AERE - PR/NP 13
INDC-215
INDC(UK)-002/G

UNCLASSIFIED

AERE - PR/NP 13

United Kingdom Atomic Energy Authority

RESEARCH GROUP

NUCLEAR PHYSICS DIVISION PROGRESS REPORT

For the period 1st May 1967 to 31st October 1967

Editor : C. F. COLEMAN

Nuclear Physics Division,
Atomic Energy Research Establishment,
Harwell, Berkshire.
1968

U.D.C.
539.1 (047.1)

NUCLEAR PHYSICS DIVISION

PROGRESS REPORT

For the period 1st May 1967 to 31st October 1967

Editor: C. F. COLEMAN

Nuclear Physics Division,
U.K.A.E.A. Research Group,
Atomic Energy Research Establishment,
HARWELL.

February, 1968.

/HMB

HL 68/714

CONTENTS

CONTENTS (cont'd)

CONTENTS (cont'd)

NUCLEAR PHYSICS DIVISION

Division Head: Dr. B. Rose

IBIS 3 MV Pulsed Van de Graaff and 5 MV Van de Graaff

Dr. A. T. G. Ferguson

Tandem Generator

Dr. J. Freeman

Electron Linear Accelerator

Dr. E. R. Rae

Proton Physics

Dr. P. E. Cavanagh

Synchrocyclotron

Mr. A. E. Taylor

Ion-Crystal Interactions

Dr. G. Dearnaley

Mössbauer Effect

Dr. T. E. Cranshaw

Miscellaneous Research

Dr. J. V. Jelley

INTRODUCTION

DR. B. ROSE

The topics to which I shall call attention in this introduction have been chosen with the object of highlighting particular aspects of the work of the Division - work recently completed or still under way which is already influencing reactor thinking, the last stages of one particular program and the first stages of several new programs, newly developed techniques and elegant applications of established techniques.

The results of most importance to the reactor program are undoubtedly those on the Pu α-value, even though they are still preliminary. The work on p-p scattering at 98 MeV represents probably the last useful contribution to this problem until techniques are materially improved and a good case is made for improved accuracy. The experiment on the total neutron cross section of aligned holmium provides one of the most direct indications that a certain nucleus is highly prolate.

The first nuclear physics experimental work is reported from the variable energy cyclotron. The analysis of a collaborative experiment carried out with University participation on Nimrod has revealed a new dipion resonance.

The technique of using high resolution germanium gamma-ray counters is being extensively developed. Preliminary results from the application of these devices to the study of nuclear lifetimes (by observing doppler shifts), of inelastic neutron scattering (by observing $(n,n'\gamma)$ processes) and of the gamma spectra following resonance neutron capture show that they will undoubtedly lead to important results in the near future.

Finally, there is an interesting contribution to lunar physics - or is it to mineralogy?

This brief introduction emphasizes the breadth of the Division's program, but there is no lack of investigation in depth, as a cursory glance at the table of contents will suggest, and a detailed study of the report will confirm.

EDITORIAL NOTE

Since the results obtained from the various machines are not easily classified according to the energy of the charged beams, individual research items are labelled with a single letter indicating on which machine the experiments were performed. These labels are as follows:-

Cockcroft Walton Generator (A. T. G. Ferguson)	A
3 MV pulsed Van de Graaff Generator IBIS (A. T. G. Ferguson)	B
5 MV Van de Graaff Generator (A. T. G. Ferguson)	C
13 MV Tandem Generator (J. M. Freeman)	D
45 MeV Electron Linac (E. R. Rae)	E
50 MeV Proton Linac : S.R.C.	F
Variable Energy Cyclotron : Chemistry Division	G
Synchrocyclotron (A. E. Taylor)	H
Nimrod Proton Synchrotron : S.R.C.	I

The running analyses for the various machines operated by the division are presented as far as possible in a uniform format, but some differences exist in the way in which the scheduling is arranged, and machines such as the Electron Linac can accommodate several experiments simultaneously.

GENERAL REACTOR TECHNOLOGIES AND STUDIES

GENERAL NUCLEAR DATA FOR REACTORS

(E) Fission cross section fluctuation analysis (G. D. James and D. A. J. Endacott)

Further attempts to identify possible causes of the significantly high values of the serial correlation coefficients $r_k(W)$[1] found in analyses of the low energy fission cross section data[1,2] have been made by introducing correlations among a set of resonance parameters for about 1700 resonances with the average properties of ^{241}Pu resonance levels. The effect on $r_k(W)$ of introducing the following correlations have been investigated for each spin sequence separately and also for both spin sequences: (a) the neutron widths were re-arranged so that decreasing neutron widths correlated with increasing level spacing, (b) the fission widths were re-arranged so that decreasing fission widths correlated with the increasing level spacing and (c) fission widths were re-arranged so that decreasing fission widths correlated with increasing neutron widths. No significantly high values of $r_k(W)$ were found for (a) and (b) but results from correlation (c) did show values of $r_k(W)$ which were significant at the 5% level for values of $W<10$ eV. Finally a periodic change in neutron widths was introduced such that neutron widths for resonances in a given spin sequence had a 'saw tooth' variation with a period of 50 eV. No obvious indication of this periodicity appeared in the values of $r_k(W)$. Again, some values of $r_1(W)$ for $W<10$ eV were significant at the 5% level and two values of $r_1(W)$, at $W = 1$ eV and $W = 2$ eV, were large (0.6 and 0.36 for 1% significance values of 0.25 and 0.26 respectively). These results probably reflect the value of the level spacing $D = 1.3$ eV.

(E) The direct measurement over the energy range 10 eV to 30 keV of alpha (E) for ^{239}Pu (M. G. Schomberg, M. G. Sowerby and F. W. Evans)

The work previously reported[3] has been continued and measurements have been made of the neutron and gamma-ray yields for two ^{239}Pu samples of thickness 1.2×10^{-3} and 5.79×10^{-4} atoms per barn respectively. In addition the relative incident neutron flux has been measured and we have made runs on Ag, Pt, Au, Ta and ^{238}U to check the efficiency of the gamma-ray detector by the "black" resonance technique[4].

The reactor physicist requires the ratio of the average capture to fission cross sections ($\langle\sigma_{n\gamma}(E)\rangle/\langle\sigma_{nf}(E)\rangle$) rather than the average value of alpha (E) ($\langle\alpha(E)\rangle$). In order to obtain the average values of these cross sections it is necessary to make multiple scattering corrections and the present experiment is not far enough advanced for this to be done. The value of $\langle\sigma_{n\gamma}(E)\rangle/\langle\sigma_{nf}(E)\rangle$ in the energy range from a few hundred eV to 10 keV is quite uncertain, since the KAPL data[5] suggest that the value is $\simeq 0.5$, while the values deduced[6] from the measured total and fission cross sections via the formula

$$\langle\sigma_{n\gamma}(E)\rangle = \langle\sigma_{nT}(E)\rangle - \langle\sigma_{nf}(E)\rangle - \langle\sigma_{nn}(E)\rangle$$

---

(1) Egelstaff P. J. Nuc. Energy 7, 35 (1958).

(2) James G. D. and Endacott D. A. J. Nuclear Physics Division Progress Report AERE - PR/NP 10, 2 (1966).

(3) Schomberg M. G., Sowerby M. G. and Evans F. W. Nuclear Physics Division Progress Report AERE - PR/NP 12 (1967).

(4) Moxon M. C. and Rae E. R. Nucl. Inst. and Meth. 24, 445 (1963).

(5) Sampson J. B. and Molino A. F. KAPL 1793 (1957).

(6) Patrick B. H., Schomberg M. G. and Sowerby M. G. Nuclear Physics Division Progress Report AERE - PR/NP 12 (1967).

are $\simeq 1$ (σ_{nT} and σ_{nn} are the total and scattering cross sections respectively). It is therefore important to get some idea of the value obtained from the present experiment. The data obtained from the thinner of the two ^{239}Pu samples have been integrated over 100 eV intervals below 1 keV, 1 keV intervals between 1 and 10 keV, 5 keV intervals between 10 and 30 keV and 10 keV intervals from 50 to 70 keV. The quantity $<\sigma_{n\gamma}(E)>/<\sigma_{nf}(E)>$ has been estimated from the formula[7]

$$\frac{n_c}{n_f} = \frac{\sigma_{n\gamma}(E)}{\sigma_{nf}(E)} S = \frac{A\frac{N_\gamma}{N_n} - 1}{B - C\frac{N_\gamma}{N_n}}$$

where n_c and n_f are the number of capture and fission events

N_γ and N_n are the number of gamma ray and neutron counts

A, B and C are constants which are found by normalisation and

S is the multiple scattering correction factor which in general is close to unity.

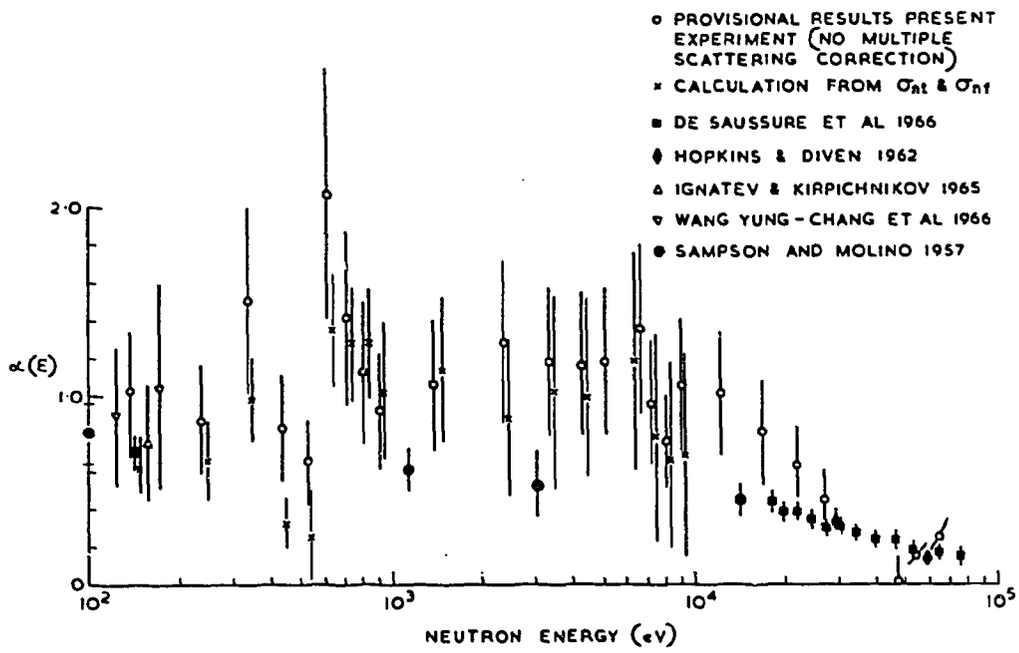

Fig. 1. α(E) for ^{239}Pu.

The values of A, B and C have been found by assuming, from the data of Derrien et al.[8], the value of α(E) for 13 well resolved resonances in the energy region below 80 eV. The estimated values of $<\sigma_{n\gamma}(E)>/<\sigma_{nf}(E)>$ are plotted in Fig. 1 along with the other available data. It can be seen that the results are in reasonable agreement with the values obtained from $\sigma_{nT}(E)$ and $\sigma_{nf}(E)$. Between 10 and 30 keV our values are higher than the values of De Saussure et al.[9] but this discrepancy is not considered significant at this stage because uncertainties in background are most important in this energy range. The errors assigned in Fig. 1 to the present experiment have arbitrarily been assumed to be ± 33% because the systematic errors, which have not been assessed, predominate. The procedure

(7) Schomberg M. G., Sowerby M. G. and Evans F. W. IAEA Symposium on Fast Reactor Physics and Related Safety Problems, Karlsruhe, SM-101/41 (1967).

(8) Derrien H., Blous J., Eggermann C., Michaudon A., Paya D. and Ribon P. Nuclear Data for Reactors 2 IAEA Vienna p. 195 (1967).

(9) De Saussure G., Weston L. W., Gwin R., Ingle R. W., Todd J. H., Hockenbury R. W., Fullwood R. R. and Lotlin A. 1966 Conference on Nuclear Data for Reactors, (IAEA), vol. 2, p. 233 (1967).

used to estimate the present values is only valid if multiple scattering corrections are small and the variation of the incident neutron flux over the energy interval used is negligible. Therefore the results should be viewed with extreme caution. However, they do show, particularly in the energy range 1 to 10 keV, where the assumptions are not too unreasonable, that the value of $\alpha(E)$ is more likely to be in the region of 1 than 0.5.

(E) ^{10}B scattering cross section (A. Asami and M. C. Moxon)

The scattering cross section of ^{10}B was measured relative to carbon using a sample changer on the 50 m spectrometer, with the two detectors set at angles of 60° and 120° to the incident neutrons. Analysis of the data includes corrections due to centre of mass motion and, in first order, to multiple scattering.

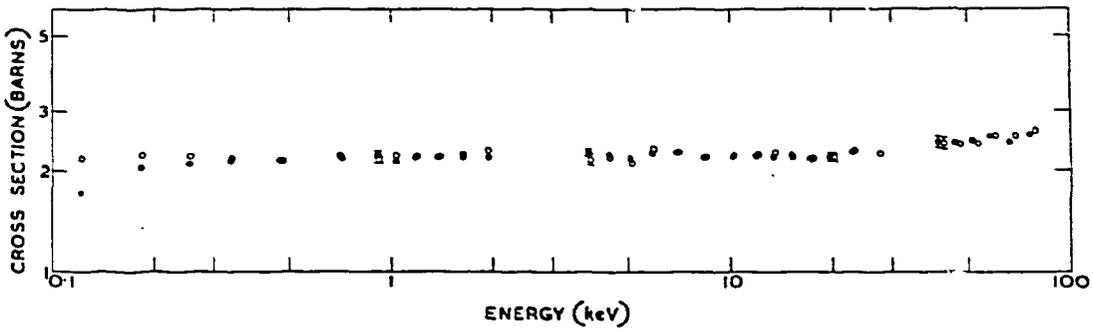

Fig. 2. ^{10}B scattering cross section.
(•, detector at 60°; ×, detector at 120°).

Preliminary results in the energy range from 200 eV to 80 keV are shown in Fig. 2. The indicated errors are only statistical. The cross sections near 3 keV, 35 keV and 90 keV are not determined because of the presence of the resonances in sodium (2.8 keV) and in aluminium (35, 90 keV). The former was used for the normalization of backgrounds.

The ^{10}B scattering cross section was calculated from the ratio of the number of neutrons scattered by the ^{10}B sample to the number scattered by a similar C sample, assuming that the carbon scattering cross section was equal to the total cross section (given by $\sigma_T = \sigma_S = 4.767 - 4.00 \times E$ (MeV)[10]), and that the scattering cross section is independent of angle in the centre of mass system.

The present results, which are however subject to further minor corrections, agree well with the recent measurements by Mooring et al.[11] (above 10 keV) and by Diment[12] (below 10 keV).

Measurements at other detector angles (35°, 145°) are in progress and analysis of the data is proceeding.

---

(10) Uttley C. A. and Diment K. M. This progress report, p. 4.

(11) Mooring F. P., Monahan J. E. and Huddleston C. M. Nucl. Phys. 82, 16 (1966).

(12) Diment K. M. AERE - R 5224.

(E) Total cross section measurements (C. A. Uttley and K. M. Diment)

I. The total cross section of carbon

The total cross section of reactor grade graphite between 70 eV and 100 keV has been measured, primarily to provide comparison scattering cross sections for determining the scattering cross section of ^{10}B[13]. The carbon measurements were made on the 120 metre spectrometer and overlap total cross section measurements made with the 300 metre spectrometer[14] at energies of up to several MeV. It is commonly assumed that the total cross section of carbon is constant from thermal energies up to at least 1 keV. The average cross section between 70 eV and 1 keV obtained from the data shown in Fig. 3, 4.767 ± 0.010 barns, is about 1% higher than the value of 4.71 barns recommended in the evaluation of Schmidt[15], which appears to attach surprisingly little weight to more recent direct measurements at energies of tens of eV, particularly that of Walton et al.[16] (4.77 ± 0.05 barns) and those of Triftshauser and Fehsenfeld[17] (4.743 ± 0.002 and 4.7264 ± 0.0024 barns). The full curve in Fig. 3, which fits the data to one per cent over the range from 0.1 to 100 keV and would be useful for multiple scattering calculations in this range, is represented by the equation

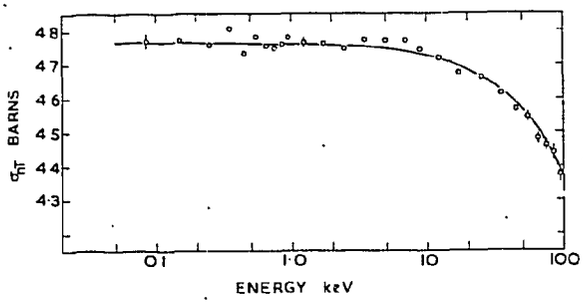

Fig. 3. Total cross section of carbon.

$$\sigma_{nT} = 4.767 - 4.00E \text{ barns}$$

where E is the neutron energy in MeV. Our earlier fit[14], based on the 300 metre data, covers the somewhat higher energies 10 → 2,000 keV, and agrees within the stated limits in the overlap region.

II. The total cross section of ^6Li

Transmission measurements on samples of Lithium enriched to 95.2% in ^6Li have been made over the energy range 70 eV to 7 MeV on the 120 metre and 300 metre spectrometers. These measurements are intended to determine the range over which the absorption cross section follows a $1/\sqrt{E}$ law. When the results are combined with accurate values for the parameters of the 250 keV resonance, the $^6Li(n,\alpha)$ cross section should provide a useful standard for neutron flux measurements below 100 keV. The results already processed are shown in Fig. 4. A preliminary fit to the data from 70 eV to 10 keV is consistent with an absorption cross section which varies with energy as $0.151 \times E^{-1/2}$ and a constant component of 0.7 barn which is attributed to potential scattering.

(E) Neutron capture cross sections of Cu and Sb (M. C. Moxon, Mrs. C. Campbell and F. Horsmann)

Neutron capture measurements on antimony and copper in the neutron energy range 5 eV to 100 keV have been carried out on the 32.5 metre flight path. The data are now being analysed. These elements, like others, showed several small resonances which were not observed in transmission measurements (see Fig. 5).

---

(13) Asami A. This progress report, p. 3.

(14) Uttley C. A. and Diment K. M. Nuclear Physics Division Progress Report AERE - PR/NP 9 (1965).

(15) Schmidt J. J. KFK 120 (EANDC-E-35'U') (1966).

(16) Walton R. B., Wikner N. F., Wood J. L. and Beyster J. R. Bull. Am. Phys. Soc. 5, 288 (1960).

(17) Triftshauser W. and Fehsenfeld P. EANDC-E-57'U' (1965).

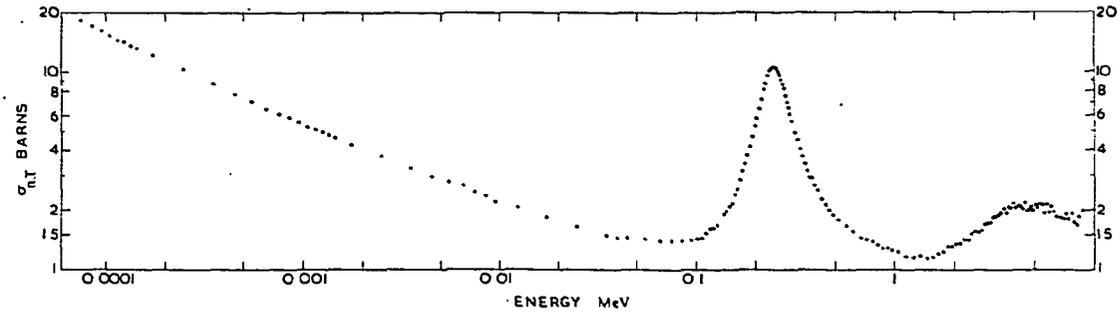

Fig. 4. Total cross section of ^6Li.

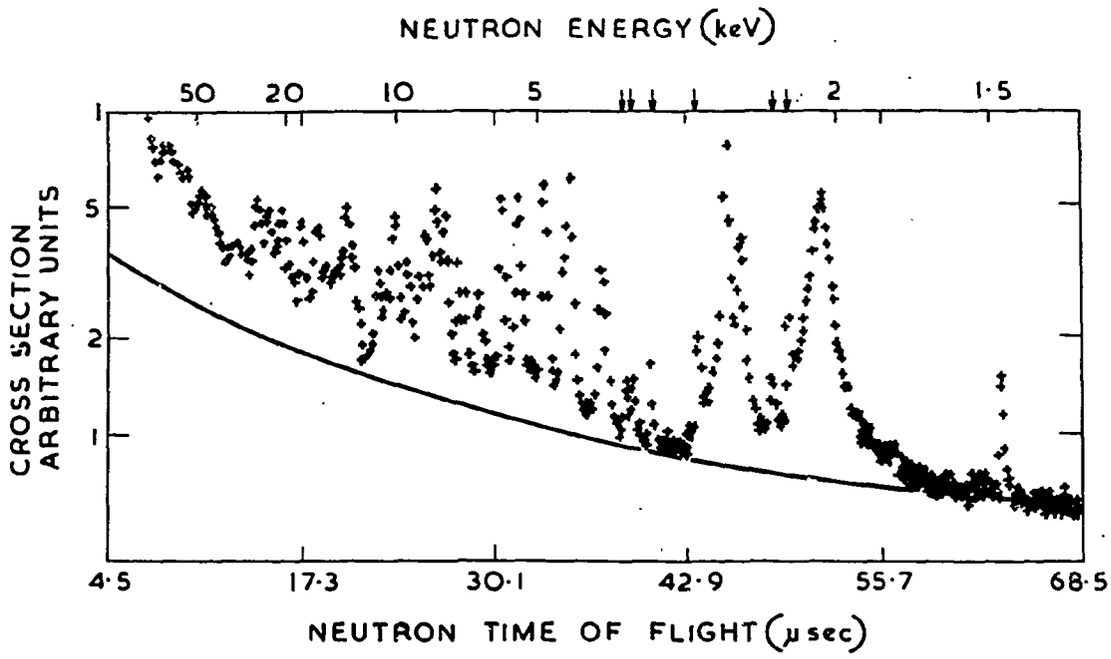

Fig. 5. Neutron capture in natural copper (0.060 ins). The smooth curve is the measured background. The resonances marked ↓ have not been observed in transmission measurements.

(E) Analysis of neutron capture cross sections to obtain resonance parameters (M. C. Moxon)

The Monte Carlo program originally written by J. E. Lynn has now been modified to include the effects of the energy resolution on the measurements. The resolution function is calculated by folding together the following factors:-

(i) the shape of the electron pulse

(ii) The build up and decay of the neutrons in the booster

(iii) the timing channel width

(iv) the angle of the flight path to the normal of the moderator being viewed

(v) the moderation time jitter[18,19,20].

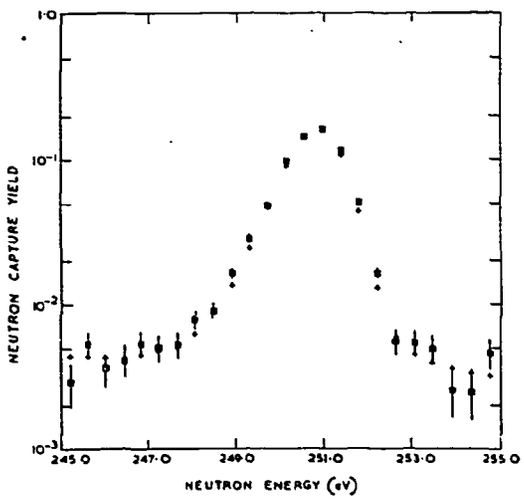

Fig. 6.

• EXPERIMENTAL DATA
• CALCULATED FIT
RESONANCE ENERGY = 250·8 (eV), SPIN = 1
NEUTRON WIDTH = 10·65 (meV), RADIATION WIDTH = 120·0 (meV)
FLIGHT PATH LENGTH = 32·54 metres
WIDTH OF ELECTRON PULSE = 200 nsec
$T_{1/2}$ FOR BOOSTER = 105 nsec
TIMING CHANNEL WIDTH = 125 nsec
MEAN FREE PATH USED TO CALCULATE MODERATION TIME JITTER 0·5cm

Fig. 6 shows the fit to a resonance at 250.8 eV in ^{109}Ag where the natural width of the resonance is small compared with the resolution width.

(E) Transmission measurements on ^{107}Ag and ^{109}Ag (N. J. Pattenden and J. E. Jolly)

Transmission measurements have been reported previously[21] on a 739 mg sample of ^{109}Ag, using the small sample spectrometer (nominal resolution ~ 16 nsec/m). More recently, samples of about 10 g of separated ^{107}Ag and ^{109}Ag metal have become available. The ^{109}Ag measurements have therefore been repeated and extended and ^{107}Ag measurements performed on a 94 m flight path (nominal resolution ~ 3 nsec/m). In the energy range from 40 eV upwards 39 resonances have been identified in ^{107}Ag and 52 in ^{109}Ag. The samples were too thin to detect with certainty resonances with reduced neutron width ($2\,g\,\Gamma_n^{o}$) values of $\lesssim$1.0 meV. A detailed resonance analysis will be performed as soon as time permits, but some points of interest can be observed from an examination of the data.

(1) The 169.80 eV resonance should probably be assigned to 107 and not 109.

(2) There are resonances in both isotopes at 173.10, 251.29, 554.51, 933.39, 1414.5 and 1586.0 eV.

(3) The 469.61 eV resonance should be assigned to 109 and the 472.20 eV resonance to 107.

The above energy values, quoted for identification purposes only, are those of Garg et al.[22].

---

(18) Groenewald H. J. and Groendijk H. Physica 13, 141 (1947).

(19) Patrick B. H., Bowey E. M., Moxon M. C. and Rae E. R. Proceedings of the Third Euratom Conference on Accelerator Targets Designed for the Production of Neutrons, Liege (September 1967) (to be published).

(20) Patrick B. H., Bowey E. M., Moxon M. C. and Rae E. R. Optimisation of moderators for pulsed neutron targets, this progress report, p. 54.

(21) Pattenden N. J. Nuclear Physics Division Progress Report AERE - PR/NP 8, p. 12 (1965).

(22) Garg J. B., Rainwater J. and Havens Jr. W. W. Phys. Rev. 137, B547 (1965).

(E) Radiative capture of thermal and resonance neutrons (W. E. Stein*, B. W. Thomas and E. R. Rae)

A system for the study of neutron capture gamma rays has been established at the Harwell linear accelerator. The boosted source and moderator provide intense bursts of neutrons with a continuous spectrum within the energy region (thermal to a few keV) of interest in this experiment. The gamma-ray spectrometer is a 30 cm^3 lithium-drifted germanium detector. The experimental arrangement is shown in Fig. 7.

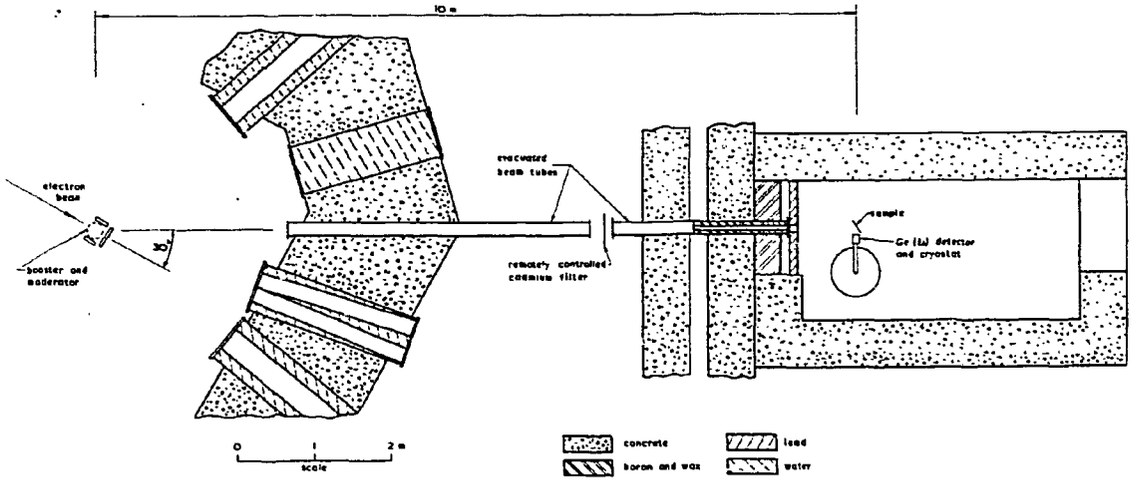

Fig. 7. Experimental arrangement for resonance neutron caputre gamma ray studies.

Neutrons from the booster are collimated onto a sample approximately 10 metres from the source. Capture gamma rays are detected by the germanium detector which is placed out of the direct beam but close to the capture sample. Neutron energies are determined from the time of flight over the distance between the source and sample. The detector and sample are situated in a two-foot thick concrete enclosure 12 ft. long, 6 ft. wide and 10 ft. high. For additional shielding the detector is protected by about 1 inch of normal lithium carbonate and wax and 3 mm of lead. In this arrangement the primary radiation or gamma flash presents no great difficulty.

Although a complete two-parameter system is being assembled, data presented here were taken with a system which was limited to ten time intervals which could be arbitrarily set to select neutron energy regions of interest. In this manner amplitude spectra for each of the ten selected time intervals were obtained simultaneously. The time resolution based on the neutron burst and flight path was about 15 ns/m. The intrinsic energy resolution of the gamma-ray spectrometer as determined from the width of the full-energy peak of a thorium source is about 6 keV. When capture gamma rays were observed in the presence of the gamma flash shorter time constants were required, which caused the resolution width to increase. Observed line widths for 100 eV and 1 keV neutrons were 11 keV and 18 keV respectively.

To date capture gamma-ray measurements have been made on tungsten, iron and copper samples. Present tungsten results are in agreement with recently published data[23]. Although analysis of the Fe and Cu data is still incomplete, a few general comments can be made about the results.

Capture gamma-ray spectra for thermal and 1.167 keV resonance neutrons incident on iron are shown in Fig. 8 (overleaf). The peak in the thermal spectrum at 6418 keV is attributed to a strong calcium background line from neutrons captured in the concrete shield. When compared with the thermal data, the resonance spectrum indicates a reduced intensity of the 5920, 6018 and 7277 keV transitions and a considerable enhancement of the 6378 keV line.

---

(23) Rae E. R., Moyer W. R., Fullwood R. R. and Andrews J. L. Phys. Rev. 155, 1301 (1967).

*On attachment from Los Alamos Scientific Library.

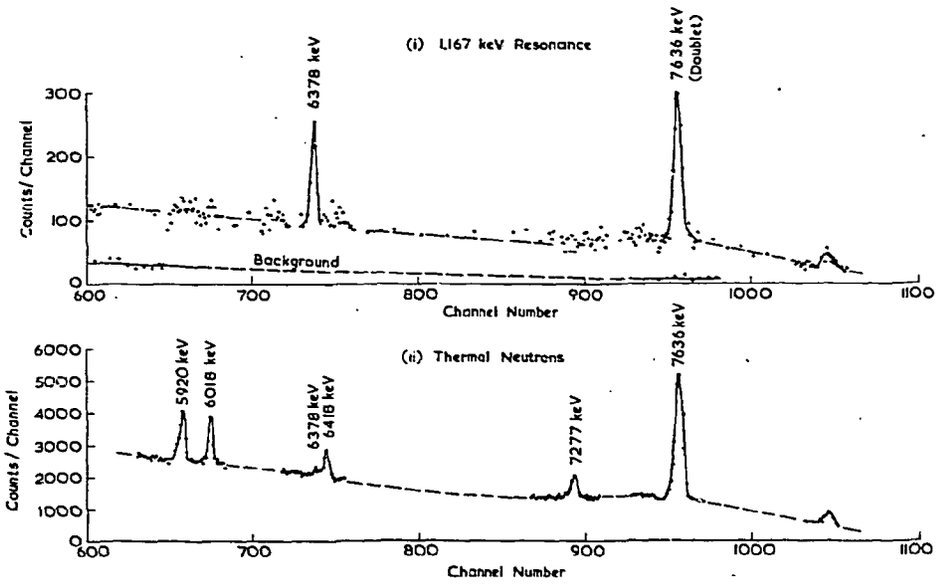

Fig. 8. Capture gamma ray spectra for $^{56}Fe\,(n,\gamma)\,^{57}Fe$.

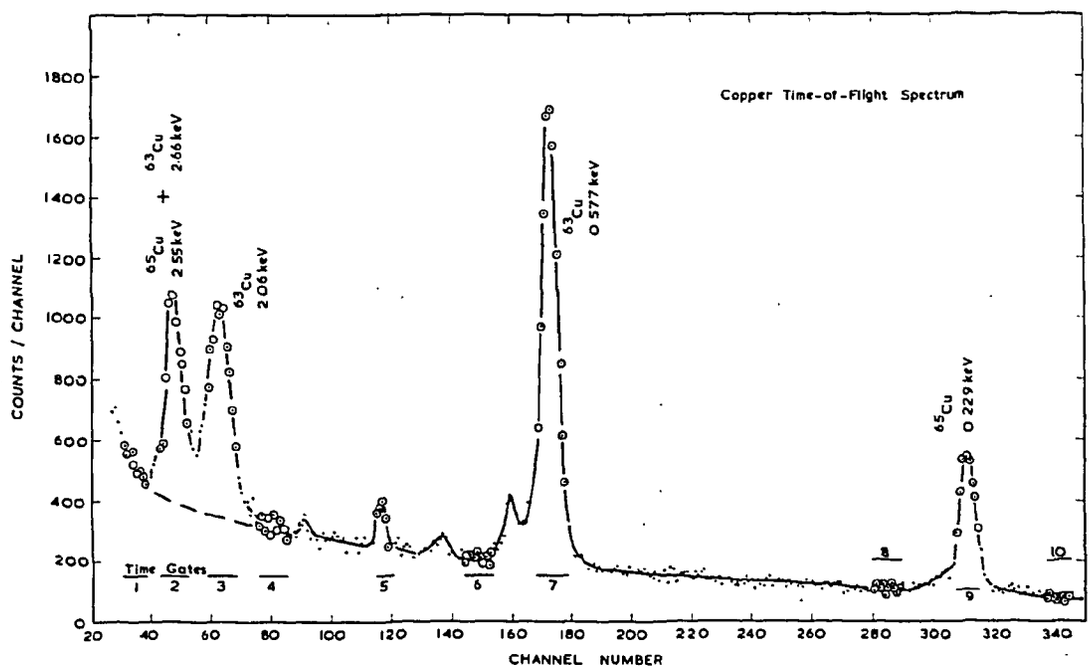

Fig. 9. Time-of-flight spectrum for a natural copper sample.

A time-of-flight spectrum for a natural copper sample is shown in Fig. 9. Bold points and horizontal lines indicate the time intervals covered by the ten timing gates. The second gate covers two unresolved resonances in ^{65}Cu at 2.55 keV and ^{63}Cu at 2.66 keV. The ^{63}Cu resonance contributes about 75% of the total counts in the observed spectrum. The observed copper gamma-ray spectra for resonance and thermal neutrons are shown in Figs. 10 and 11 (see page 10 for Fig. 11). Backgrounds for the resonance data were obtained by setting the timing gates between resonances. For the thermal

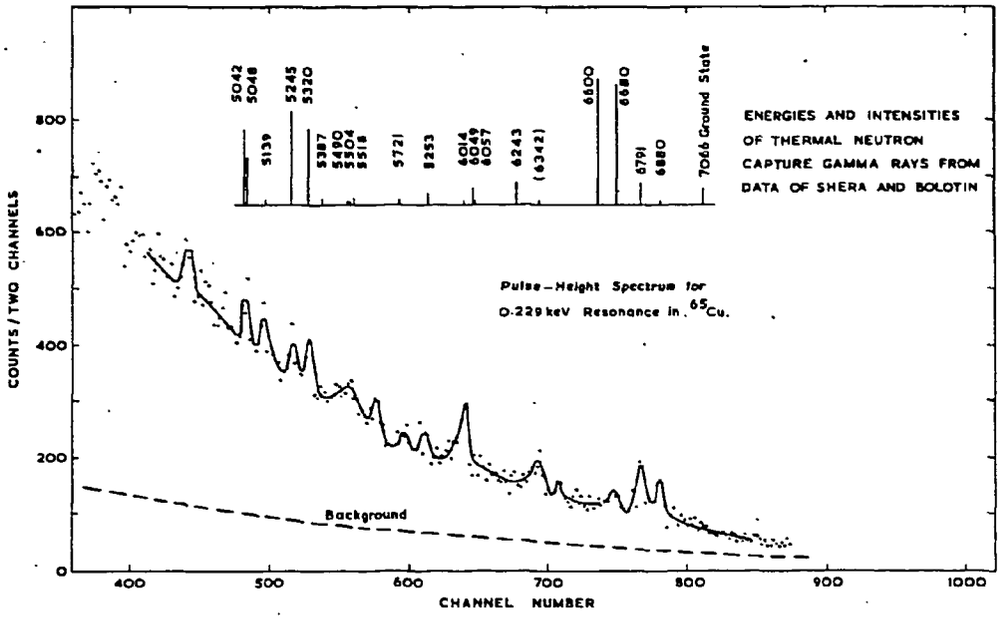

Fig. 10. Gamma ray spectrum for neutrons captured in the 0.229 keV resonance of ^{65}Cu. The energy scale and relative intensities of transitions observed by Shera and Bolotin[23] for thermal neutron capture in ^{65}Cu are given in the insert.

neutron measurements the detector was shielded by lead in order to reduce the intensity of gamma rays from the iron and calcium in the surrounding materials. To provide comparable slow neutron scattering in these background measurements, the copper sample was replaced by a graphite sheet of appropriate thickness.

The dominant feature of these spectra is the fluctuation in intensity of the primary transitions. The strong ground state transition observed in the thermal spectrum is not seen in the 0.577 keV data. Instead the strongest transition for this resonance is to the first excited state at 160 keV. Another striking feature of the 0.577 keV resonance data is the appearance of five strong lines between 4540 and 5150 keV. These lines represent about 11% of the total gamma-ray intensity or about 70% of the strength of the transitions to the first four excited states. There is no known explanation at the present time for strong transitions to particular states approximately 3 MeV above the ground state.

Our present ^{63}Cu data have been analysed to obtain the combined intensities of the transitions to the ground and to the three lowest excited states. These summed intensities are 43, 16.4, 2.2 and 6.6 per cent for thermal, 0.577 keV, 2.06 keV and 2.66 keV neutrons respectively. It is improbable that this dramatic change is due to resonance-resonance interference at thermal neutron energies, but it may be a manifestation of intermediate structure effects.

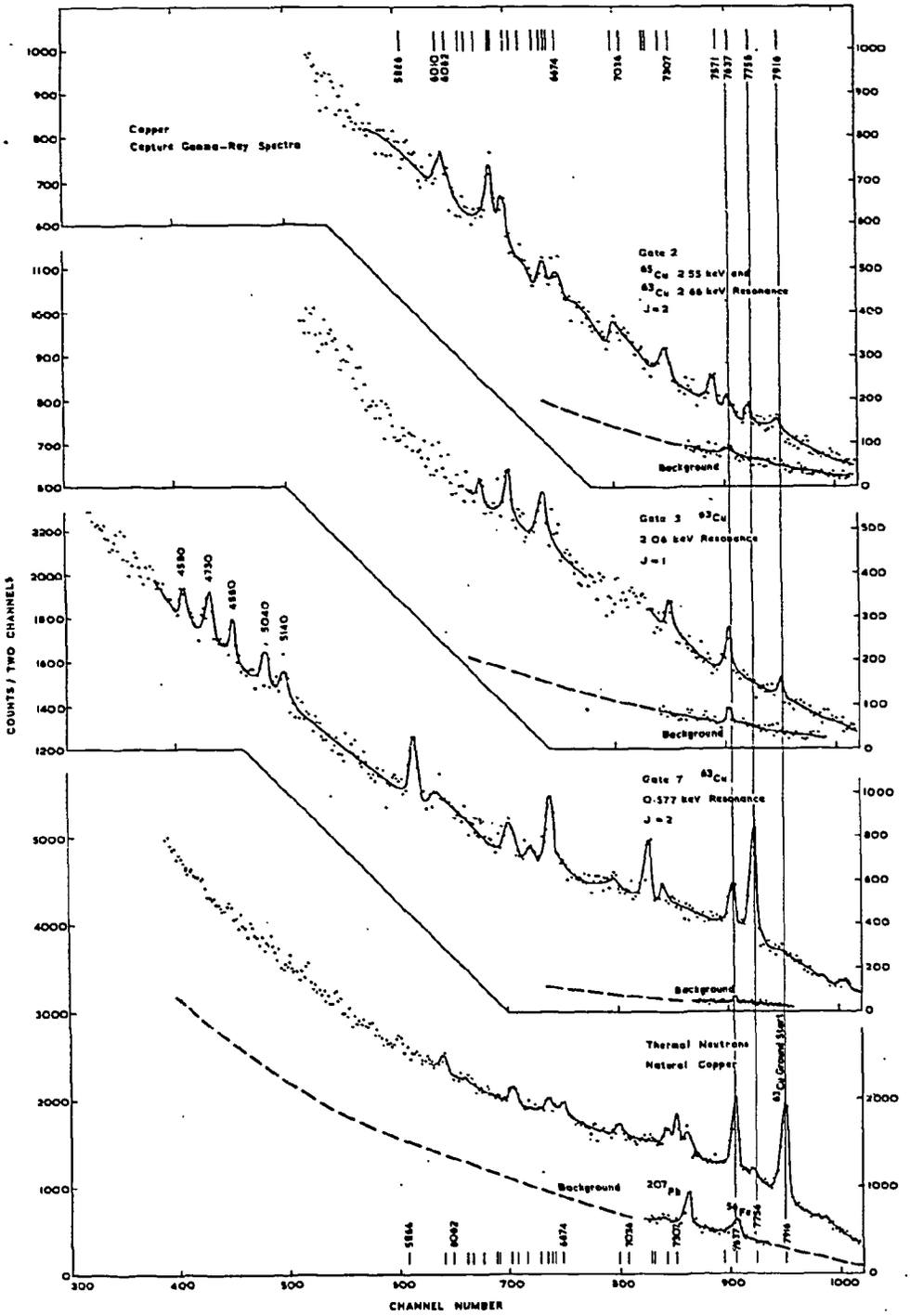

Fig. 11. Copper capture gamma ray spectra for thermal and resonance neutrons. The scales at the top and bottom give the energies of transitions observed by Shera and Bolotin[24] for thermal neutron capture in ^{63}Cu.

(24) Shera and Bolotin, private communication, Los Alamos Scientific Laboratory.

FUNDAMENTAL AND BASIC RESEARCH

NUCLEAR STRUCTURE AND DYNAMICS

B. The reactions $^{17}O(^{3}He,n)^{19}Ne$ and $^{18}O(^{3}He,n)^{20}Ne$ (B. H. Armitage, K. Gul and B. W. Hooton)

The neutrons resulting from these reactions were studied by time-of-flight techniques using a 3.1 MeV ^{3}He beam. The angular distributions of the neutron groups leading to excited states in ^{19}Ne and ^{20}Ne were analysed using the D.W.B.A. method.

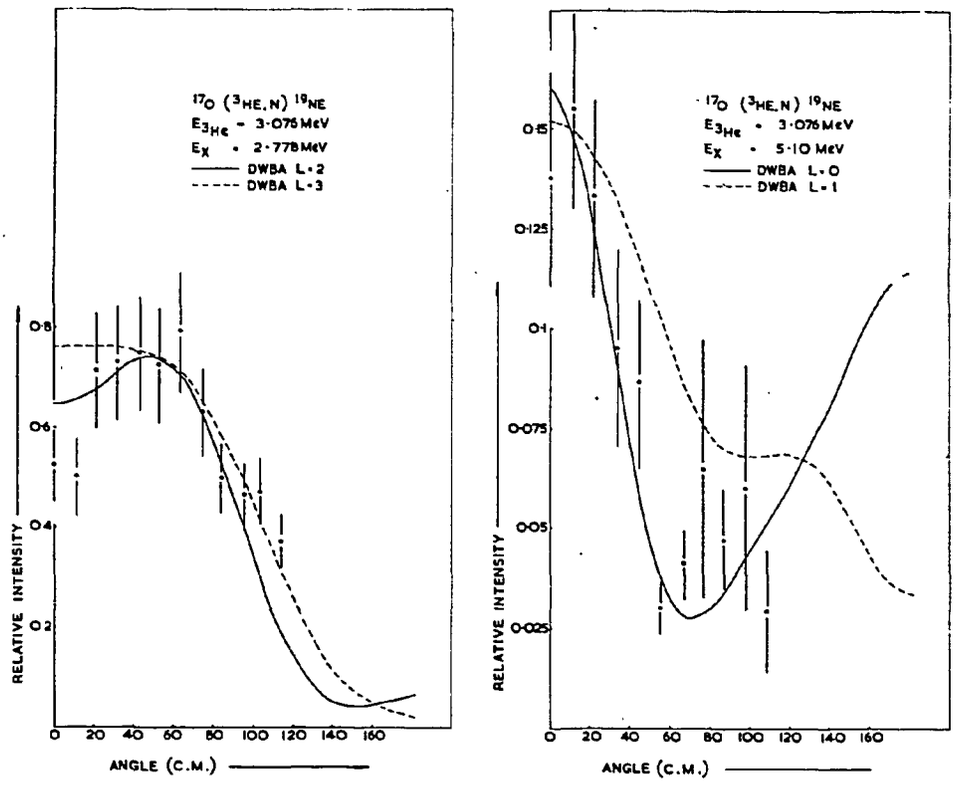

Fig. 12. Angular distribution for the reaction $(^{3}He,n)$ leading to the 2.778 and 5.10 MeV states of ^{19}Ne.

$^{17}O(^{3}He,n)^{19}Ne$

Many of the peaks in the neutron spectra correspond to excitation of more than one level and the only angular distribution which gave reasonable agreement with a D.W.B.A. calculation is shown in Fig. 12. The L=2 distribution was calculated by putting both protons in the 1d orbit, the L=3 distributions, by putting one proton in the 1d and the other in the 1f orbit. The L=2 distribution is a better fit at forward angles and is consistent with an expected spin of $9/2^{+}$. This work concludes a series of investigations into the mass 19 system[25].

(25) Nuclear Physics Division Progress Report AERE - PR/NP 12, p. 23 (1967).

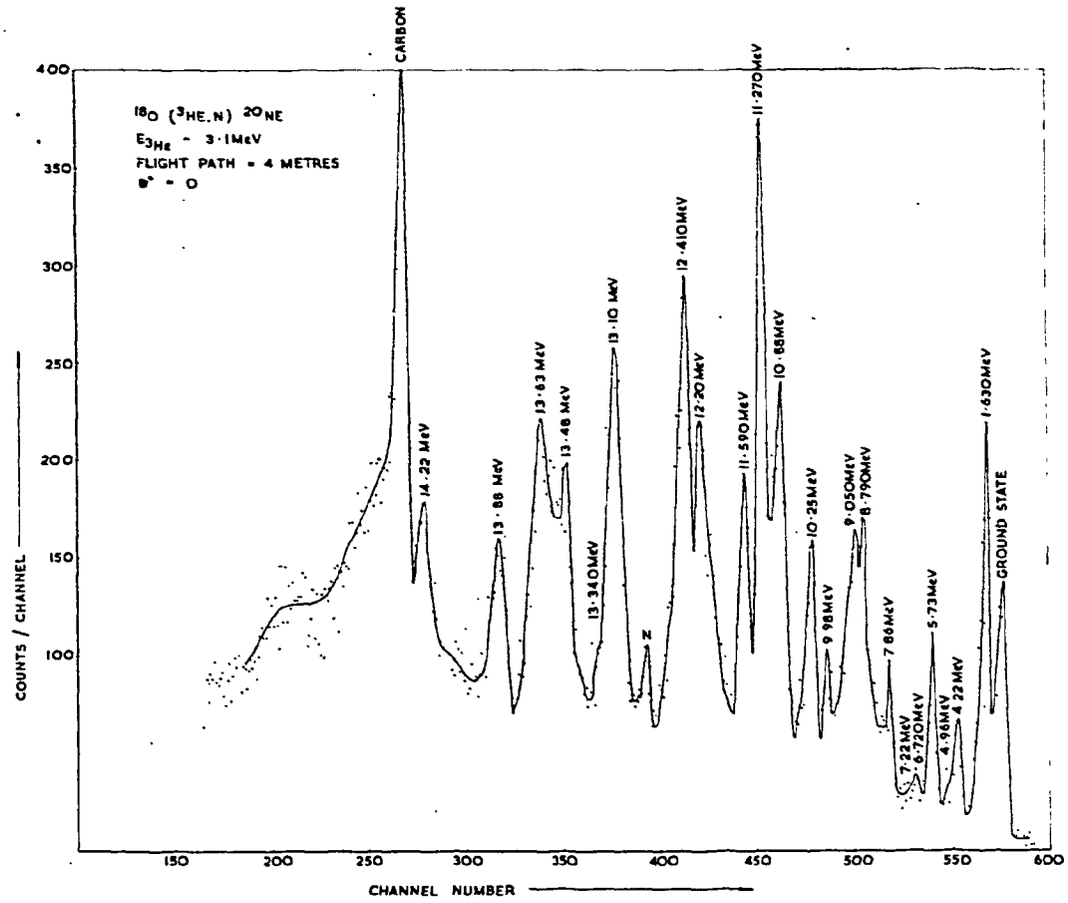

Fig. 13. Spectrum for the reaction $^{18}O(^3He,n)\,^{20}Ne$.

$^{18}O(^3He,n)^{20}Ne$

A typical neutron spectrum is shown in Fig. 13. Since the ground state of ^{18}O is 0^+ the spin and parity of the final state is determined uniquely by the orbital angular momentum of the captured diproton (assuming no spin flip and therefore S=0). A selection of angular distributions is given in Fig. 14. In general for a given L value more than one angular distribution is possible. In particular the distribution to the 1.63 MeV 2^+ state is shown to be due to the $(1d)^2_{j=2}$ rather than the $(1d, 2s)_{j=2}$ configuration. A summary of the results is given in Table I (see page 14). In certain cases relative spectroscopic factors and two particle fractional parentage coefficients have been obtained and are being compared with theory. The significance of our failure to observe known 0^+ states[26] at 6.72 and 7.20 is under investigation.

(26) Siemssen R. H., Lee Jr. L. L. and Cline D. Phys. Rev. 140B, 1258 (1956).

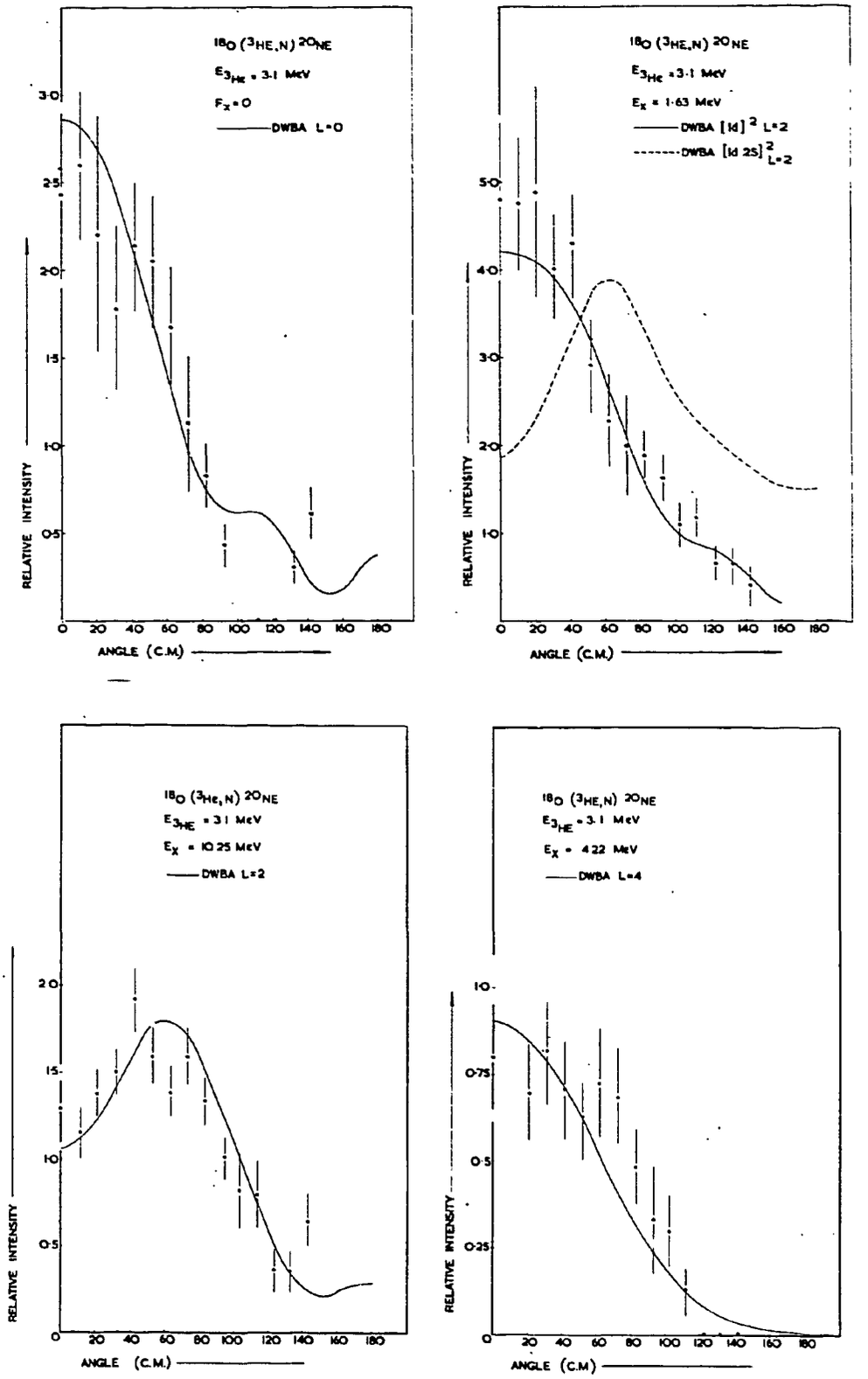

Fig. 14. Angular distributions for the reaction (^{3}He,n) leading to the 0, 1.63, 4.22 and 10.25 MeV levels of ^{20}Ne.

TABLE I

Present Work		Previous Work[27,28,29]	
E	J	E	J
1.63	2^+	1.632	2^+
4.22	4^+	4.248	4^+
5.73	1^-	5.63	3^-
		5.8	1^-
10.25	2^+	10.27	2^+
10.88			
11.27	0^++, 2^+, 3^-	11.276	
11.59		11.56 ± .04	
12.20	2^+	12.16	
		12.24	
12.41	0^+, 1^-	12.39	
13.10	0^+, 1^-	13.086	

(B) The measurement of gamma-rays following inelastic neutron scattering from Fe and P (B. H. Armitage, A. T. G. Ferguson, G. C. Neilson* and W. D. N. Pritchard+)

The gamma-ray spectra arising from the reactions $^{56}Fe(n,n'\gamma)^{56}Fe$ and $^{31}P(n,n'\gamma)^{31}P$ induced by 4.7 MeV and 5.5 MeV neutrons have been measured. The coincidence technique used to reduce the effect of neutron induced backgrounds in the 30 cc Ge(Li) detector has already been described[30]. The Fe sample was a hollow circular cylinder 4.8 cm in length with inner and outer diameters of 3.18 and 3.8 cm respectively. The 90° differential cross sections for production of the various gamma-rays were obtained by using the value of the production cross section for the 0.845 keV gamma-ray published by Benjamin et al.[32] combined with measurements of the energy dependence of the detection efficiency obtained by the method described by Freeman and Jenkin[31].

The efficiency calibration is required for a thick source distributed uniformly through the material of the Fe sample. For this purpose a replica of the sample was divided into two equal parts by making an oblique cut through the curved surface of the cylinder. A suitably shaped ring of absorbent paper was loaded as uniformly as possible with a solution of one of the calibration sources and dried out, and the two halves of the sample were then reassembled with the ring trapped between them. The detection efficiency was then measured at the sample to detector distance used in the scattering experiments, but

---

(27) Ajzenberg-Selove F. and Lauritzen T. Nucl. Phys. 11, 1 (1959).

(28) Landolt-Borstein (Berlin-Gottingen, Heidelberg, Springer-Verlag, 1961).

(29) Pearson J. D. and Spear R. H. Nucl. Phys. 54, 434 (1964).

(30) Armitage B. H., Braid T., Ferguson A. T. G.., Neilson G. C. and Pritchard W. Nuclear Physics Division Progress Report AERE - PR/NP 12, p. 18 (1967).

(31) Freeman J. M. and Jenkin J. G. AERE Report - R 5142 (1966).

(32) Benjamin R. W., Buchanan P. S. and Morgan I. L. Nuclear Physics 79, 241 (1966).

*On leave from University of Alberta.

+On attachment from University of Exeter.

with several different sample orientations. In this way separate corrections for the self-absorption of gamma-rays in the sample were avoided.

A typical (n,n′γ) spectrum is shown in Fig. 15. Additional information on the energy levels of ^{56}Fe obtained from measurements with the Ge(Li) detector of the gamma-spectrum of ^{56}Co forms a valuable addition to that obtained from the (n,n′γ) measurements, since the decay from the 4^+ ground state of ^{56}Co leads to a selective population of ^{56}Fe states which is quite different to that produced by the ^{56}Fe(n,n′γ)^{56}Fe reaction. The analysis of the data is not yet complete.

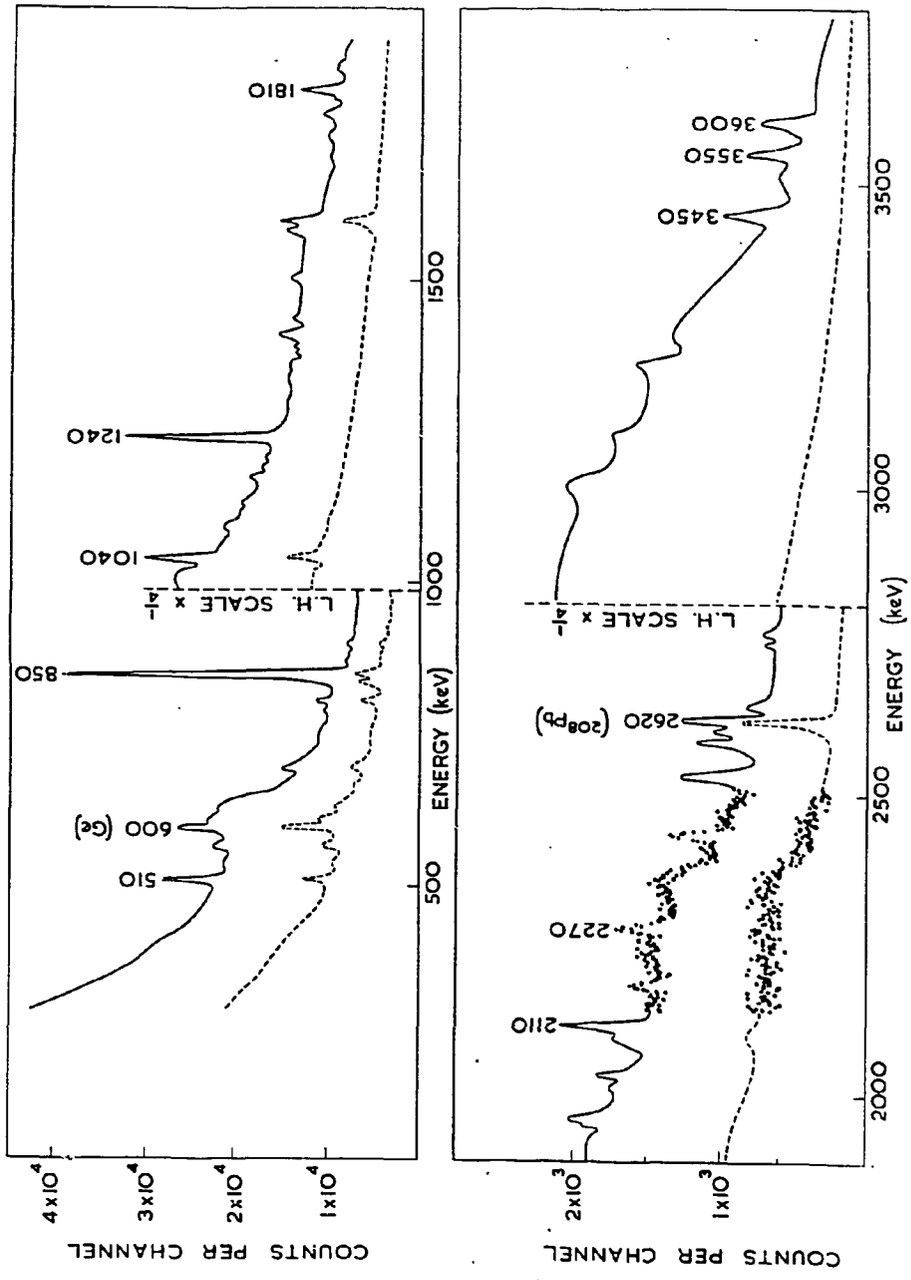

Fig. 15. Spectrum of gamma-rays produced by the inelastic scattering of 5.5 MeV neutrons from an Fe sample observed in a Ge(Li) detector. The data were taken at ~ 20 keV per channel.

(B) Studies of the $^{9}Be(\alpha,n)^{12}C$ and $^{13}C(\alpha,n)^{16}O$ reactions (J. M. Adams and C. McKenzie)

Preliminary studies have been made of the above reactions, which could usefully supplement existing sources of monoenergetic neutrons. At the energies available on IBIS (up to 3.5 MeV) the $^{13}C(\alpha,n)$ reaction gives monoenergetic neutrons ($Q_0 = 2.20$ MeV) while the $^{9}Be(\alpha,n)$ reaction gives two groups with an energy separation of 4.43 MeV. Neutron spectra have been obtained and excitation functions measured from 1.4 MeV - 3.5 MeV with targets of 50-100 $\mu g/cm^2$. The neutron spectra show all groups to be exceptionally clean and free from background. Further work motivated both by nuclear and applied considerations will be pursued.

(B) Neutron scattering from Cr, Fe, Co, As, Y and Ce at MeV energies (J. Martin with D. T. Stewart and J. Mirza (University of Glasgow))

Following the completion of a program of 6 MeV neutron scattering from Aluminium, Silicon, Phosphorus and Sulphur, reported earlier[33], we have extended the range of our investigations to heavier nuclei. Differential elastic and inelastic cross sections at 6 MeV have been measured for natural iron and chromium targets, and these results are now being corrected for multiple scattering effects. We hope to interpret the inelastic scattering to the first excited 2+ states in these nuclei by a combination of statistical model and direct interaction predictions, which we use successfully to interpret our results for silicon and sulphur. The shape elastic scattering, obtained by subtracting a statistical contribution from the measured elastic scattering cross section, will be compared with the predictions of the Perey and Buck non-local optical model[34]. In order to subject this model to more extended tests we have also measured scattering cross sections at 6 MeV from targets of Arsenic, Yttrium, Cobalt and Cerium. In these nuclei the inelastic scattering is rather weak (indicating that the reaction mechanism is predominantly compound nuclear) and only the elastic scattering has been measured reliably. However, it is hoped that improvements in our fast electronics may enable the measurement of the inelastic scattering cross sections, either at 6 MeV or lower energies. Such data can be a powerful spectroscopic tool for investigating some of the heavier elements.

A model for the analysis of fine structure observed in proton scattering via analogue resonances (A. M. Lane and S. Ramavataram)

Investigation of the fine structure underlying analogue resonances is particularly relevant to a theoretical understanding of line-broadening[35], and to this end a general description of fine structure states which allows for a smooth transition from the bound to the unbound region would be very useful.

Using the procedure outlined by Lane[35] and invoking the "picket-fence" model we have obtained a description of the fine structure states which does have this property. The validity of the theory has been tested by comparison with the fine structure data[36] for ^{40}A.

The essential features of the theoretical model may be summarised as follows: we note that the individual resonances are poles of an $\underline{S}$-matrix given by

$$\underline{S} - \underline{1} = \underline{\Omega}\,(1 + 2i\,\underline{P}^{1/2}\,\underline{R}_{K.P.}\,\underline{P}^{1/2})\,\underline{\Omega}\ ;\ \underline{R}_{K.P.} \text{ is the Kapur-Peierls R-matrix}$$

By specialising to the case of no internal mixing and a single channel, we can obtain the condition for poles as

$$R_{WE} = \frac{1}{\Delta L}$$

---

(33) Nuclear Physics Division Progress Report AERE - PR/NP 11, p. 11 (1967).

(34) Perey F. G. and Buck B. Nucl. Phys. 32, 353 (1962).

(35) Lane A. M. (Invited lecture given at the Birmingham Conference, 1967, to be published).

(36) Keyworth G. A. et al. Nucl. Phys. 89, 590 (1966).

where R_{WE} is the Wigner-Eisenbud R-function defining the zeroth-order energies and widths of the fine structure states and ΔL is the boundary condition difference between $R_{K.P.}$ and R_{WE}. Separating out the special state $|0\rangle$ from the fine structure ($|\mu\rangle$) states we can write the above equation as

$$\sum_{\mu} \frac{\gamma_\mu^2}{E_\mu - E} + \frac{\gamma_o^2}{E_o - E} = \frac{1}{\Delta L}.$$

The "picket-fence" approximation implies that:

$$\Sigma \frac{\gamma_\mu^2}{E_\mu - E} = \langle \gamma_\mu^2 \rangle_{av} \Sigma \frac{1}{E_\mu - E} = \pi S_b \cot \pi \frac{(E_\mu - E)}{D}$$

where $S_b = \langle \gamma_\mu^2 \rangle_{av}/D$ is the background strength function

and D = average level spacing

Hence the equation for poles reduces to

$$\frac{1}{\Delta L} - \frac{\gamma_o^2}{E_o - E} = \pi S_b \cot \pi \frac{(E_\mu - E)}{D}$$

Assuming that $P = 0$ we obtain for the energy eigenvalues E_r the formula

$$\cot \frac{\pi}{D} (E_\mu - E_r) = -\frac{\Delta}{\frac{1}{2}\Gamma^{\downarrow}} \left[\frac{E_o - E_r + \Delta}{E_o - E_r} \right] \qquad \text{(A)}$$

where Δ = shift factor

$\Gamma^{\downarrow}$ = spreading width associated with boundary condition mixing.

The (real) fine structure reduced widths may be obtained by a Taylor expansion of $R_{K.P.}$ around $E = E_r$ and we obtain

$$\frac{\theta_r^2}{D} = \frac{\dfrac{S_b (E_o - E_r)^2}{1 + Y^2}}{\left(\dfrac{E_r - E_o - \Delta}{1 + Y^2} \right)^2 + \dfrac{\Gamma^{\downarrow} D}{(1 + Y^2) 2\pi} + \dfrac{\Delta^2 Y^2}{(1 + Y^2)^2}} \qquad \text{(B)}$$

where $Y^2 = (\frac{1}{2}\Gamma^{\downarrow}/\Delta)^2$

Introducing a coupling strength parameter x defined by

$$\Gamma^{\downarrow} = 2\pi D x^2$$

we characterise the coupling strength as

(a) strong if $x^2 \approx 2$

(b) intermediate if $x^2 \approx 1$ to $1/4$

(c) weak if $x^2 \approx 1/4$ to $1/16$

With these definitions, and choosing the ratio $\Delta/\Gamma^{\downarrow}$ to be in the range –3 to –6 the energies are computed from equation (A) and for any given value of x^2. The energy eigen-values are substituted into equation (B) to give the reduced width spectrum. A comparison of the spectra thus obtained with the ^{40}A data (Keyworth et al.[36], Table I) suggested that

(a) for the $3/2^-$ state the best fit is obtained with $-\Delta/\Gamma^{\downarrow} = 3$, $\Gamma^{\downarrow}/D \approx 1$ and $x^2 \approx 1/6$,

(b) for the $1/2^+$ state the best fit is obtained with parameters $-\Delta/\Gamma^{\downarrow} = 3$, $\Gamma^{\downarrow}/D \approx 1.6$ and $x^2 \approx 1/4$.

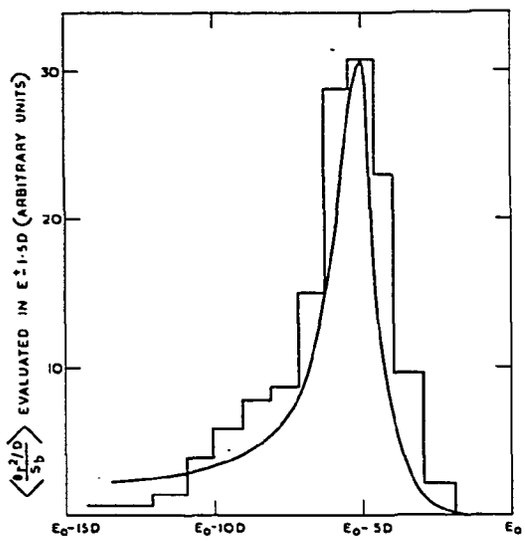

Fig. 16. Differential strength function plot for ^{40}A.

In an attempt to obtain a more accurate fit to the data for the $1/2^+$ state we constructed a differential strength function plot of the theoretical (best fit) spectrum using an averaging interval of $E \pm 1.5\,D$ (Fig. 16). The histogram thus obtained was fitted with the Robson enhancement factor

$$|f|^2 = \left|\frac{E_A - E - \Delta}{E_A - E - \frac{1}{2}i\Gamma}\right|^2 ;$$

the values of the parameters which optimise the fit are in good agreement with those used by other workers (see Keyworth et al., Fig. 13) and correspond to $D \sim 10$ keV.

We found on investigation that this formalism could be generalised to multi-channel cases and $P > 0$ in a relatively straightforward manner.

<u>Estimate of the parameters of analogue resonance theory for realistic nuclear potentials, with an analysis of the $^{207}Pb(p,p')$ reaction (A. M. Lane and S. Ramavataram)</u>

In an earlier analysis[37] of the $^{207}Pb(p,p')$ data[38] we found that calculations using the "cut-off" potential model definitions[39] for the shift (S_c) and the penetration (P_c) factors[40] and "strong absorption model" estimates for the strength function, were not in satisfactory agreement with experiment.

The analysis has now been carried out by obtaining the relevant parameters from a Saxon-Wood potential. By definition[39], S_c and P_c for open channels are given by:

$$S_c^+ = \mathrm{Re}\,(kr\, O_c^{+\prime}/O_c^+); \quad P_c^+ = \mathrm{Im}\,(kr\, O_c^{+\prime}/O_c^+)$$

where O_c^+ is the outgoing wave in channel C. We now write

$$O_c^+ = \phi_2 + i\cdot\phi_1 \xrightarrow{\text{asymp}} G_c + i\,F_c$$

---

(37) Nuclear Physics Division Progress Report AERE - PR/NP 12, p. 20 (1967).

(38) Anderson B. L., Bondorf J. P. and Madsen B. S. Phys. Letters 22, 651 (1966).

(39) Lane A. M. and Thomas R. G. Rev. Mod. Phys. 2, 257 (1958).

(40) Lane A. M. and Robson D. Comprehensive theory of nuclear reactions, Part II (to be published).

where ϕ_2, ϕ_1 are the complex, regular and irregular solutions (for a Saxon-Wood potential). The procedure for obtaining these functions is briefly described below.

Suppose that at a given energy E there are two solutions to the Schrodinger equation, ψ_1 and ψ_2. At a point (r) in the nuclear interior we write

$$\alpha\psi_1 = \phi_1\,(1 + S_1) + i\phi_2\,(1 - S_1) \xrightarrow{\text{asymp}} F_1\,(1 + S_1) + iG_1\,(1 - S_1)$$

and

$$\beta\psi_2 = \phi_1\,(1 + S_2) + i\phi_2\,(1 - S_2) \longrightarrow F_1\,(1 + S_2) + iG_1\,(1 - S_2)\,,$$

where α,β are the normalisation coefficients and S_1,S_2 are the scattering matrix elements associated with ψ_1 and ψ_2 respectively. Eliminating ϕ_2 and then ϕ_1 from the above equation we obtain:

$$\phi_1 = \frac{\alpha(1 - S_2)\psi_1}{2(S_1 - S_2)} - \frac{\beta(1 - S_1)\psi_2}{2(S_1 - S_2)}$$

and

$$\phi_2 = \frac{i\alpha(1 + S_2)\psi_1}{2(S_1 - S_2)} - \frac{i\beta(1 + S_1)\psi_2}{2(S_1 - S_2)}$$

$S_1(S_2)$ may be obtained by eliminating $\alpha(\beta)$ from the asymptotic equations for $\psi_1(\psi_2)$ at two points (r_2) and (r_3). The normalisation coefficients can then be obtained by substituting for the known quantities S, ψ, G and F at (r_2) or (r_3). A useful check on the ϕ_1 and ϕ_2 functions thus obtained is the value of the Wronskian

$$W_c^+ = (O_c' I_c - I_c' O_c)^+ = 2i \quad \text{where} \quad I_c^+ = (\phi_2 + i\phi_1)^*$$

A programme has been written for the I.B.M. 'STRETCH' computer which calculates S_c^+ and P_c^+ according to the procedure outlined above. The real and imaginary parts of the background R-matrix[37] were also evaluated by using the equation

$$\frac{1}{f_c(E) - S_c^+ - iP_c^+} = R^o_{cc}\,,$$

where $f_c(E)$ is the logarithmic derivative of the solution ψ_1.

The shift factor S_n for the $|nA\rangle$ channel[37] was calculated by a separate 'STRETCH' program which solves the bound-state problem for a Saxon-Wood potential. The normalised wave functions $U_c(a)$ obtained in this calculation provide the zeroth-order reduced widths[40] $\gamma_{\lambda c}$; we use the relations[37]:

$$\gamma_c^2 = \frac{\hbar^2}{2ma}\left[U_c(a)\right]^2 \;;\; \gamma_{\lambda c}^2 = \frac{2j_c + 1}{2T_o + 1}\,\gamma_c^2$$

A comparison of the radial dependence of the quantities $(S_c^+ - S_n)$ and P_c^+ for the Saxon-Wood and "cut-off" potential models indicates that for $R \sim 8.0$ F the latter model applied to the ^{207}Pb nucleus may cause the parameters to be underestimated by as much as 50%. Asymptotic values are reached for $R > 10.0$ Fermi. These results suggest that the usual choice of $R = r_o A^{1/3}$, where $r_o = 1.30$ to 1.45 and evaluation of parameters using the "cut-off" model would lead to inconsistencies.

The radial dependence of the total width parameter Γ and of the sum over partial widths $\Sigma_c\Gamma_c$, were also examined and the best fits to the observed values[38] were obtained for a radius of 9.50 Fermi.

(D) Experiments relating to pure Fermi beta decays and to theories of weak interactions (J. M. Freeman, D. C. Robinson, G. Murray (Manchester) and W. E. Burcham (Birmingham))

Last year it was pointed out[41] that, although the seven accurately measured ft values for pure Fermi transitions between $J=0^+$, $T=1$ isobars were reasonably consistent, there were nevertheless deviations of the order 1%, implying the existence of effects which might significantly influence the value deduced for the weak interaction vector coupling constant. Since then a number of new calculations have been made of the Fermi functions and of the radiative corrections. Blin-Stoyle and Nair[42] have calculated the Fermi functions, which involve electron radial wave functions evaluated at the nuclear radius R, by solving the Dirac radial equations with a potential corresponding to a spherical nuclear charge distribution of radius R with allowance for the screening effect of the atomic electrons. A number of other groups have independently made similar calculations[43], with general agreement to within about 0.2%. It is concluded that the f values for the heavier nuclei (mass 42 to 54) derived earlier from the Fermi function tables of Bhalla and Rose and of Dzhelepov and Zyrianova are in error by amounts increasing with Z to 1% in the case of ^{54}Co. The new ft values are represented in Fig. 17. Also incorporated in these results are the new calculations of radiative corrections made by Källén[44] for the specific case of Fermi decays.

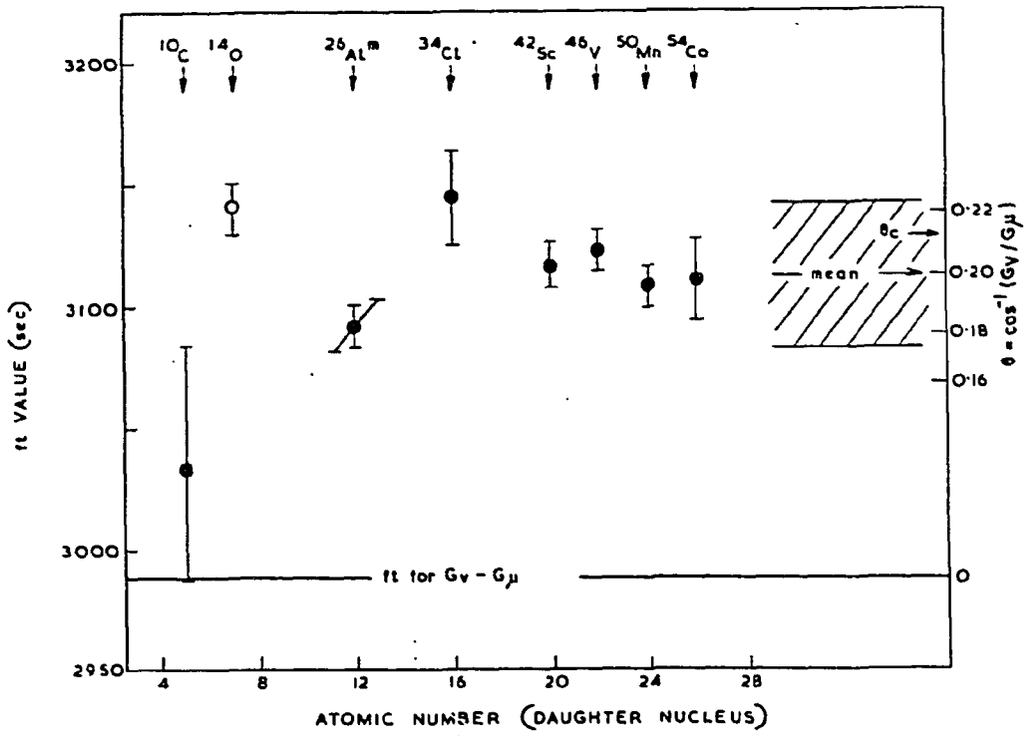

Fig. 17. ft values for pure Fermi decays.
The open circle is the ^{14}C result of Bardin et al.[27], the closed circles are Harwell results. The shaded area about the mean value represents the limits of the systematic uncertainty in the radiative correction. Θ_C represents the presently accepted position of the Cabibbo angle inferred from the rate of $K^+ \rightarrow \pi^0 e^+ \nu$ decay.

(41) Freeman J. M., Jenkin J. G., Murray G. and Burcham W. E. Phys. Rev. Letters 16, 959 (1966).

(42) Blin-Stoyle R. J. and Nair S. C. K. E.M.R. Contract No. 1662 (to be published).

(43) Suslov Yu. P. Jadernaja Fizika 4, 1187 (1966); Matese J. J. and Johnson W. R. Phys. Rev. 150, 846 (1966); Behrens H. and Bühring W. (to be published); Bhalla C. P. (to be published).

(44) Källén G. Nuclear Physics B1, 225 (1967).

The ft values for the higher Z nuclei now being somewhat lower, the result for $^{26}Al^{m}$ does not appear as anomalous as before, but the possibility of significant fluctuations remains particularly amongst the ft values for lower Z. Work is therefore continuing on the ^{14}O decay, the ^{10}C decay, and the investigation of possible charge-dependent effects on the nuclear matrix elements.

I. The Fermi decay $^{10}C(\beta^{+})^{10}B^{**}$

The branching ratio for the Fermi decay mode determined from measurements of the relative yields of 1022 and 718 keV gamma-rays following the ^{10}C decay has been reassessed, taking into account small variations in the shapes of the full energy peaks, and coincidence losses. After allowance for the upper limit deduced for a possible beta branch to the third excited state of B the branching ratio is found to be $(1.499\,^{+0.024}_{-0.026})$ per cent. Combining this value with the weighted mean value for the total half-life[45] and with the previously deduced values for the positron end-point, (888.0 ± 1.9), and applying the appropriate radiative correction (2.1%), we obtain the ft value $3079\,^{+60}_{-56}$ sec. The weighted mean of this result and our previous measurement[46] is $3033\,^{+50}_{-45}$ sec, which is lower than but not statistically inconsistent with other ft values, as illustrated in Fig. 17.

II. The decay $^{14}O(\beta^{+})^{14}N^{*}$

Our previous measurement of the β end point for this decay, made by measuring the $^{14}N(p,n)^{14}O$ threshold, was rendered somewhat unsatisfactory because of difficulties with ^{14}N targets and weak alpha calibration sources. We have now made further measurements using melamine targets. Much data remains to be analysed, but so far the results for the end point confirm our previous measurement[47] which remains some 3 keV lower than the value obtained by Bardin et al.[48].

We are now also making accurate measurements of the ^{14}O half life.

III. The decay $^{42}Sc(\beta^{+})^{42}Ca$

This decay, as described in a previous progress report[47] offers the possibility of detecting any reduction in the Fermi matrix element due to charge-dependent mixing between the second excited (0^{+}) state of ^{42}Ca (1.84 MeV) and the ground state, and between the corresponding states in ^{42}Sc.

We have used a 20 cc Ge(Li) detector to search for a 1.53 MeV gamma-ray, which would indicate the presence of a β branch to the 1.84 MeV state, and therefore, since this is a forbidden transition, the presence of some mixing between ground and 1.84 MeV states.

The 1.53 MeV gamma was not seen, and the experiments allow us to put an upper limit on the extent of the matrix element reduction arising from this mixing. Our preliminary figure for this limit is 0.15% which is of the order of magnitude of the reduction predicted theoretically[49]. A considerable improvement in the sensitivity of the experiment is desirable, but with our present system this would be rather difficult.

---

(45) Nuclear Physics Division Progress Report AERE - PR/NP 12, p. 23 (1967).

(46) Nuclear Physics Division Progress Report AERE - PR/NP 10, p. 28 (1966).

(47) Nuclear Physics Division Progress Report AERE - PR/NP 11, p. 16 (1967).

(48) Bardin R. K., Barnes C. A., Fowler W. A. and Seeger P. A. Phys. Rev. 127, 583 (1962).

(49) Blin-Stoyle R. J., Nair S. C. K. and Papageorgiou S. Proc. Phys. Soc. 85, 477 (1965).

IV. Accurate analysis of half-life data

The work described in the last progress report[47] has been continued to establish the effect of (a) number of counts, (b) varying counting times, and (c) background, on the results obtained by the usual and by our refined methods of analysis.

To facilitate the work and to make certain that rate dependent effects were not influencing the results, a computer program was written to generate "ideal" artificial decay curves which are being analysed in various ways.

(D) Nuclear spectroscopy of ^{129}Te via (d,p) reactions (B. W. Hooton, R. K. Jolly and M. K. Zaman)

Nuclear structure studies in the Te isotopes using (d,p) reactions were made by one of us[50] with ~ 40 keV energy resolution. Although almost all of the strong transitions were correctly analysed, it was obvious that many doublets and even multiplets had not been resolved and that possibly several of the weak transitions had been completely missed. It was, therefore, considered advisable to repeat some of the previous measurements with an improved energy resolution. Some of these measurements on ^{122}Te and ^{124}Te have been previously reported[51].

An experiment involving detailed angular distribution measurements (from 5° to 145° in 5° and 7.5° steps) of protons produced in ^{128}Te (d,p) by 13 MeV deuterons from the tandem Van de Graaff accelerator has been started. The data will be accurately normalised in a separate measurement and the cross sections analysed with distorted wave Born approximation calculations. A proposed study of some of the ^{128}Te(d,p)^{129}Te energy spectra using the extremely good resolution (3-7 keV) of the Enge split pole spectrograph at Pittsburgh should determine whether our energy resolution, (10 → 15 keV), is adequate.

Spin of the 1.52 MeV state in ^{55}Cr (R. K. Jolly, F. R. Maxson, G. C. Neilson and G. A. Jones)

Following up our earlier work[52] we have carried out further polarisation measurements with the reaction ^{54}Cr(p,p$_0$)^{54}Cr. A strong resonance which appears at E_p = 3.58 MeV in excitation functions measured at θ_{Lab} = 125° and 150° is the analogue of the 1.52 MeV state in ^{55}Cr. This state is known[53,54] to arise from a strong l = 1 transition in the reaction ^{54}Cr(d,p)^{55}Cr. Since the ground state of ^{55}Cr is known[55] to be $p_{3/2}$ and there are two other p states[53] within 600 keV of the ground state shell model considerations lead one to expect that the 1.52 MeV state will be $p_{1/2}$.

In Fig. 18 our polarisation results are compared with the theoretical curves of Adams et al.[56]. Although there is some uncertainty in the zero for the experimental polarisations the results clearly show that the state has $J^{\pi} = 1/2^{-}$, and support the same assignment for the isobaric analogue at 1.52 MeV in ^{55}Cr.

(D) Quadrupole and octupole excitations in Ti, Cr, Fe and Ge isotopes (R. K. Jolly)

A programme of systematic studies on the one phonon states of even-even spherical nuclei has been started[57] using position sensitive detectors in the focal plane of a Buechner spectrograph.

---

(50) Jolly, R. K. Phys. Rev. 136, B683 (1964).

(51) Nuclear Physics Division Progress Report AERE - PR/NP 11, p. 17 (1967).

(52) Nuclear Physics Division Progress Report AERE - PR/NP 12 (1967).

(53) Bochin V. P., Zherebtsova K. I., Zolotarev V. S., Komorov V. A., Krasnov L. V., Litvin V. F., Nemilov Yu A., Novatsky B. G. and Piskorzh Sh. Nuclear Physics 51, 161 (1964).

(54) Bjerregaard J. H., Dahl P. F., Hansen O. and Sidenium G. Nuclear Physics 51, 641 (1964).

(55) Nuclear Data Sheets, National Academy of Sciences, Washington.

(56) Adams J. L., Thompson W. J. and Robson D. Nuclear Physics 89, 377 (1966).

(57) Jolly R. K., Goldberg M. D. and Sengupta A. K. (to be published).

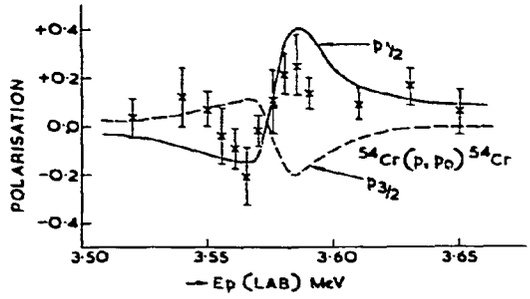

Fig. 18. Polarisation excitation function for $^{54}Cr(p,p_0)\,^{54}Cr$ at a laboratory angle of 150°. The theoretical curves shown assume a total width ~20 keV.

The one phonon quadrupole and octupole states were excited via direct interaction inelastic scattering of 11.8 MeV deuterons from the Tandem Generator. It was demonstrated that accurate measurement of differential cross sections subsequently analysed with careful, zero range, distorted wave Born approximation calculations for a deformable potential, using complex coupling and including the effects of Coulomb excitation, would yield very reliable values of B(E2; 0 → 2) and B(E3; 0 → 3). The present studies form the second series of measurements in this programme. Preliminary work on the inelastic deuteron spectra from the nuclei $^{46,48,50}Ti$, $^{50,52,54}Cr$, ^{56}Fe and $^{72,74}Ge$ is underway. It is planned to measure detailed differential cross sections for the collective 2^+ and 3^- states in these nuclei. The elastic scattering cross sections in Ge and some other cases may also be measured if necessary to provide optical model parameters for DWBA calculations.

(C) Nuclear lifetimes by the doppler shift attenuation method (W. M. Currie, L. G. Earwaker and J. Martin)

We have further improved the twin target doppler shift technique described earlier[58] by making use of a Ge(Li) detector. Most of the early doppler shift measurements made in other laboratories with Ge(Li) detectors have suffered from the fact that the detectors were quite small, so that coincidence measurements could not readily be carried out. The consequences were that (1) either the reaction had to be used near threshold so as to limit the direction of recoil, or assumptions had to be made about the distribution of reaction products, and (2) that the beam energies had in any case to be kept low to avoid population of the state under observation by cascade γ-ray transitions. In view of these limitations the measurements had in general to be made under the worst possible conditions (i.e. with low and partially undefined recoil velocities) so that the slowing down and scattering of heavy ions are not well known. This may explain why two independent studies[59,60] of levels in ^{30}Si yielded lifetimes for the first excited state which differ by a factor of almost 2.

Till now we have been using coincidence techniques in conjunction with a NaI(Tl) detector, an approach which can reduce these systematic errors but which, because of the much inferior energy resolution, increases the statistical errors. With the advent of larger Ge(Li) detectors, coincidence measurements with these devices have become feasible and thus a number of the earlier drawbacks can be partially overcome, while at the same time the improvement in energy resolution makes possible the detailed observation of line shapes. In this situation the measurement of lifetimes by the Doppler shift technique no longer requires an act of faith. On the Van de Graaff we have been using a coaxial 50 cc detector with a specified resolution of 3.4 keV (F.W.H.M.) for 1 MeV γ-rays. Under experimental conditions beam instabilities caused the γ-ray count rate to fluctuate violently, so that the observed resolution over long runs was degraded even with spectrum stabilisation, and ranged in one case, with 22 MeV gamma rays, from 4 keV to 7 keV, depending on conditions, while the overall time resolution for proton-gamma coincidences varied from 7 to 14 ns F.W.H.M. using pulse height compensation.

With this Ge(Li) detector we have repeated measurements on the first and second excited states of ^{30}Si, ^{31}P and ^{33}P, which were originally performed with NaI(Tl). Through the use of varied backing

(58) Nuclear Physics Division Progress Report AERE - NP 12, p. 29 (1967).

(59) Broude C., Smulders P. J. M. and Alexander T. K. Nuc. Phys. A90, 321 (1967).

(60) Lieb, K. P., Grawe H. and Ropke H. Nuc. Phys. A98, 145 (1967).

materials, chosen to give a range of slowing down times and mass numbers, we hope to reduce the remaining systematic errors and so to extract accurate lifetimes. For the present measurements the geometry was essentially the same as that described in the earlier progress reports.

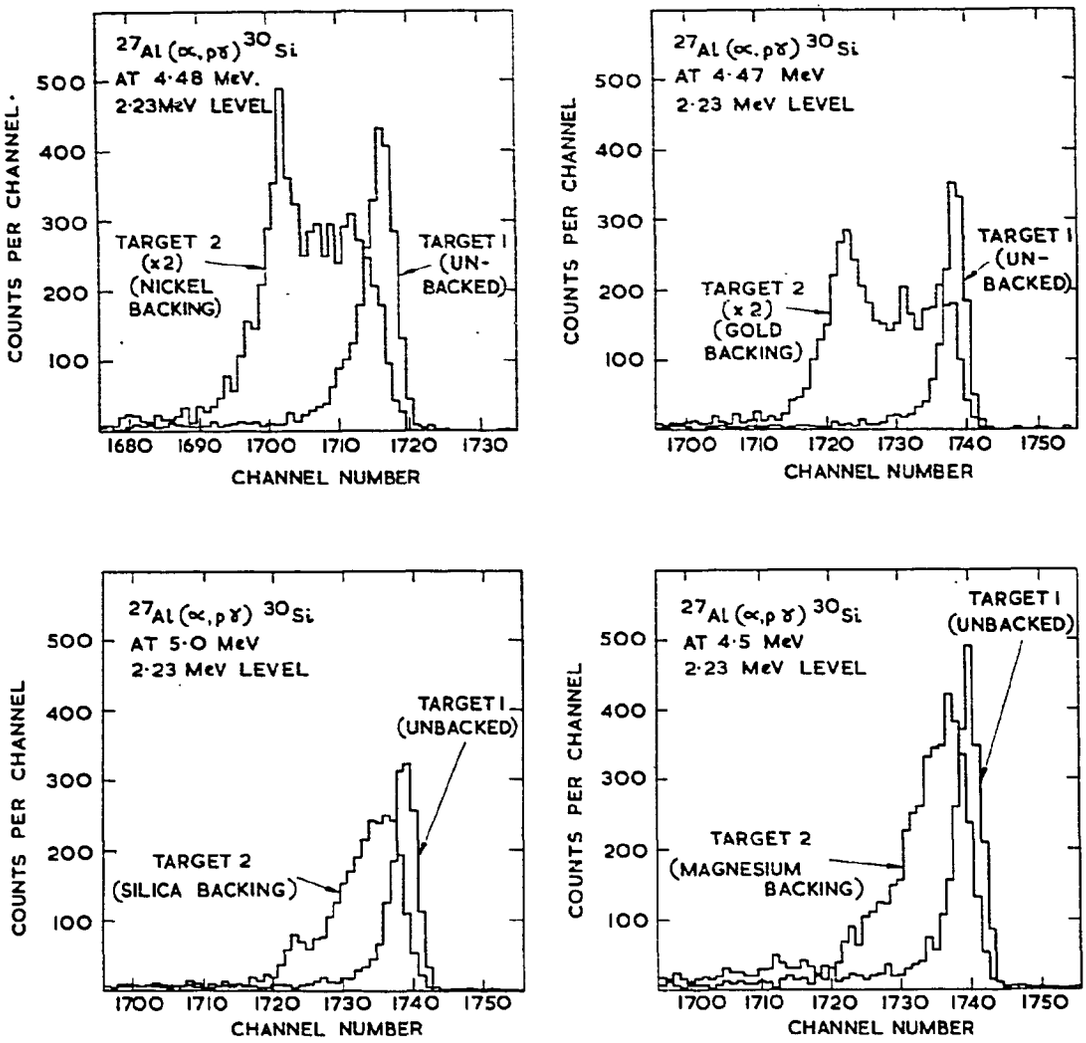

Fig. 19. Photopeak line shapes for coincidence γ-rays detected simultaneously from two targets. Those from target 1 have suffered a full Doppler shift, determined by reaction kinematics alone, while in the case of target 2 the shift has been attenuated by backing material in which the radiating nuclei were slowing down.

Fig. 19 shows some line shapes for the first excited state of ^{30}Si obtained by the $^{27}Al(\alpha,p)^{30}Si$ reaction induced by a singly charged beam with an energy of about 4.5 MeV. Similar line shapes obtained with a doubly charged 7 MeV beam are shown in Fig. 20. No detailed analysis of these curves has yet been made, but if approximate slowing down times of 3.3, 3.7, 7.0, 8.0 and 10.0×10^{-13} sec are assumed for Ni, Au, Sn, SiO_2 and Mg respectively then it can be seen by inspection (cf. Fig. 35 in ref. 61 and Fig. 13 in ref. 62) that the line shapes are all consistent with a lifetime lying somewhere between the values 2.6 and 4.6×10^{-13} sec[59,60]. Furthermore the detailed analysis of these line

(61) Litherland A. E. in "Nuclear Structure and Electromagnetic Interactions", Oliver and Boyd (1965).

(62) Warburton E. K. Available as BNL11484.

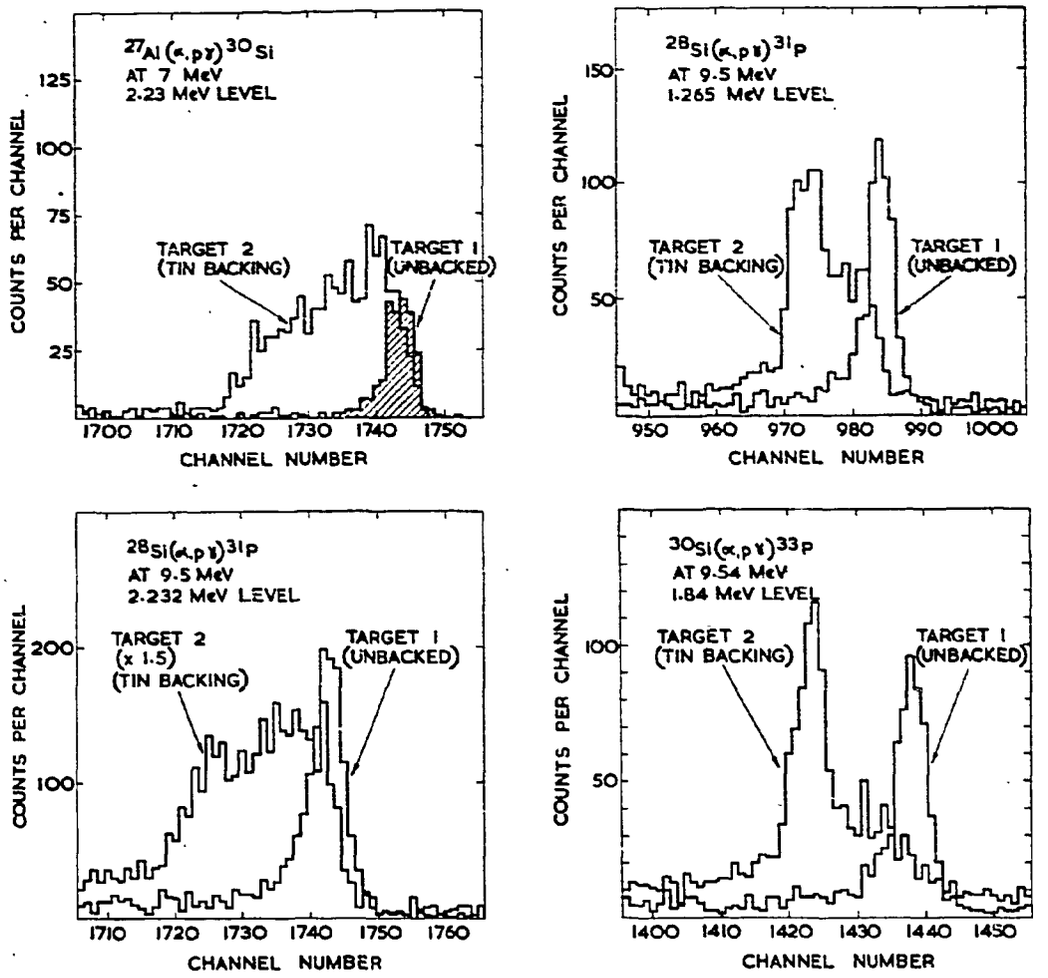

Fig. 20. Photopeak line shapes for coincidence γ-rays detected simultaneously from two targets. Those from target 1 have suffered a full Doppler shift, determined by reaction kinematics alone, while in the case of target 2 the shift has been attenuated by backing material in which the radiating nuclei were slowing down.

shapes should provide quantitative information on the importance of nuclear (as opposed to electronic) scattering and on the accuracy of our calculated corrections, based on the paper of Blaugrund[63].

Fig. 20 shows some results for levels in ^{31}P and ^{33}P obtained under difficult machine conditions and with high γ-ray count rates. The resolution is poorer and the backgrounds are higher, but with the large ratio of (full shift/resolution) it should be possible to give a fairly detailed interpretation of the line shapes.

(G) Location and characterisations of isomeric states in the region Z=63→83 (T. W. Conlon)

A search for isomeric states with half-lives in the range 10^{-4} to about 10^{-1} seconds occurring in nuclei in the region Z=62→83 has been started on the V.E.C.

---

(63) Blaugrund A. E. Nucl. Phys. 88, 501 (1966).

The energies of the gamma rays depopulating isomeric states are measured using a Ge(Li) detector. The energies and times of arrival of photons following bombardment of the target by a pulsed beam are measured simultaneously by a 4096 pulse height analyser operating in a two-dimensional mode. From the spectra thus produced the Z of the final nucleus, α_k for the delayed transition, the precise energies and relative intensities of the isomeric and cascade photons and the transition probability for decay of the long-lived state by E-M processes can be obtained directly.

One expects to reach isomeric states principally by the (p,Xn) and (p,pYn) reactions, where for 50 MeV protons incident on rare earth targets X and Y are typically 7 and 6. At first sight one might expect the excitation of new isomeric states to be unlikely, but in fact a recent survey[64,65] at a much lower proton energy, where only the (p,n) and (p,pn) reactions were energetically possible, revealed some twenty-three isomeric states, six of which had not been previously observed. In that survey considerable insight into the operation of the K-selection rule of the Unified Model and the selection rules on the asymptotic quantum number of the Nilsson scheme was obtained, together with a large amount of spectroscopic information. Since a much wider range of final nuclei can be reached at V.E.C. energies one may expect that the number of such transitions observed and the amount of information extracted will be correspondingly increased.

A pulsed beam system suitable for this work is under development. At the time of writing the filament ion source of the V.E.C. can be pulsed. The pulser can be triggered externally and a pulsed beam has been obtained with "beam off" intervals of from 500 μs up to 100 ms and an average residual beam of $< 1 \times 10^{-7}$ of the "beam on" intensity.

The isomer search programme is now in progress using the beam line and scattering chamber system described by B. W. Ridley[66].

(F) Nuclear structure of the tin isotopes (P. E. Cavanagh, C. F. Coleman, A. G. Hardacre and J. F. Turner)

I. Determination of occupation numbers from quasiparticle energies (C. F. Coleman)

Baranger[67] has discussed the application of a pairing model analysis to residual interactions of a rather general form. He denotes the 'j' values of the active configurations by the symbols j_a, the appropriate single particle energies in a nucleus of neutron number N by $\epsilon_a(N)$ and the gap parameters by $\Delta_a(N)$ (for the simple pairing model these are the same for all configurations), and finds that he has also to introduce a self binding energy $\mu_a(N)$ which is zero for the simple pairing model, but for more general interactions increases monotonically with N. He defines the quantities

$$\eta_a(N) \equiv \epsilon_a(N) - \mu_a(N) - \lambda(N)$$

and obtains the equations

$$E_a(N) = \sqrt{\eta_a(N)^2 + \Delta_a(N)^2} \quad \text{(A)}$$

$$V_a^2(N) = \tfrac{1}{2}(1 + \eta_a(N)/E_a(N)) \quad \text{(B)}$$

$$= \tfrac{1}{2}(1 \pm \sqrt{1 - \Delta_a(N)^2/E_a(N)^2}) \quad \text{(C)}$$

In the past attempts to extract the occupation numbers $V_a^2(N)$ from the experimental quasiparticle energies $E_a(N)$ have been based on the use of equation (C) with the simple pairing model. However there

(64) Conlon T. W. Nucl. Phys. A100, p. 545 (1967).

(65) Conlon T. W., Naumann R. A. and McCarthy A. L. Nucl. Phys. A104, p. 213 (1967).

(66) Nuclear Physics Division Progress Report AERE PR/NP 12, p. 31 (1967).

(67) Baranger M. Phys. Rev. 120, 957 (1960).

is no satisfactory experimental method for fixing the $\Delta_a(N)$, and the values of $V_a^2(N)$ computed from this equation are critically dependent on the difference $E_a - \Delta_a$ when this quantity is small, a condition which arises when the configuration is about half full. These facts combined with the sign ambiguity have made it very difficult to form a clear impression of the way in which the $V_a^2(N)$ increase with N, and this increase is most rapid just when $V_a^2(N) \sim ½$, in fact, in the archetype of the pairing model situation. Unfortunately in this situation occupation numbers obtained by comparing the experimental pickup cross sections with DWBA calculations are also unreliable, since here the transferred nucleon is certainly not well described by a single shell model eigenfunction.

We have therefore attempted for each particular configuration to make use of the complete set of values of $E_a(N)$ simultaneously. Each quasiparticle energy was taken as the mean of the excitation energies of all the levels belonging to the given configuration, weighted by the corresponding pickup cross sections, and the corresponding quasiparticle vacuum energy was taken as the mean of the ground state binding energies for the neighbouring even isotopes. Starting values of the gap parameters $\Delta_a(N)$ were taken from the theoretical calculations of Arvieu[68], and were substituted with the $E_a(N)$ into equations (A), which were then solved for the $\eta_a(N)$. The $\Delta_a(N)$ were then adjusted empirically for each configuration until the calculated $\eta_a(N)$ became as nearly as possible linear functions of N. Quadratic curves were then fitted to these $\eta_a(N)$ and smoothed values read off the curves along with the adjusted values of the $\Delta_a(N)$ were substituted into equation (B) to determine the $V_a^2(N)$, a procedure which was repeated several times to optimise the fit to the mass condition $\sum_a (2j_a+1)V_a^2(N) = N-50$. The values of $\eta_a(N)$ and $V_a^2(N)$ so determined are shown in Figs. 21 and 22, together with theoretical occupation

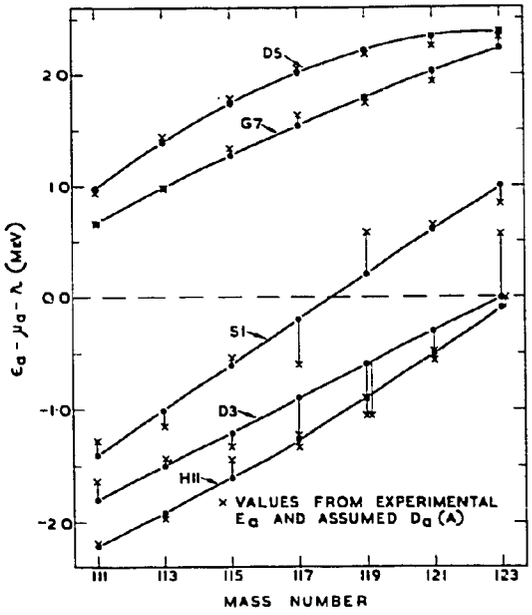

Fig. 21. Values of the quantities e_a-μ_a-λ extracted from the mass dependence of the experimental quasi-particle energies for the odd tin isotopes.

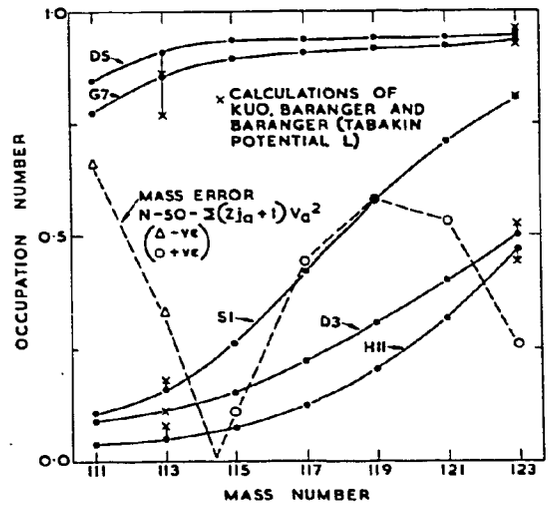

Fig. 22. Values of the occupation numbers V_a^2 (A) determined from the experimental quasi-particle energies for the odd tin isotopes.

(68) Arvieu R. Paris thesis (1963).

numbers calculated by Kuo et al.[69] for ^{113}Sn and ^{123}Sn, and the agreement is quite good. Values of $E_a(N)$ calculated from the smoothed $\eta_a(N)$ and the adjusted $\Delta_a(N)$ agree with the experimental values within an R.M.S. error of 50 keV, the fit for the $d_{3/2}$ configuration being much the worst and the fit for the $s_{1/2}$ configuration only moderately satisfactory. The error in N varies systematically between the limits ± 0.6. Since the $\Delta_a(N)$ are specifically chosen to give satisfactory interpolation through the neighbourhood of $V^2 \sim 1/2$, while when $V^2 \sim 0$ or 1 it is relatively insensitive to the exact value of the corresponding gap parameter, the values of the $V_a^2(N)$ obtained in this way should be fairly reliable, especially since they are also subject to the mass condition. Comparison of these results with the occupation numbers obtained by taking the ratios of the experimental pickup cross sections to those obtained from DWBA calculations indicates that the theoretical cross sections are too low by a factor ~ 2 when $V_a^2(N) \lesssim 1/2$, a condition under which the pairing interaction must seriously distort the wave-function of the transferred neutron.

II. DWBA analysis of (p,d) angular distributions (P. E. Cavanagh)

This work is now complete and is being prepared for publication.

III. Analysis of (p,t) and (p,p′) measurements (C. F. Coleman)

All the tin results to date were read out from the analyser onto five hole punched paper tape. The The earlier (p,d) results were subsequently converted to punched card form on the Atlas Laboratory Atlas computer, and further manipulation was carried on STRETCH using the card input. For the (p,p′) and (p,t) measurements programs were written so that the date on the punched paper tape could be read through the PDP8 computer in B 8.9 and transferred on magnetic tape to STRETCH, where it would subsequently be read onto a binary magnetic tape data store. This transfer has proved extremely slow, apparently because of faults in the paper tape reader, but normalised printouts and machine plotted graphs are now available for all the (p,t) measurements, and analysis is proceeding. The difference between the line widths for odd and even mass targets[70] has been traced to very small scale irregularities in the thickness of the particular odd targets used[71], which were much less pronounced in the even targets.

IV. Measurements with 30 MeV polarised protons (P. E. Cavanagh, C. F. Coleman, A. G. Hardacre and J. F. Turner)

An attempt was made to measure the polarisation sensitivity of elastic scattering for 30 MeV protons incident on targets of some of the even tin isotopes, using a spark chamber to determine the angle of scattering over the range 35° to 105°, backed by three pyramidal NE102 scintillation counters, each covering a range of 23°, to determine the energy of the scattered particles. The polarisation state was switched automatically at intervals of about two minutes, and the two dimensional output data plus an additional bit to indicate the polarisation state were recorded on a ¼" four track 18 bit block digital tape recorder. The spark chamber worked excellently, but the resolution of the detectors was disappointing, with the octupole states of the even isotopes barely resolved, and considerable trouble was experienced with the recorder, possibly associated with the rather high rates obtained with the very large solid angle defined by the spark chamber. Despite these difficulties it was evident that the technique is potentially very powerful, since systematic differences between the 'up' and 'down' angular spectra were clearly visible after running for only a few minutes.

The beam emerging from the scattering target was transported to the N 1/2 spectrometer, which was set up to observe deuterons from the reaction $^{118}Sn(p,d)^{117}Sn$. The resolution in this experiment was somewhat marginal for the purpose, being limited by the energy spread of the output beam from the

---

(69) Kuo T. T. S., Baranger E. and Baranger M. Nuclear Physics 81, 241 (1966).

(70) Cavanagh P. E. and Coleman C. F. Nuclear Physics Division Progress Report AERE - PR/NP 12, p. 32 (1967).

(71) Turner J. F. Private communication (1967).

P.L.A., since any attempt to reduce this spread by magnetic analysis would have produced prohibitive loss in intensity. Trouble with the coupled switching of the polarisation state and the analyser sectors vitiated some of the results, but the main 'd' line clearly showed a substantial (~ 20%) polarisation sensitivity at the peak of the angular distribution.

(G) Energy dependence of the elastic scattering of ^{3}He and ^{4}He from ^{40}Ca and ^{58}Ni (T. H. Braid*, T. E. Conlon and B. W. Ridley)

A systematic investigation of the elastic scattering from ^{40}Ca and ^{58}Ni of ^{3}He and ^{4}He has been carried out on the V.E.C., using ^{4}He beams with energies of 52.3, 58.9, 67.7 and 85.6 MeV, and ^{3}He beams of 51.4, 73.2 and 83.5 MeV. Monitor counters at ± 14° to the beam line were used to correct for the effects of beam wandering on a non-uniform target, and for changes in the mean direction of the beam, and a mass gate was employed for the ^{3}He measurements. The results, together with data obtained elsewhere at lower energies, are being analysed by an optical model program using a uniform geometry with real potential well depths of the order of 180 MeV in an attempt to determine the energy dependence of the non-geometric parameters. Figs. 23 and 24 show some of the ^{3}He data with the optical model fits, while Fig. 25 (overleaf) shows preliminary results for the energy variation of the main optical model parameters.

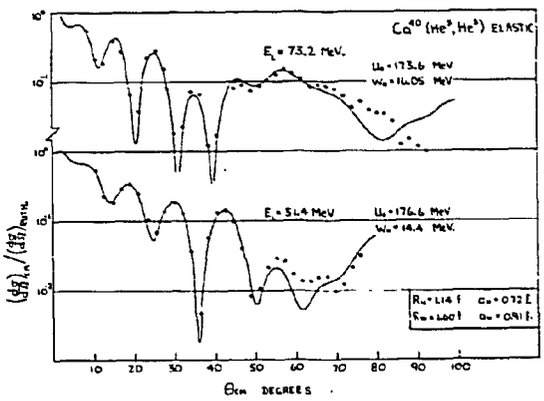

Fig. 23. Angular distribution of ^{3}He ions elastically scattered from ^{40}Ca at energies of 51.4 and 73.2 MeV, with optical model fits.

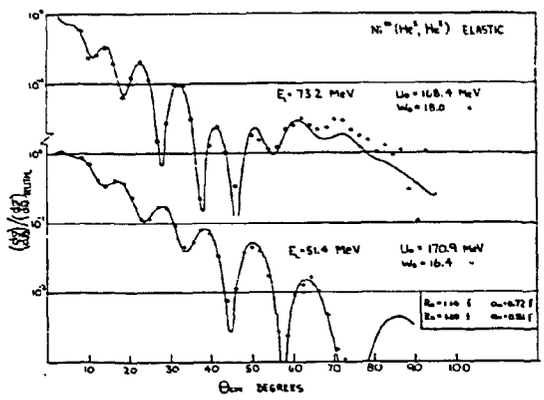

Fig. 24. Elastic scattering of ^{3}He ions from ^{58}Ni.

(H) Total cross section of aligned holmium nuclei (H. Marshak (N.B.S. Washington) and A. Langsford)

The holmium nucleus is a highly deformed prolate spheroid which can be aligned by the application of a high magnetic field at a sufficiently low temperature. The purpose of the present experiment was to measure the change in neutron total cross section over the energy range 2 to 120 MeV when previously unaligned holmium nuclei were aligned with their major axis lying in the direction of the neutron beam. A ^{3}He cryostat and superconducting magnet was made for this purpose at the National Bureau of Standards and then transported to Harwell. Two runs were made, during which a temperature of 0.32°K was obtained and measurements were made in magnetic fields of up to 55 kOe.

Fig. 26 (see page 31) shows results in which the temperature averaged 0.38°K and the magnetic field was 50 KOe. The degree of nuclear alignment under these conditions is approximately 0.27. More accurate values of the alignment parameters are at present being evaluated for all the data. Earlier

*On attachment from the Argonne National Laboratory, U.S.A.

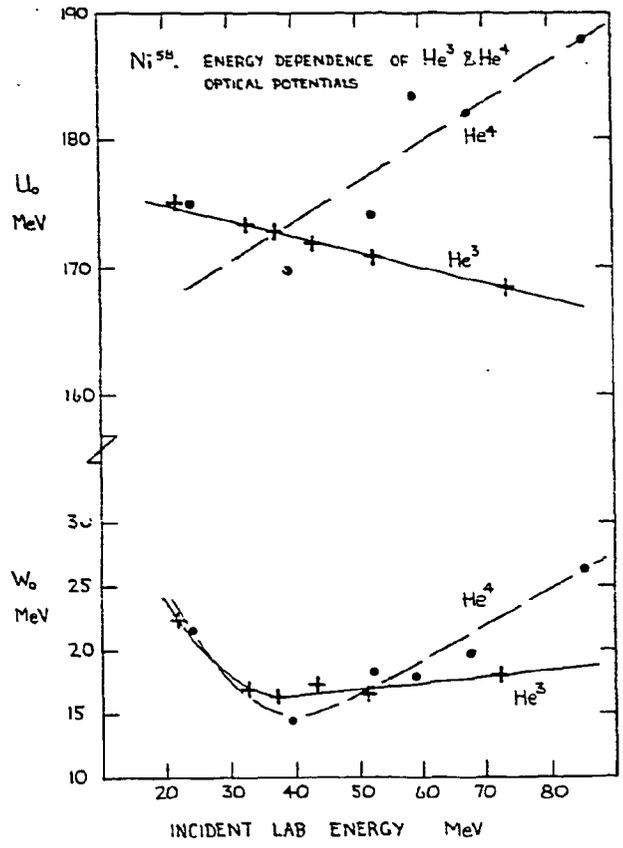

Fig. 25. Variation with incident energy of parameters for 'fixed geometry' optical model fits to elastic scattering of ^3He and ^4He ions from ^{58}Ni.

measurements by Marshak[72] and by Shelley[73] at Stanford are also shown, normalised to the degree of nuclear alignment achieved in the present experiment.

The most noticeable feature of the curve is the pronounced oscillations in the cross section difference as a function of neutron energy. If the holmium nucleus were opaque the cross sectional area presented by the aligned nuclei to the neutron beam would be less than that for unaligned nuclei.

The variations in the cross section difference with energy are due to the varying interference between the neutron wave passing through the nucleus and that going around it. Since the path length through the nucleus is greater when it is aligned the maxima and minima in the total cross section curve under this condition appear at slightly higher momenta. The energy dependence of the difference between these two cross sections yields the observed effect. The solid curve in Fig. 26 is the result of an elementary optical model calculation with an approximate treatment of the absorption of the neutron wave. This approximation may account for the poor agreement between calculated and measured cross section differences above 40 MeV. However at lower energies the model describes both the positions and magnitudes of the maxima and minima in cross section difference so well that one feels that this simple description of the interaction contains the essential physics, and that good agreement between model and experiment can be obtained from a full optical model treatment. Optical model calculations are at present being carried out at Oak Ridge under the direction of Tamura.

To check the model of the holmium crystal structure used to calculate the nuclear alignment, cross section differences were also measured as a function of the specimen temperature, but the results of these measurements have still to be analysed.

(H) Cross section and polarization in p-p scattering at 98 MeV (M. R. Wigan (Oxford), P. Martin (Grenoble), R. Bell (Oxford), O. N. Jarvis, J. P. Scanlon)

This experiment has now been completed and is being prepared for publication. The final values of the polarization measurements are shown in Fig. 27, together with various phase-shift analysis predictions. There is an overall uncertainty of ± 0.85% in the absolute normalization of the data, due to the uncertainty in the beam polarization[74]. The results for the cross section measurements are shown in Fig. 28, together with the prediction as before. The absolute normalization error is about ± 1%. An interesting feature of the cross section results is that the integrated cross section (from 12° to 90° cm.)

---

(72) Marshak H., Richardson A. C. B. and Tamura T. Phys. Rev. Lett. 16, 194 (1966).

(73) Shelley E. G. et al. Phys. Lett. 19, 684 (1966).

(74) Jarvis O. N., Rose B. and Scanlon J. P. Nuc. Phys. 77, 161 (1966).

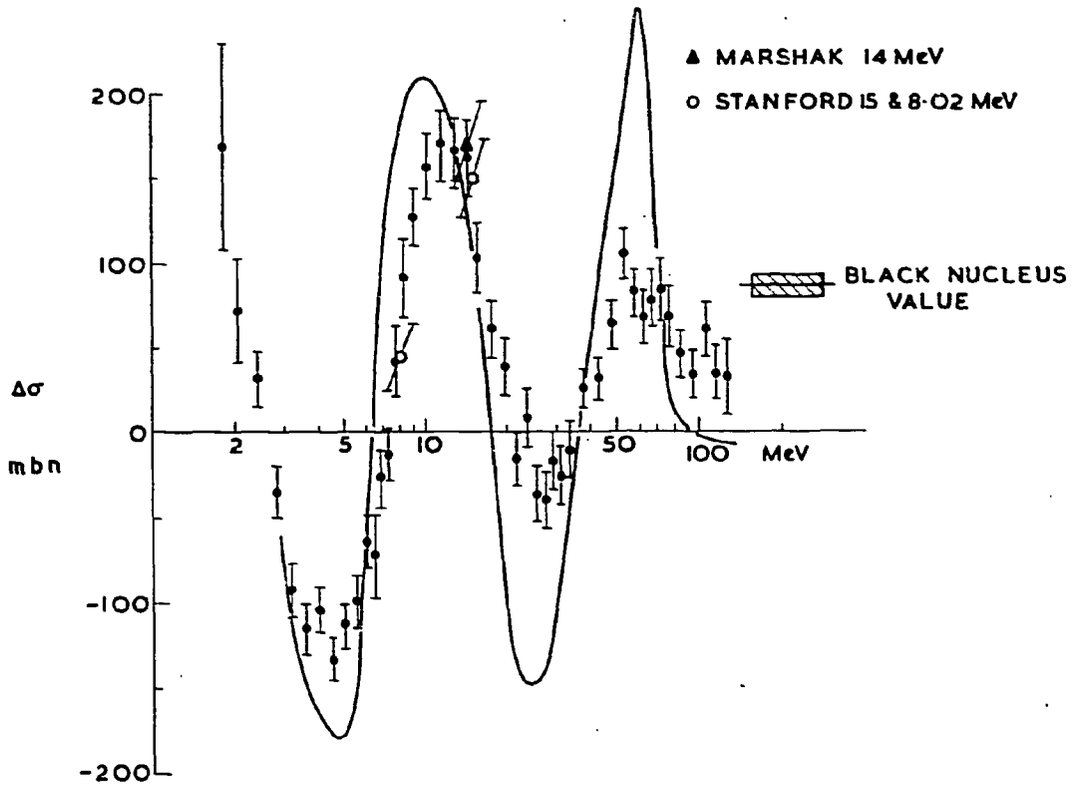

Fig. 26. Energy dependence of difference between the total neutron cross sections for aligned and unaligned holmium nuclei.

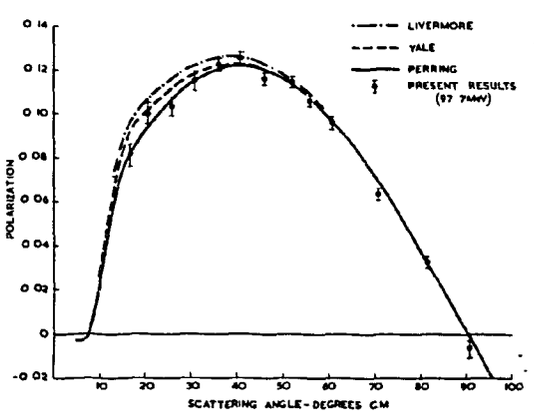

Fig. 27. Polarization in p-p scattering near 98 MeV.

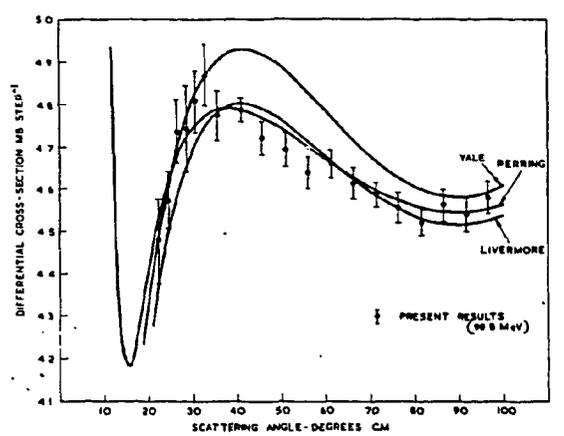

Fig. 28. Differential cross section for p-p scattering near 98 MeV.

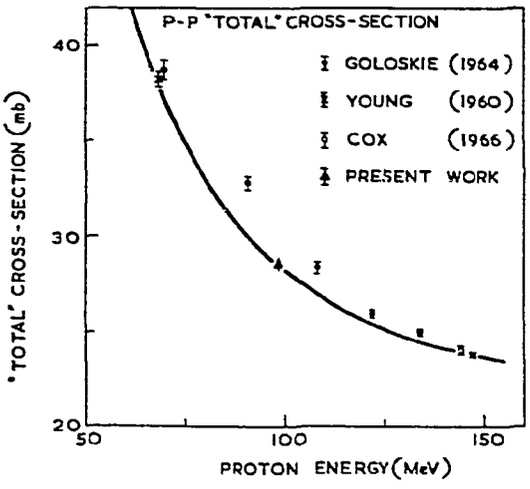

Fig. 29. Predicted (full line) and experimental p-p total cross sections.

is about 8% below the value obtained by Goloskie and Palmieri[75] in a direct measurement with a quoted accuracy of ± 1%. This disagreement is the more interesting in that Goloskie and Palmieri also determined the total cross sections to ~ 1% near 68 MeV and 140 MeV, and obtained results in excellent agreement with the integrated differential measurements of Young and Johnston[76] and of Cox et al.[77] respectively. These data are shown in Fig. 29, in which the solid curve is the prediction for the variation of the "total" cross section obtained from the recent multi-energy phase-shift analysis of MacGregor et al.[78].

(H) Asymmetry in charged particle production for 100 MeV polarized neutrons (A. Langsford with J. G. McEwan, G. C. H. Sharman and R. F. George (Southampton University) and T. G. Walker (R.H.E.L., Chilton))

In order to see whether carbon or aluminium spark chamber plates would be suitable as their own analysers of neutron polarization, targets of these materials were bombarded by the polarized neutron beam[79] from the synchrocyclotron. The asymmetry in the charged particles so produced was measured using an array of counters and spark chambers, which gave information on the direction of the outgoing charged particles, their range and specific ionization. Targets of polyethylene and heavy water were also used in order to calibrate the spark chamber system over a range of energies and angles with both protons and deuterons.

The spark chambers were viewed by a television camera. The video signal was digitised and processed on-line by a PDP8 computer which monitored the quality of the data. Spark co-ordinates were recorded on magnetic tape for subsequent processing, and in all 112,000 events were obtained in 56 hours of useful data taking. By placing a neutron counter of known efficiency in the beam absolute production cross section were measured as a function of neutron energy. The proton energy resolution was about 10 MeV over the 50 to 120 MeV energy range of the experiment. The data is at present being analysed.

(I) Studies of π p inelastic interactions between 3.1 and 3.6 Gev/c (C. Whitehead in collaboration with Southampton University, University College, London and the Rutherford Laboratory)

Analysis has continued and the data were presented at the Heidelberg International Conferance on Elementary Particles.

In addition to the f^0 enhancement, which is found at 1270 ± 15 MeV/c^2 with a width of 160 ± 20 MeV/c^2, a 3.5 standard deviation effect of a narrow enhancement at 1085 MeV/c^2 is found. We have considered the possibilities that this enhancement results from biases in our experimental configuration, or fortuitously, from ambiguous events, and we are confident that the effect cannot be ascribed to these causes. A search of the literature revealed other experiments[80,81,82] in which a slight enhancement at this mass is seen. Individually these effects are barely significant, but a combined mass plot shows a

(75) Goloskie R. and Palmieri J. N. Nuc. Phys. 55, 463 (1964).

(76) Young D. E. and Johnston L. H. Phys. Rev. 119, 313 (1960).

(77) Cox G. F., Eaton G. H., Van Zyl C. P., Jarvis O. N. and Rose B. AERE - R 5585.

(78) MacGregor M. H., Arndt R. A. and Wright R. M. UCRL - 70075.

(79) Bowen P. H. et al. Nuc. Instr. and Methods 15, 31 (1962).

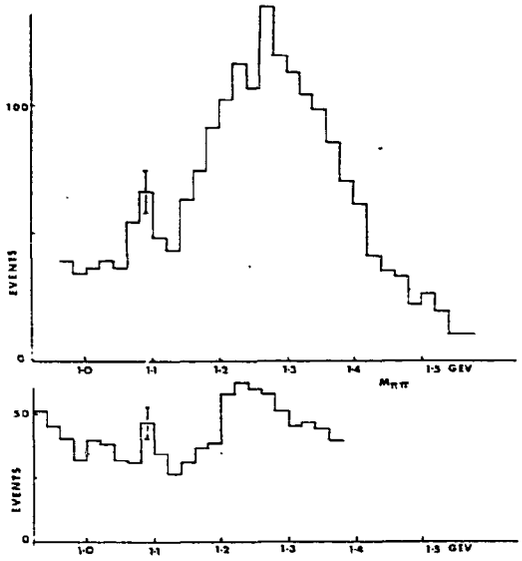

three standard deviation peak at approximately 1090 MeV/c^2. In Fig. 30 the upper histogram shows the data from the present experiment, and the lower histogram the summed data from references 80, 81 and 82.

At the Heidelberg Conf[illegible] was suggested that the peak we observe is [illegible] the $\pi\pi$ decay mode of the S* resonance[8[illegible]] [illegible] so far only in the K_1K_1 decay mode. However, there exists considerable discrepancy in the widths (Γ(1085) < 25 MeV/c^2; 100 MeV/c^2 < Γ(S*) < 170 MeV/c^2) which could possible be explained by threshold effects in the S* → K_1K_1 mode, although the estimates given by Beusch et al.[84] have already had a mass dependent width in their analysis of the S*.

Fig. 30. Upper histogram shows the missing mass distribution for the reaction $\pi^- + p \to n + \pi^+ + \pi^-$ for momenta from 3.1 Gev/c to 3.6 Gev/c showing a 3.5 standard deviation enhancement at 1085 ± 10 MeV/c^2 in addition to the 1270 ± 15 MeV/c^2 f^0 enhancement with width 160 ± 20 MeV/c^2. The lower histogram is the summed data from freferences 75, 76 and 77.

The S* has been described as $J^P = 0^+$, I = 0[83]. Analyses of our data and comparisons with the data of references 80, 81 and 82 are consistent with I = 0 for this $\pi\pi$ enhancement, although there is only a 90% confidence level against the assignment I = 1. I = 2 is strongly ruled out. Our angular distribution in the region of 1090 MeV/c^2 is adequately fitted by S and D waves, P wave interference effects not being required, thus indicating an even spin assignment, which in turn supports the assignment I = 0. However, as long as the width of the resonance is not much less than our upper limit of 25 MeV/c^2, detailed cross section arguments together with the assumption of peripheral production and of the validity of the OPE Born term model show that the present data, though they do not favour spin zero, do not strongly conflict with this assignment. On balance we believe at present that the evidence indicates that the 1085 MeV peak is not the $\pi\pi$ decay mode of the S*. A paper is being prepared for publication.

The angular distribution of events in the mass range 1200-1300 MeV/c^2 has been analysed by fitting to the equation

$$W(\cos\theta^*) = \rho_{0,0}\left(Y_2^0\right)^2 + 2\rho_{1,1}\left(Y_2^1\right)^2 + 2\rho_{2,2}\left(Y_2^2\right)^2$$

where the ρ's are the density matrix elements and are further related through the condition that their trace must be unity.

Table II (overleaf) gives in column 1 the values of the density matrix elements obtained in this experiment, in column 2 the results of the Aachen-Berlin-Cern[85] collaboration, in columns 3 and 4 the results of the Aachen-Berlin-Cern collaboration analysis of the data of Lee et al.[80] and of the Aachen-Birmingham-Bonn-Hamburg-London I.C.-Munich collaboration experiment respectively, and in column 5 our estimate of the density matrix elements from the data of de Rosny and Fleming[86]. In all cases the

(80) Lee Y. Y. et al. P.R.L. 12, 341 (1964).

(81) Bonder L. et al. Phys. Lett. 5, 153 (1963).

(82) Hagopia V. and Selove W. P.R.L. 10, 533 (1963).

(83) Crennell D. J. et al. P.R.L. 16, 1025 (1966).

(84) Beusch W. et al. Private communication, to be published.

(85) Aachen-Berlin-Cern collaboration. Phys. Lett. 22, 533 (1966).

(86) de Rosny G. and Fleming P. Nuovo. Cim. 68, 1137 (1967).

TABLE II

Density matrix representation of the angular distribution of the decay of the f^o for the present experiment and those analysed in references 85 and 86

	Present Expt. $\pi^- p \to n f^o$ 3.1 - 3.6 Gev/c	$\pi^+ p \to N^{x++} f^o$ 8 Gev/c	$\pi^- p \to n f^o$ 4 Gev/c	$\pi^- p \to n f^o$ 3.7 Gev/c	$\pi^+ d \to pp f^o$ 6 Gev/c
ρ_{oo}	0.93 ± 0.07	0.85 ± 0.10	1.01 ± 0.20	0.64 ± 0.07	0.92 ± 0.10
ρ_{11}	0.27 ± 0.02	0.19 ± 0.04	0.21 ± 0.09	0.29 ± 0.06	0.27 ± 0.03
ρ_{22}	−0.24 ± 0.02	−0.12 ± 0.06	−0.22 ± 0.09	−0.11 ± 0.06	−0.23 ± 0.04

data is for the f^o mass region. A pure spin state resonance has positive values of the density matrix elements and the negative value of $\rho_{2,2}$ corresponds to interference effects and to the observation at values near $\cos \theta^* = 0$ of far fewer events than would be expected for a J = 2 resonance(87). It is pointed out that although the experiments quoted above do not give a simple spin assignment, they all yield a consistent description of the resonance in terms of density matrix elements, even though different production mechanisms and final states are involved.

MISCELLANEOUS STUDIES IN PHYSICS

Mössbauer Group (T. E. Cranshaw, G. Lang, M. S. Ridous, W. Oosterhuis, C. E. Johnson (S.S.P.) and B. Window (Fellow, S.S.P.))

^{119}Sn in magnetic systems (T. E. Cranshaw and A. P. Jain)

The work on ^{119}Sn in AuMn, AgMn, CuMn, AuFe has been published(88). Further work on these systems is being carried out by B. Window.

The preliminary work on ^{119}Sn in cobalt has also been published(89), and a tentative explanation of the anomalous temperature dependence given in terms of a temperature dependent "transferred byperfine field". Collaboration on N.M.R. measurements on ^{117}Sn and ^{119}Sn in Co, which should provide a crucial test of this mechanism has been started with D. T. Edmonds (Clarendon Laboratory). It is also proposed to examine the system FeMn with the same mechanism in mind.

Measurements on ^{119}Sn in Ni have been made for two concentrations of Sn. The field at Sn is found not to follow the magnetisation of the alloy, but to be mainly dependent on how many Ni neighbours it possesses. This result is unexpected, since the results of diffuse neutron scattering show a long range disturbance round the Sn site, and the magnetisation measurements are in good agreement with a "band filling" model.

---

(87) Nuclear Physics Division Progress Report AERE - PR/NP 12 (1967).

(88) Jain A. P. and Cranshaw T. E. Phys. Lett. 25A, 421 (1967).

(89) Jain A. P. and Cranshaw T. E. Phys. Lett. 25A, 425 (1967).

Dilute alloys (M. S. Ridout)

Gold - Iron

Our room temperature spectra of gold-iron alloys with iron concentrations between 0.5% and 12.8% show structure which increases in complexity with iron concentration (Fig. 31). Violet and Borg[90]

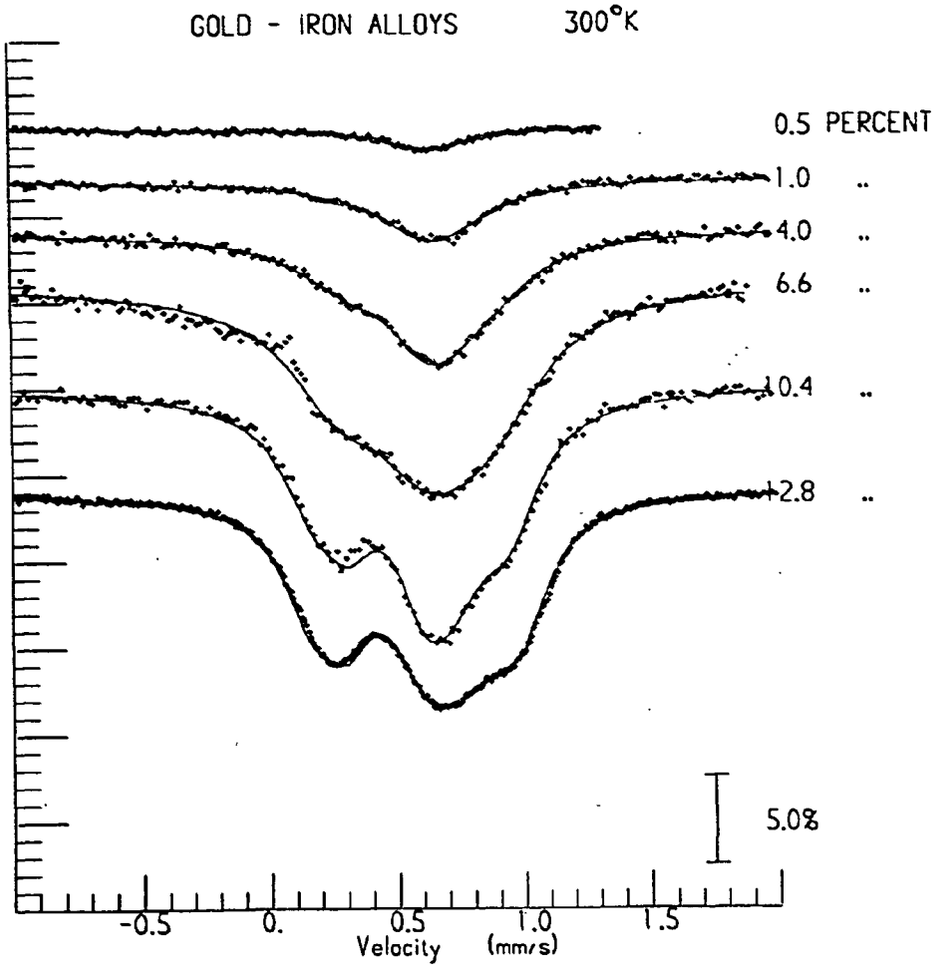

Fig. 31. Mössbauer spectra of iron in gold-iron alloys shown as a function of iron concentration.

obtained similar spectra which they interpreted as two doublets with a small shift between them. One doublet, with small splitting, was associated with iron atoms with no iron atoms in the nearest neighbour shell, while the other doublet was associated with iron atoms with one or more iron atoms in the nearest neighbour shell. In order to fit the data they had to invoke the Goldanskii effect[91], which produces unequal intensities in the lines of the doublet. In our work the analysis has been extended to allow for different spectra for iron atoms with 0,1,2,3 and 4 iron atoms in the nearest neighbour shell.

---

(90) Violet C. E. and Borg R. J. To be published.

(91) Gol'danskii V. I., Markarov E. F. and Khrapov V. V. Soviet Physics JEPT (Eng. Trans.) 17, 508 (1963).

The relative contributions from each configuration were calculated on the assumption that the solute atoms were randomly distributed in the lattice, and the quadrupole splittings and shifts were obtained from a least squares fit to the data. It was not necessary to invoke the Goldanskii effect. The results of the fitting are shown in Fig. 31 and the parameters obtained are tabulated below.

No. of neighbours	*Q*	*C*
0	0.054 ± 0.017	0.633 ± 0.016
1	0.318 ± 0.015	0.613 ± 0.022
2	0.294 ± 0.044	0.480 ± 0.052
3	0.110 ± 0.007	0.699 ± 0.071
4	0.207	0.378

The units are mm/sec; the errors for the 4 - neighbour case are not quoted as in the most concentrated alloy this configuration accounted for only 4% of the total absorption.

The large value of Q for 1 and 2 iron neighbours together with the small value for no iron neighbours is consistent with the view that the local symmetry of the F.C.C. lattice is perturbed by the substitution of iron for gold atoms in the nearest neighbour shell. The small but finite Q for no iron neighbours indicates that effects due to iron atoms in the next nearest shell are small but significant. The reduced value of Q for the 3 neighbour case indicates that the symmetry has increased. The data are not good enough to determine whether or not there is any tendency to a non-random arrangement.

Copper - Iron

The spectrum of a sample containing 0.19% iron usually shows two lines, one of which is attributed to iron in solution, and the other to precipitated γ-Fe.

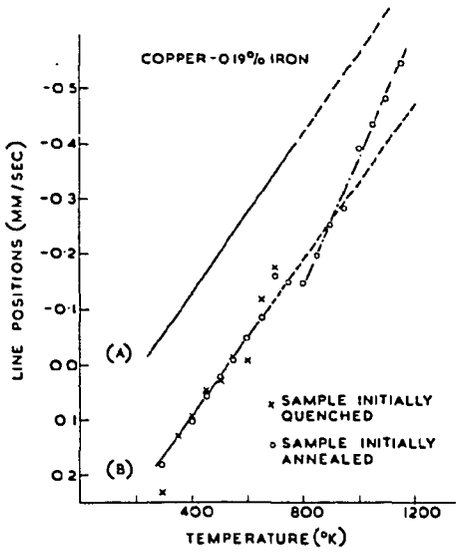

Fig. 32. Temperature dependence of line positions in copper-iron alloys. Curve (A) is the precipitated γ-Fe and curve (B) is due to iron in solid solution.

Measurements have been made from room temperature to 1150°K. The temperature dependence of the positions of the two lines is shown in Fig. 32. The increased slope of curve (B) above 800°K shows that the mean squared velocity $\langle v^2 \rangle$ increases more rapidly with temperature than the Debye theory of solids predicts. Similar, but less accurate, measurements of the temperature dependence of the line intensity show that the mean squared displacement $\langle x^2 \rangle$ increases less rapidly with temperature than expected. Experiments are proceeding to determine the source of this behaviour.

Nuclear quadrupole moment of $^{57}Fe^m$ (C. E. Johnson)

The quadrupole moment Q of a nucleus is usually deduced from a measure of the coupling $\Delta E_Q = \frac{3}{4I(2I-1)} e^2Qq$ with the electric field gradient q produced by the electrons. q involves the effective value $\langle r^{-3} \rangle_{eff}$ of the electron wave function in the solid state, which is less than that calculated for the free atom because of covalency (f) and screening (1-R) effects, and can be written

$$\langle r^{-3} \rangle_{eff} = f(1-R) \langle r^{-3} \rangle_{free\ atom}$$

Hence although ΔE_Q may be measured with precision, the value of Q may have large uncertainties because of the difficulties of estimating $\langle r^{-3} \rangle_{eff}$. For $^{57}Fe^m$ the uncorrected value deduced from

measurements on ferrous fluosilicate ($Fe\,Si\,F_6$, $6\,H_2O$), which has an almost pure orbital ground state, is 0.12 b using the value $\langle r^{-3}\rangle_{UHF} = 5.1$ a.u. (Johnson, Marshall and Perlow)[92]. Estimates of f and (1-R) have increased this value up to 0.3 b.

The quantity $\langle r^{-3}\rangle_{eff}$ also occurs in the expression for the magnetic hyperfine interaction. Although it is not obvious that the screening factor (1-R) is the same for electric and magnetic interactions (in the former it arises from Coulomb effects, in the latter from inter-atomic exchange) it has been calculated (Freeman and Watson[93]) that for the Fe^{++} ion they are the same to within 10%, which is considerably better than the uncertainties hitherto involved. The anisotropy of the hyperfine field is due to the orbital and dipolar fields at the nucleus and for ferrous fluosilicate

$$H_{\parallel} - H_{\perp} = 4\beta \langle r^{-3}\rangle_{eff} (g_{\parallel} - g_{\perp}) - \frac{3}{14}$$

and

$$q = \frac{4}{7}\langle r^{-3}\rangle_{eff}$$

where β is the Bohr magneton, and susceptibility data has shown that $g_{\parallel} = 2.00$, $g_{\perp} = 2.14$.

The Mössbauer spectrum of a single crystal of ferrous fluosilicate has been measured between 1.7 and 4.2°K in external magnetic fields of up to 30 kG. The values found for the parallel and perpendicular components of the hyperfine field were $H_{\parallel} = -550$ kG and $H_{\perp} = -248$ kG from which it is estimated that

$$\langle r^{-3}\rangle_{eff} = 3.5 \text{ a.u.}$$

and

$$Q(^{57}Fe^{m}) = +0.18 \text{ b}$$

Biological molecules (G. Lang)

Leghaemoglobin (G. Lang, P. J. Dart (Rothamstead Agricultural Experimental Station) and A. Thomson (W.R.E.))

The spectra of a preparation of leghaemoglobin cyanide have been found to be closely similar to those of rat haemoglobin cyanide. Spectra of whole root nodules indicate the previously unsuspected presence of non-protein iron. This discovery is being followed up by tracer studies at Rothamstead.

Haemoglobin (G. Lang and M. Winter (Inorganic Chem. Lab. Oxford))

A comparison of the spectra of ordinary and deuterated acid methaemoglobin seems to indicate that the protons of the water ligand are broadening the former through magnetic hyperfine interaction. A dependence of low temperature spectra on ionic strength has also been observed. However elucidation of these effects will require the preparation of additional samples because of the difficulty in achieving reproducible results.

---

(92) Johnson C. E., Marshall W. and Perlow G. J. Phys. Rev. 126, 1503 (1962).

(93) Freeman A. J. and Watson R. E. Phys. Rev. 131, 2566 (1963).

Cytochrome C (G. Lang, T. Yonetani (Johnson Foundation) and D. Herbert (Microbiological Research Establishment))

Measurements have been made on ^{57}Fe enriched cytochrome C obtained from yeast. The spectra are similar to those of haemoglobin cyanide and cyanate, and agree well with a theory using similar crystal field parameters.

Radio pulses from extensive air showers (W. N. Charman, J. H. Fruin and J. V. Jelley)

(a) The installations at AERE and WRL

The synchronous gate circuits described in the last report, built to suppress pulses from the navigational beacon near Wantage and the Linac modulator pulses from AERE, have been modified so as to increase the fractional observing time from 0.37 to 0.90, a factor of ~ 2.5. A second scintillator, similar in area to the first, has been set up so that horizontal muons from showers may be detected by operating the two units in time coincidence. This system has an effective projected sensitive area of 2 m^2 oriented perpendicular to the axes of the two 55 MHz antenna beams, and an acceptance cone of ~ 0.13 sr. Following the report(94) that radio pulses from showers have now been detected at 520 MHz i.e. at frequencies higher than those for which mutual coherence effects are expected from the main disc of the shower, two further radio channels are in the course of construction, one at 200 MHz and one at 500 MHz.

The installation at Grove is complete but its operation is at present hampered by an unknown source of intermittent pulse interference.

(b) Observations

During a selected six week period of observation, it was found that the coincident events recorded by the 55 MHz system could be divided broadly into three categories (a) those in which the recorded pulses were sharp, single and bandwidth-limited, (b) those in which the pulse was single but had structure, and (c) those in which a long sequence of narrow pulses filled the 5 μ second time-bases. A detailed analysis of these observations has been presented elsewhere(95). It is believed that some but not all of the 'a' events are random coincidences, that the 'b' events may be partly or wholly due to cosmic-ray showers, and that the 'c' events are dominantly due to interference.

In ~ 160 hours of elapsed running time, two scintillator pulses only were recorded in coincidence with ~ 1000 time-bases fired by the 55 MHz radio channels. However this count is still significant, since the random rate for this type of event is quite negligible.

A search for high-energy γ-rays from the Crab nebula (Under EMR Contract No. 1561) (W. N. Charman, J. H. Fruin and J. V. Jelley, jointly with N. A. Porter and others at University College, Dublin)

Experiments last winter using the Harwell installation of Cherenkov light receivers(96) at the dark site in Glencullen, County Dublin, gave tentative evidence(97) for the detection of high-energy γ-rays from the Crab nebula. To exploit this possibility it was decided to improve the existing system by lowering the energy threshold and by increasing the discrimination between γ-ray and proton induced

---

(94) Fegan D. J., McBreen B., O'Mongain E. P., Porter N. A. and Slevin P. Tenth International Conference on Cosmic-Rays, Calgary, Canada. July 1967. Paper EAS-69.

(95) Charman W. N., Fruin J. H. and Jelley J. V. Tenth International Conference on Cosmic-Rays, Calgary, Canada. July 1967. Paper EAS-60.

(96) Jelley J. V. and Porter N. A. Quarterly J. of the R.A.S. 4, 275 (1963).

(97) Fegan D. J., McBreen B., O'Mongain E. P., Porter N. A. and Slevin P. Tenth International Conference on Cosmic-Rays, Calgary, Canada. July 1967. Paper OG-9.

showers. The following improvements to the Glencullen installation have now been completed: (1) the two f/0.5 rear-silvered mirrors have been replaced by four f/2.0 front-aluminised mirrors, (2) the field of view of the mirrors has been reduced from 1.5° to 0.5°, thus lowering the background light and improving the angular resolution, (3) the electronic resolving time has been reduced from 15 μs to $\sim$ 3 ns, (4) an improved servo-system has been introduced[98] and (5) the random rate is recorded continuously. These changes should significantly increase the sensitivity of the installation for observations this coming winter.

A cooled image intensifier system for astronomical spectroscopy (W. N. Charman, J. H. Fruin and A. V. Hewitt)

The analysis of the astronomical observations made on the coudé spectrograph of the 30" telescope at the Royal Greenwich Observatory, Herstmonceux, is now complete. The quality of our observations with a time resolution $\sim$ 1 minute on the variable star VZ Cnc (period $\sim$ 4 hrs) equalled that of the photographic observations of Danziger and Oke[100] at the 200" Palomar telescope, while the linearity of the system was confirmed by comparing the photometered results on the Orion association with those obtained by Sharpless[99] using conventional photoelectric photometry at the 84" McDonald telescope, so that the overall performance of the intensifier is most satisfactory. This work is now being prepared for publication.

The channelling of protons in thin crystals (G. Deamaley, I. V. Mitchell, R. S. Nelson (Met. Division), M. W. Thompson and B. W. Farmery (Univ. of Sussex))

The first phase of the work has now been completed and is being prepared for publication.

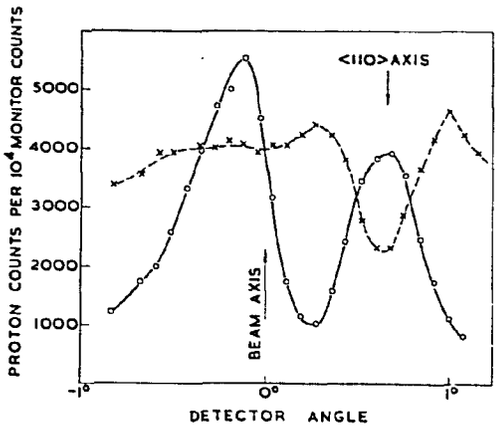

Fig. 33. Angular distribution of channelled (-o-o-) and non-channelled (-x--x-) protons transmitted through an Si crystal near the <110> axis, measured along the {110} plane.

The idea of a potential barrier around an axial channel has been further developed, and an explanation of this barrier in terms of the atomic potentials has also been provided. This idea is supported by studies of the angular distribution of 2 MeV protons transmitted through silicon crystals at angles slightly away from an axial direction (Fig. 33). The split peak we observe in the angular distribution for the channelled beam has one component along the <110> direction and another which shows an angular displacement of incoming particles away from the <110> direction, suggesting that, for particles incident at an angle $\sim$ ½° to the <110> axis, capture into the <110> direction competes with planar channelling. The view proposed by Appleton et al.[101], that axial channelling results merely from the superpositron of channelling along the various crystal planes, would require that the peak for planar channelling should be symmetric about the direction of the incoming beam.

A study of the spectrum of particles emerging within 5° of the beam axis revealed no evidence for a high energy-loss component[102] associated with proton channelling near planar directions. Since such a component was reported in measurements in which protons scattered at angles up to 70° were detected[101], its angular distribution must be very diffuse.

(98) Fruin J. H. and Jelley J. V. Tenth International Conference on Cosmic-Rays, Calgary, Canada, July 1967, Paper TECH-5.

(99) Sharpless S. Ap. J. 136, 767 (1962).

(100) Danziger I. J. and Oke J. B. Ap. J. 147, 151 (1967).

(101) Appleton B. R., Erginsoy C. and Gibson W. M. Phys. Rev. 161, 330 (1967).

(102) Gibson W. M. et al. Phys. Rev. Letters 15, 357 (1965).

Further experiments are in preparation in order to investigate the effects of temperature on proton channelling, i.e. on the angular distribution and energy loss of channelled ions. This work will be closely integrated with similar studies for heavy ions, which form part of the ion implantation programme. A theoretical study of the energy loss of fast-moving ions in crystals has been initiated.

Silicon surface barrier detectors (G. Dearnaley)

A new theory of the mechanism of surface barrier formation in these detectors has been developed. The gold layer is now envisaged as the source of nucleation centres from which structural changes take place in the unsaturated silicon oxide on the semiconductor surface. These changes are encouraged by the presence of an electric field. Thus the work function and nature of the metal electrode are important in determining the rate at which the surface states at the silicon-oxide interface develop, but once this development has occurred, the barrier height is governed by the surface state density and the metal plays a lesser role. Aluminium is favourable as a rear contact material because it reduces the rate of formation of surface states.

These ideas have arisen from a study of the behaviour of certain thin film Au-SiO-Al devices which have been prepared by STL, Harlow. It appears that the same ideas of structural change in the unsaturated oxide leading to electronic conduction along filaments can explain the negative resistance and memory characteristics of the SiO devices.

The same theory has also been applied to the oxide-coated thermionic cathode, and it is suggested that the activation of such cathodes results in the formation of conducting filaments through the unsaturated oxide. Electron emission then takes place from local hot spots. Experiments to test the validity of these hypotheses are now being prepared.

(H) Study of the luminescent properties of rocks, meteorites and natural glasses under proton bombardment (J. M. Blair in collaboration with J. A. Edgington (Queen Mary College, London))

The background to this project has been given earlier[103]. The work is now complete, and a preliminary account has been submitted for publication. The results are summarised in Table III, and the more significant features are illustrated in Figs. 34→36 (see page 42).

Discussing first the geological samples, we observed that the luminescent intensities were in all cases similar at +20° and +100°, but greatly enhanced at −180°C (see Fig. 34). In similar studies[104] Nash found that the response of a basalt sample was unaffected by a temperature change from +120° to −80°C; we too find that a reduction to −80°C does not sensibly alter the response of basalts or granites, but that a further reduction to −180°C has a dramatic effect. We show in Fig. 36(a) the blue response of a granite specimen as a function of temperature and conclude that between −80° and −180°C the relative probability of radiative transitions increases sharply for these common minerals. The granites show this low temperature enhancement most strikingly; their total brightness at −180°C is of the same order as that of NE 102A plastic phosphor, corresponding to an energy efficiency of the order of one per cent. The granites show also an extremely intense red thermoluminescence, with peaks near −140° and −30°C, and thermoluminescent energy efficiencies of the order of 10^{-3}; a typical glow curve is shown in Fig. 36(b). In these respects the granites proved to be the most outstanding rocks tested.

Of meteorites, we studied eleven chondrites, cosmologically the most abundant class, and three achondrites. Our results for irradiation at +20°C agree generally with those of Geake and Walker[105]. The enstatite achondrite Khor Temiki, with an efficiency of about one per cent, was easily the most intensely luminescent. Our spectrum for this, together with that of Geake and Walker for comparison, is shown in Fig. 35(a). The effects of temperature variation are interesting. Some classes of meteorite

---

(103) Nuclear Physics Division Progress Reports AERE - PR/NP 11 and 12 (1967).

(104) Nash D. B. Journal of Geophysical Research 71, 2517 (1966).

(105) Geake J. E. and Walker G. Geochimica et Cosmochimica Acta.

TABLE III

Summary of luminescent properties of rocks, natural glasses and meteorites under proton bombardment

		Average light output*			C.E.F.**	Thermo-luminescence
		+20°C	−180°C	+100°C		
Geological Samples						
I	Basic ferromagnesian rocks and minerals (dunite, enstatite, augite, olivine)	13	30	11	2.7	Nil
II	Extrusive rocks and breccia (five specimens of ash, pumice and basaltic lava)	25	68	27	2.5	Nil
III	Ancient volcanic breccia (Ordovician ash and tuff)	57	460	63	7.3	Weak blue peaks near −140°C
IV	Potash felspar (orthoclase)	266	449	320	1.4	Intense blue peak near +20°C
V	Granites (seven specimens)	238	3352	266	12.6	Intense red peaks near −30° and −140°C
Meteoric Samples						
VI	Hypersthene chondrites (Sinai, Tenham)	12	24	14	1.7	Nil
(VIa	Barwell	30	28	38	0.7	Strong green-blue) peak above +180°C)
VII	Bronzite chondrites (Cobija, Momans, Ogi, Sindhri)	18	19	28	0.7	Strong blue peak above +180°C
VIII	Pigeonite chondrite (Karoonda)	8	25	13	1.9	Nil
IX	Enstatite chondrites (Daniel's Kuil, Khaipur)	92	97	119	0.8	Very strong red peak near 0°C
X	Carbonaceous chondrites (Cold Bokkeveld, Orgueil)	8	10	5	2.0	Nil
XI	Hypersthene achondrite (Johnstown)	11	36	10	3.6	Nil
XII	Enstatite achondrite (Khor Temiki)	1778	1730	1997	0.9	Intense red peak near 0°C
XIII	Plagioclase achondrite (Juvinas)	115	132	89	1.5	Weak red peak near 0°C
Glasses						
XIV	Tektites (Australite, Bediasite, Indochinite, Rizalite)	11	14	10	1.4	Nil
(XIVa	Moldavite	48	85	54	1.6	Nil)
XV	Natural glasses (Darwin glass, Ries impactite)	15	158	12	13.2	Nil
(XVa	Libyan Desert glass	471	1345	350	3.8	Nil)

*These figures are the integrated light output from 3800 A - 7400 A.
In this Table and on the Figures, one unit corresponds to the emission of 2×10^6 photons per second, which for our proton flux is equivalent to an energy efficiency of about 7×10^{-7} (assuming an optical depth of 40μ).

**Ratio of light output at −180° to that at +100°C.

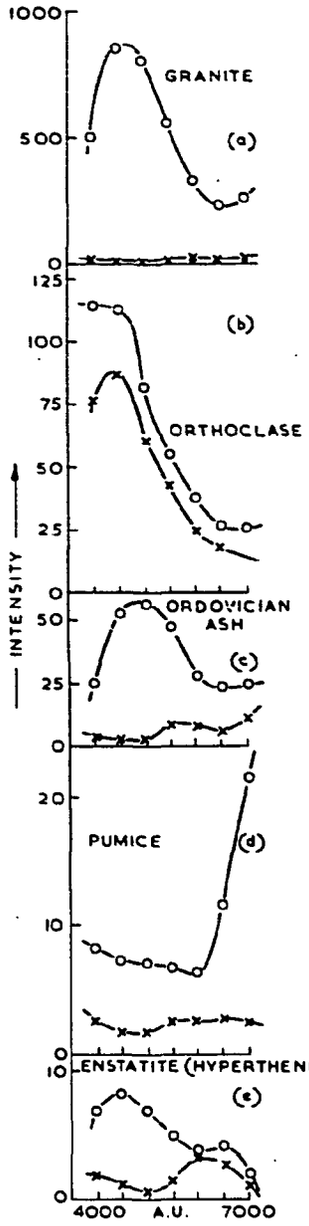

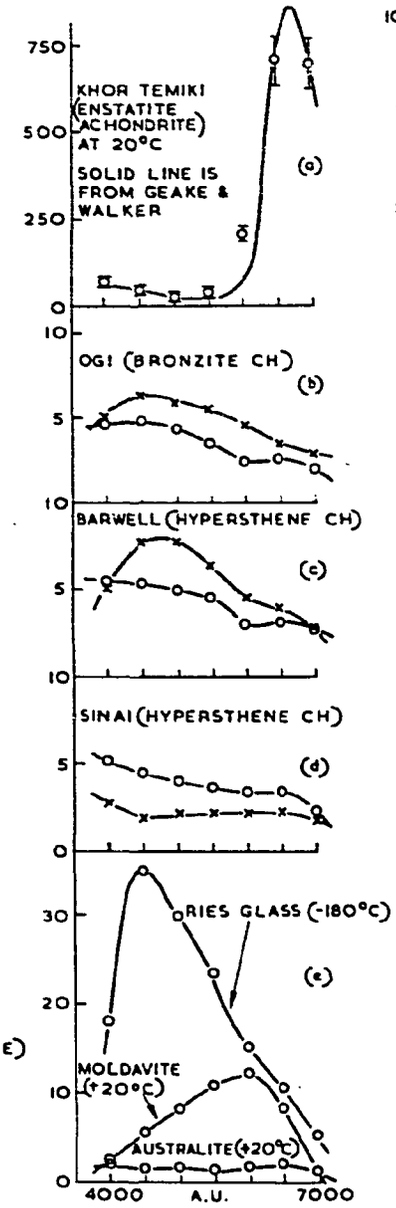

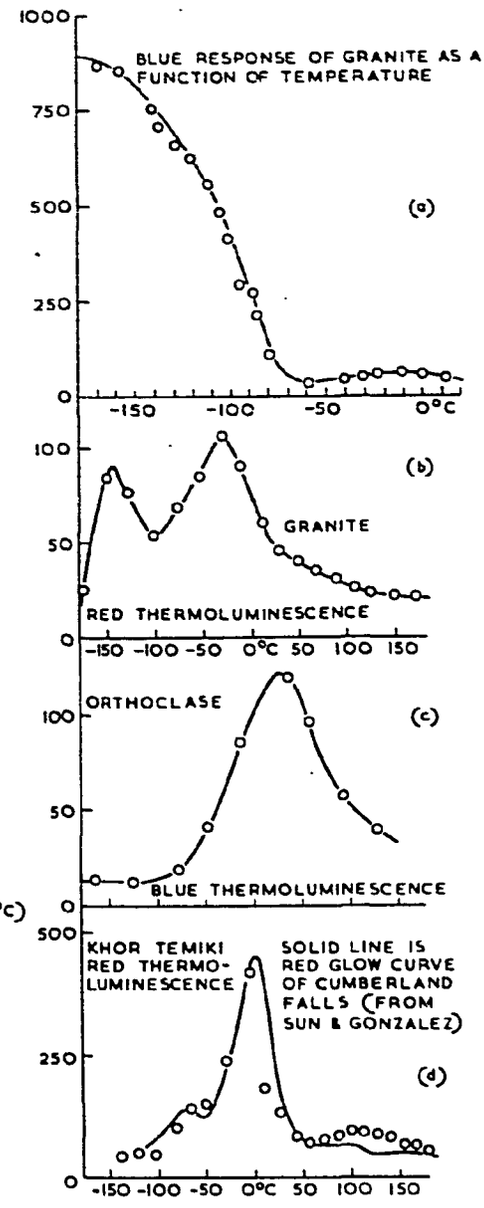

Fig. 34. Luminescent spectra of various geological samples. Open circles represent data at -180°C; crosses are data at +100°C.

Fig. 35. Luminescent spectra of various meteoritic and vitreous samples. Open circles represent data at -180°C; crosses are data at +100°C (except where stated otherwise).

Fig. 36. Luminescent response as a function of temperature (a), and thermoluminescent effects (b, c, d), for various samples.

(bronzite and enstatite chondrite, enstatite achondrite) are brighter at +100° than at −180°C, unlike any terrestrial rocks we studied. This behaviour, typified by a cold enhancement factor less than unity, is accompanied by thermoluminescence near to or above room temperature. We show in Fig. 36(d) the red thermoluminescence of Khor Temiki, with for comparison the glow curve obtained[106] by Sun and Gonzalez for Cumberland Falls, another enstatite achondrite. The recent fall, Barwell, appears anomalous. In all respects it resembles the bronzites more than the hypersthenes with which it is classified[107] on a mineralogical basis. Figs. 35(b), (c) and (d) show the spectra at −180° and +100°C of Sinai (a typical hypersthene), Ogi (a bronzite), and Barwell respectively. This observation appears to us significant and (in view of the clear mineralogical distinctions[108] between the classes of chondrites, particularly falls) somewhat surprising.

Finally, we studied five specimens of tektites and three terrestrial glasses. Four of the tektites are very similar; they have featureless spectra of low intensity and exhibit only a small low temperature enhancement and no thermoluminescence, as may reasonably be expected of such vitreous, homogeneous materials. The Moldavite, on the other hand, has a strong orange-red peak and a total light output about five times that of the others. Fig. 35(e) compares its spectrum at +20°C with that of the Australite. Also shown is the low temperature spectrum of Ries impactite glass; its resemblance to that of the Moldavite is intriguing, but the difference in cold enhancement factors would seem to rule out any genetic relationship between these two geographically associated glasses. Our conclusion is that the Moldavite is not in this respect a "typical" tektite; further work would be interesting in view of the problem of the origin of tektites.

Our observations of the intense thermoluminescence of granites suggest an explanation of the transient red glows seen repeatedly in regions of the moon which from their distribution are believed[109] to be prone to tectonic disturbances. In such active regions it must sometimes happen that cold subsurface material, possibly granitic, is suddenly disturbed and exposed to surface insolation; having been irradiated for millenia by high energy solar protons it glows on heating. Using values for proton fluxes cited[110] by More and Tiffany, we calculate, for instance, that lunar material at a depth of about 10 gm cm^{-2} will absorb about 10^{10} MeV gm^{-1} cm^{-2} $year^{-1}$. Such irradiation at −120°C for about half a million years might then yield, on sudden heating, light outputs of the same order as that of reflected sunlight.

MISCELLANEOUS TECHNIQUES

The six gap beta-ray spectrometer (R. Chapman)

During September the spectrometer and its associated equipment were transferred from the Nuclear Physics Division, A.W.R.E.

When finally set up, the spectrometer should be capable of detecting electrons with energies ranging from 5 keV np to at least 5 MeV and with momentum resolution settings of 0.4, 0.8 and 1.4% at transmission values of 1, 5 and 10% respectively. It will be used mainly to look at the prompt internal conversion electron spectra produced during bombardment of isotopically enriched nuclear targets by beams of charged particles accelerated by the Tandem Van de Graaff.

---

(106) Sun K. H. and Gonzalez J. L. Nature 212, 23 (1966).

(107) Jobbins E. A., Dimes F. G., Binns R. A., Hey M. H. and Reed S. J. B. Mineralogical Magazine 35, 881 (1966).

(108) Mason B. Meteorites, Wiley, 1962 (p. 78).

(109) Middlehurst M. B. and Moore P. A. Science 155, 449 (1966).

(110) More K. A. and Tiffany O. L. Proceedings of the Symposium of Radiation Hazards in Space, 1962, p. 682 (USAEC, TID-7652, 1963).

Because extensive modifications have recently been made to the spectrometer magnet assembly the extensive checks on the pole plate profiles carried out some months ago at A.W.R.E. will require to be repeated.

The computer hardware developed at A.W.R.E. to link the various spectrometer monitoring and control facilities to the Aldermaston PDP7 computer will require some modification before being used in conjunction with the PDP8 computer at Harwell. When these changes have been made the following pieces of apparatus will be automatically controlled by computer:

(1) a digital voltmeter - used to monitor spectrometer magnet current,

(2) a stepping motor - used to increment current through coils,

(3) relay - used to reverse current through coils,

(4) Harwell type scaler - used to record number of electrons detected at each spectrometer current setting,

(5) current integrator - used to monitor beam on target.

The preparation of lithium-drifted germanium detectors for gamma-rays (G. Dearnaley, D. A. Elliott and I. V. Mitchell)

The first two samples of 3 in. diameter germanium crystals, grown by GEC Wembley under contract AE/A/1943, have now been received. Planar drifting of these samples, our contribution to the evaluation of this material, has begun.

A 7.5 cm × 1 cm disc of similar material has been drifted to a depth of about 8 mm, but published techniques for surface stabilization did not reduce the leakage to a value acceptable for detector use. It is clear that final surface preparation of drifted diodes remains the major obstacle in detector fabrication.

The preparation of lithium-drifted germanium particle detectors (G. Dearnaley, A. G. Hardacre and B. D. Rogers)

Our objective remains the production of 1 cm^2 germanium particle detectors with an energy resolution for 50 MeV protons of 25 keV. A thin entrance window to the depletion layer is to be obtained by use of a Ga^+ implanted ion contact.

Two detectors with the required area have now been produced but the depletion layer is still only about 4 mm thick. An adequately low leakage current ($\sim 10^{-9}$ A at 300 V) has been achieved, and the resolution obtained for ^{60}Co gamma-rays (5 keV line width) indicates that there is no serious trapping. Tests with 5 MeV alpha-particles indicate that the window thickness is about 1 micron, which is thin enough to allow the Landau spread for 30-50 MeV protons to be neglected.

The liquid nitrogen cryostat which has been designed for use with these detectors in the VEC scattering chamber is nearing completion.

Some further assistance in the preparation of germanium particle detectors for use with 150 MeV protons from the 110 in. cyclotron has been provided to Dr. C. Whitehead's group. A careful final ion-drift appears to be important in achieving high and uniform charge collection efficiency in these devices, and for this process a refrigerated bath has been built.

Preparation of lithium-drifted germanium detectors for the synchrocyclotron (C. Whitehead and A. C. Sherwood)

We have prepared and tested two more germium detectors with dimensions of 5.5 cm × 1 cm, the material coming from the same billet as the counter reported previously.

A FWHM resolution of 10 keV was obtained with both counters with collection voltages between 300 and 500 V and leakage currents from 0.5 to 5 na.

The uniformity of the detectors was investigated as before[111] by mapping the 4.5 cm x 5.5 cm surfaces with a 1 mm x 1 mm beam of 150 MeV protons. Fig. 37 shows a photograph of the response models built up from the investigations. Model A is the counter reported previously and models B and C the latest counters. It is clear that except for edge effects the bulk of the detectors B and C are uniformly sensitive with none of the defective areas displayed by counter A.

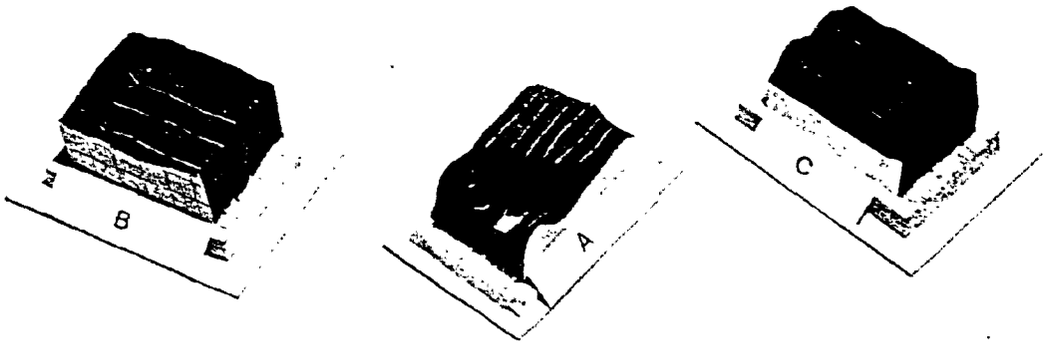

Fig. 37. Models of the sensitive volumes of three lithium difted germanium counters.

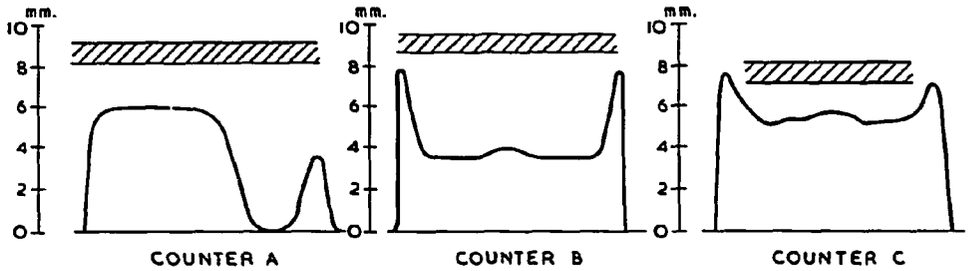

Fig. 38. Variation of sensitive depth across the centre lines of three detectors. Hatched areas show the sensitive depth as indicated by the copper staining technique.

Fig. 38 shows both the sensitive depths of the counters obtained by scanning along their centre lines and the extent of drift as indicated by the copper stain method (shown by the hatched areas). In all three cases the copper stain technique appears to overestimate the general drifted depth and it is probable that it indicates only surface features.

(111) Nuclear Physics Division Progress Report AERE - PR/NP 12 (1967).

The charge collection model of Day et al.[112] shows that for electron and hole trapping lengths very large compared to the collection distance and for collection efficiencies approaching 100% the fractional resolution of a detector due to incomplete charge collection is given by $\frac{dv}{v} = 0.2\ (1-\epsilon)$ where ϵ = collection efficiency.

Using this equation and measuring the variation of mean pulse height from 150 MeV protons as a function of collection voltages we estimate the contribution to the dispersion from incomplete charge collection in these detectors to have a maximum value of 70 keV FWHM.

This effect appears to be the dominant contribution to the intrinsic resolution of these detectors for 150 MeV protons, the next most significant contribution arising from statistics on ion pair production which would contribute a FWHM dispersion of 20 keV. The overall resolution of the device plus electronics is then estimated to have a maximum value of 74 keV FWHM. This is appreciably less than the beam energy resolution expected from the converted synchrocyclotron.

It is now intended to produce greater drifted depths and to prepare smaller detectors suitable for the deuteron, ^{3}He and alpha particle beams which will have a maximum range in germanium of only 8 mm compared with 45 mm for 150 MeV protons.

A 50 cc lithium drifted germanium γ-ray detector, on loan from Electronics and Applied Physics Division, was used to investigate the potential and limitations of such a device for nuclear structure experiments with the synchrocyclotron. The detector was placed at approximately 90° to a beam of 150 MeV protons which irradiated a series of targets. The detector had a resolution of 7 keV FWHM at 1.33 MeV and a full energy peak : Compton ratio of 6:1. γ-rays up to $\sim$ 1 MeV were very easily seen, even though they were superimposed on a rising background due to neutrons generated in the target, a background which will eventually limit the sensitivity of the detector. At higher energies two further limitations become apparent. Firstly each γ-ray produces three peaks : total energy, single escape and double escape, and secondly the 550 MeV/c momentum of the beam produces substantial döppler broadening in the de-excitation of some levels, e.g. a FWHM of 125 keV for the 4.43 MeV level of ^{12}C, which again limits the sensitivity of the detector. This second limitation can be alleviated if counters are used to define the reaction kinematics, when the döppler effect will produce a shift rather than a broadening. Under such conditions fewer γ-rays will be observed, so that the threefold multiplication of peaks can probably be tolerated. Such a technique demands highly efficient γ-ray detectors, and volumes in excess of 50 cc are desirable.

Ion implantation in semiconductors (G. Dearnaley, P. D. Goode and M. A. Wilkins)

Further concentration profiles of ^{32}P implanted into silicon crystals have been measured, and a fairly complete picture of the behaviour is now available. Fig. 39 shows channelled profiles along the <110> direction at two energies, and it can be seen that above about 100 keV a definite channelled peak is developed; this should be even more pronounced at the higher energies we will have available from the modified 500 kV Cockcroft-Walton.

The dose dependence of channelled ^{32}P profiles has been investigated, using simultaneous ^{31}P and ^{32}P implantations. The onset of radiation damage limits the P^+ ion density in the plateau region of a 40 keV profile to about 4×10^{17} ions/cm^3. This value is not greatly affected by implanting at higher temperatures, and it seems that lattice vibration effects on the channelled ion trajectories are pronounced, and that these counteract the effect of annealing during irradiation. Profiles for implantation along the <110> and <111> directions have been compared (Fig. 40): the channelled range is strongly dependent on the channel dimensions, and the reasons for this are now being considered from a theoretical standpoint. In the case of <110> channelling of ^{32}P the extrapolated range is found to vary with energy E approximately as $E^{0.6}$ over the range 10-100 keV.

---

(112) Day R. B., Dearnaley G. and Palms J. M. I.E.E.E. Trans. in Nuclear Science NS-14, No. 1 (1967).

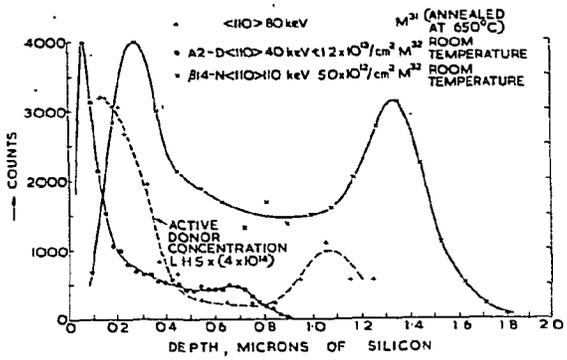

Fig. 39. Profiles for the channelled implantation of 40 and 110 keV ^{32}P and of 80 keV ^{31}P ions along the <110> direction in silicon.

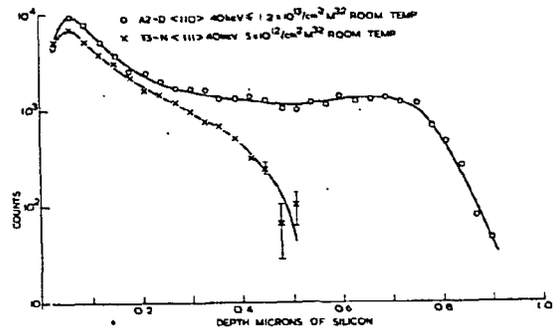

Fig. 40. Profiles for the channelled implantation of 40 keV ^{32}P ions along the <110> and <111> directions in silicon.

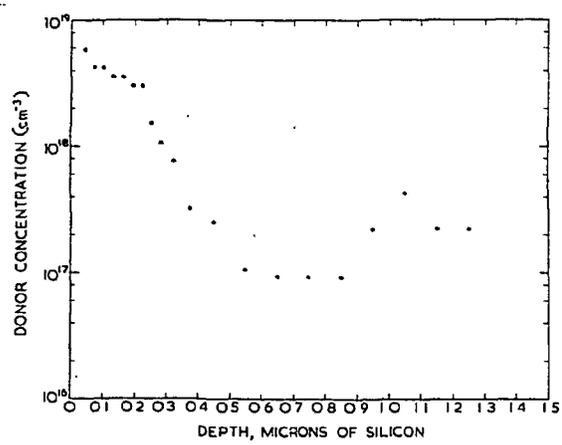

Fig. 41. Concentration profile of electrically active donors from ^{31}P implanted in silicon.

A target stage has been designed and built which will allow the Mark I E.M. separator to be used for implantation at temperatures down to 77°K, so that the influence of temperature on the channelled profiles and on the electrical behaviour after annealing can be further explored.

The electrical conductivity of phosphorus implanted into silicon has been measured as a function of depth, using the Van der Pauw geometry (a Maltese-cross shaped mask and peripheral contacts). Initial contact problems have been overcome and the results indicate that about 50% of 80 keV $^{31}P^{+}$ ions channelled at room temperature into silicon which is subsequently annealed at 650°C are electrically active (see Fig. 41). This is in strong disagreement with the results of Gibson et al.(113) who reported that with 400 keV ions, but otherwise similar conditions only about 1% of the implanted phosphorus became electrically active.

Many more crystal wafers have been oriented to high precision (± 0.02°) by the technique of 10 MeV proton channelling, using the Tandem Generator. A paper describing this technique has been published.

(D) Position sensitive detectors to fill the focal plane of a Buechner spectrometer (R. K. Jolly and G. V. Ansell)

A project is underway to span 2/3 of the focal plane of the Buechner spectrometer with between 8 and 12 identical 1 mm deep position sensitive detectors. Whenever a charged particle impinges on one of these detectors two signals can be picked up; one of these is the E signal corresponding to the energy loss of the charged particle in the detector, the other, the E × X signal which depends both on E and the location X of the point of impact. The reaction products are incident at an angle of 60° to the detector surfaces which lie along the focal plane, doubling the effective thickness of the detectors and thus enabling them to stop the most energetic products of reactions induced by beams from the 13 MeV tandem generator. True position signals X from a given detector will be obtained by an analogue division of the E × X signal by the E signal and will usually be analysed in coincidence with particle selection signals. The latter will be obtained by pulse height selection of the energy range appropriate to the particle of interest for a given magnetic rigidity. The detectors will be arranged in two rows in a "square wave train" pattern to avoid gaps in coverage between the ends of neighbouring detectors and each experimental

(113) Gibson W. et al. Proc. Conf. on Applications of Ion Beams to Semiconductor Technology, Grenoble, May 1967.

run will be split into two with each row of detectors in turn centred on the focal plane. The position signals X from consecutive detectors (treating the two runs as a single continuous one) will be mixed, digitized and routed into consecutive equi-partitioned sections of a PDP8 computer memory so that they can be displayed or read out as a single continuous X-spectrum. It is expected that the complete system will be capable of processing at least two thousand counts/sec without appreciable dead time losses.

Since a very large quantity of equipment is involved in this system, it has been decided to connect all the components of the system in its Universal mode and then "freeze" it with the exception of the freedom to manipulate dials and replace faulty units. To simplify fault tracing, the components handling the signals from a detector will be arranged in a "flow diagram" pattern and colour coded. Graphs will be provided to enable experimenters to set reasonably close values for various dial settings for typical reaction studies. It is hoped that with these aids an experimenter with a reasonable amount of previous preparation will be able to take data within twelve hours of coming on the accelerator provided everything is operating normally.

Aluminising (P. G. Davies)

Over 50 mirrors, ranging in size from 6 inches square to over five feet in diameter have been aluminised during the current period for various customers, including R.H.E.L., Dr. J. V. Jelley, Southampton University and the Research Reactors Division.

ACCELERATOR OPERATION, MAINTENANCE AND DEVELOPMENT

Cockcroft-Walton 0.5 MV generator (A. T. G. Ferguson, F. D. Pilling, K. C. Knox, S. Waring and W. E. Sparrow)

Analysis of machine running

	Hours	Hours	%
Total scheduled time	123		100.0
Installation work		-	-
Scheduled maintenance and conditioning		-	-
Setting up ion source and beam line		12	9.8
Scheduled experimental time		111	90.2
	111		100.0
Time lose through breakdowns		7	5.7
Available experimental time		104	84.5
	104		100.0
Experimental usage			
(1) Analytical Sciences Division		92	88.5
(2) Health Physics and Medical Division		12	11.5

Modification programme for 0.5 MV Cockcroft-Walton generator (G. Dearnaley)

Work on the modification is proceeding satisfactorily, and most of the components are now ready for installation. The major item, the analysing magnet, has been received from AWRE and is being installed.

The resistor column has been overhauled. Since it showed signs of overheating additional cooling has been provided. A new stabilisation system for the accelerator is under construction.

A general purpose target chamber for implantation experiments has been designed in co-operation with Vacuum Generators Ltd.

3 MV pulsed Van de Graaff generator IBIS (A. T. G. Ferguson, D. R. Porter, F. D. Pilling and E. A. Gove)

Analysis of machine running

	Hours	Hours	%
Total scheduled time	2132		100.0
Installation work		150	7.0
Scheduled maintenance and conditioning		40	1.9
Setting up ion source and aligning beam		92	4.3
Scheduled experimental time		1850	86.8
	1850		100.0
Time lost through breakdown		190	10.3
Available experimental time		1660	89.7
	1660		100.0
Experimental usage			
(1) Nuclear Physics Division		597	36.0
(2) Analytical Sciences Division		274	
(3) Solid State Physics Division		7	
(4) Metallurgy Division		66	
Sub total - other AERE Divisions		347	20.9
(5) Glasgow University		156	
(6) Exeter University		182	
Sub total - University users		338	20.4
(7) AEE Winfrith		130	7.8
Machine development		248	14.9

A working platform has been installed to facilitate the use of a second beam line for among other things preliminary work on the production of small diameter beams. Using suitable defining apertures target currents of 60-80 nanoamps have been focused through a 30 micron diameter hole, and free beams down to 10 microns diameter are envisaged in the immediate future.

A second platform round the original target area is being designed. In an attempt to increase the maximum voltage obtainable from the machine the normal insulating gas was replaced with pure SF_6 at a

pressure of 50 p.s.i.g. Stabilisation difficulties appeared, and even when these were partially overcome by increasing the gas pressure to 160 p.s.i.g. and adding N_2 and CO_2 the maximum machine voltage was still limited to 3.9 MV.

5 MV Van de Graaff generator (A. T. G. Ferguson, F. D. Pilling, K. C. Knox, S. Waring and W. E. Sparrow)

Analysis of machine running

	Hours	Hours	%
Total scheduled time	2414		100.0
Installation work		-	-
Scheduled maintenance and conditioning		94	3.9
Setting up ion source and beam lines		134	5.5
Scheduled experimental time		2186	90.6
	2186		100.0
Time lost through breakdowns		98	4.5
Available experimental time		2088	95.5
	2088		100.0
Experimental usage			
(1) Nuclear Physics Division		1022	48.9
(2) Health Physics and Medical Division		350	
(3) Analytical Sciences Division		82	
(4) Metallurgy Division		78	
(5) Electronics Division		45	
(6) Solid State Physics Division		166	
Sub total - AERE Divisions		721	34.5
(7) Oxford University		229	
(8) Manchester University		41	
(9) Sussex University		20	
(10) Exeter University		41	
Sub total - University Users		331	15.9
(11) AEE Winfrith		14	.7

The machine ran out its scheduled programme and the modification began on 3rd November as planned.

Modification (A. T. G. Ferguson, K. C. Knox, F. D. Pilling and S. Waring)

The stack and top plate have been assembled and the tank intershield and top terminal are on site. The magnet and accelerator tube are the only major items not yet to hand.

13 MeV Tandem Generator (P. Humphries)

Analysis of machine running

	Hours	Hours	%
Total scheduled time	1902		100.0
Installation work and conditioning		-	-
Scheduled maintenance		143	7.5
Setting up ion source and beam		111	5.8
Not required		76	4.0
Scheduled experimental time		1572	82.7
	1572		100.0
Time lost through breakdowns		2	0.2
Available experimental time		1570	99.8
	1570		100.0
Experimental usage			
(1) High Voltage Laboratory		819	52.2
(2) H.V.L. Manchester, Birmingham (collab.)		225	14.3
(3) Ion-crystal Group		40	2.5
(4) Analytical Sciences Division		86	5.5
(5) Exeter University		94	6.0
(6) Oxford University		41	2.6
(7) Cambridge University		14	0.9
(8) Manchester University		194	12.4
(9) Medical Research Council		7	0.4
(10) Farnborough Space Research		6	0.4
Machine Tests		44	2.8

Machine Performance

The machine has run very steadily since the shut-down which terminated at the end of February 1967. The new "standard" accelerator tubes are behaving in much the same manner as the previous similar pair that were in use for 20,000 hours. Terminal voltages of 6.5 MV can now readily be achieved.

Since the installation of the modified foil mechanism (i.e. the exclusion of possible outgassing materials) the stripper foil lifetime appears to have increased at all but the highest energies.

The magnetic quadrupole lens situated directly below the lower accelerator tube has functioned satisfactorily up to 12.5 MeV; its installation eases maintenance problems and makes it possible to consider simultaneous control of the currents fed to the quadrupole and to the bending magnet, but beam handling appears to be practically the same as when the electrostatic quadrupole is used.

Although by using the ion-pump installed in the stripper body the vacuum has been improved from approximately 5×10^{-5} mm to 5×10^{-6} mm, fairly lengthy tests indicate that this change has produced no appreciable improvement in foil life or in running conditions at extra high energies. Further tests will be carried out in the near future.

Machine Facilities

The target lines are being re-arranged to accommodate experimental equipment that is to be transferred from AWRE Aldermaston, i.e. the mulfi-gap spectrograph, a beta spectrometer and an angular correlation table.

The experimental equipment racks in the control room are being re-arranged to increase the number by 30% and to make more room for the data processing computer.

Installation of a mercury pool cathode ion-source (R. H. V. M. Dawton and P. Humphries)

Progress on this has been considerably hampered by delays in the supply and initial testing of manufactured items and new equipment. The ion source is now being assembled on the new pressure vessel lid, in Hangar 10. It is intended to test this during December and install it on the Tandem during January and February 1958. During this shut-down period preparatory building work for the installation of the multi-gap spectrograph will also be carried out. In addition an alpha particle test will be carried out on the main analyser magnet to redetermine the optimum position of the fringe-field magnets.

Negative helium ion-source development (R. H. V. M. Dawton)

A potassium vapour donor has been used with the duoplasmatron source and steady He^- beams of 2 μA obtained using a voltage of 12 kV. No trouble has been experienced with the potassium evaporator nor has the presence of potassium resulted in high voltage troubles, although admittedly the system has been operated for only about 50 hours with the evaporator at working temperature. A test will later be made with lithium instead of potassium vapour, when we are sure that the furnace is reliable at 600°C. In the final helium injector the ion source extract potential will be made independent of the charge-exchange energy so that the optimum values may be used.

The duoplasmatron extract system still has to be improved. The filaments, which last some 50 hours, have been replaced by a mercury pool cathode; its design has not been finalized but a satisfactory ion beam performance has been obtained.

On the purely experimental side a modified ion source in H.10 has given a 1 μA focussed beam of negative copper ions.

Installation of the negative helium ion source on the tandem will have to be delayed until the summer of 1968 to allow a reasonable operational time for the first ion source and associated modifications (see above).

45 MeV electron linear accelerator (P. P. Thomas)

Analysis of machine running

	Hours	Hours	%
Total scheduled time	4392		100.00
Scheduled maintenance and installation work		408	9.30
Scheduled experimental time		3984	90.70
	3984		100.00
Time lost through breakdown		236	5.93
Machine off at users' request		30	0.75
Available experimental time		3718	93.32
	3718		100.00

Analysis of machine running (cont'd)

		Hours	%
Experimental usage			
(1)	Irradiations for Analytical Sciences Division Dr. C. Baker	54	1.45
(2)	Experimental Runs - Cell I Mr. N. J. Pattenden, N.P. Dr. C. A. Uttley, " Dr. G. D. James, " Dr. M. G. Sowerby, " Mr. M. G. Schomberg, " Mr. M. C. Moxon, " Dr. A. Asami, " Dr. B. H. Patrick, " Miss E. M. Bowey, "	3301	88.80
(3)	Experimental Runs - Cell II Dr. B. H. Patrick, N.P. Dr. H. Medicus, " Miss E. M. Bowey, "	198	5.32
(4)	Experimental Runs - Cell II Mr. M. C. Moxon, N.P.	165	4.43
(5)	Experimental Runs - Cell III Dr. R. Sinclair, A.P. Mr. D. Day, "	2308	SEE BELOW
(6)	Experimental Runs - Cell III Dr. M. S. Coates, N.P.	150	

In the above table, Cell III running hours are less than Cell I running hours because either the Cell III users asked that the beam to Cell III be switched off or because Cell III fault conditions made it impossible to provide an adequate beam at the Cell III target. The breakdown for Cell III is as follows:

	Hours	Hours	%
Available Cell III experimental time	3355		100.00
Experimental Runs - Cell III		2458	73.30
Cell III off at users' request		667	19.90
Cell III off due to faults and beam transport difficulties		230	6.80

Machine development

During the current period this has included the design and installation of equipment to enable a pre-determined number of pulses to be run into a target, the design and installation of a continuously indicating pulse position indicator for Cell I, the partial rebuilding of the gun cathode modulator to improve reliability and ease rapid fault diagnosis, the installation of further stabilised power units on machine and beam handling circuits, and minor improvements to the machine vacuum system.

PDP4 data processor (E. M. Bowey, G. B. Dean and J. L. Wilbourn)

The computer was used for 1490 hours and two system modules failed during the period of this report.

A double register unit was designed, using available integrated circuits. This unit is now installed and ready for use and will enable a 'two-parameter' experimenter to be run on-line, with 8k timing channels and 4k amplitude channels. Both registers can operate at 16 MHz clock frequency, but due to the simple method used for staticising the timing channel register, the minimum channel width is limited to ⅛ μsec.

A new 35 mm automatic camera has been mounted on a 5 inch oscilloscope run in parallel with the main computer display, thus leaving this large oscilloscope available for light pen operation when needed.

(E) Optimisation of moderators for pulsed neutron targets (B. H. Patrick, E. M. Bowey, M. C. Moxon and E. R. Rae)

The spectrum of neutrons produced by injecting bursts of charged particles into a heavy element target generally peaks at ~ 500 keV and contains very few neutrons in the range below 10 keV. To increase the number of neutrons in this energy range, moderators may be placed close to the target, but the increase is usually obtained at the expense of an increase in the width of the neutron burst leaving the moderator. Michaudon[114] in a series of Monte Carlo calculations has estimated the effect of the moderator on the number of neutrons leaving the surface and also on the broadening of the neutron pulse. He showed that the moderator can be characterised at an energy E by a "figure of merit" F given by $F = \frac{N}{\sigma^2}$, where N is the number of neutrons leaving the moderator with energy E and σ^2 is the variance of the time distribution, assuming that the contribution from the incident fast neutron pulse is negligible. For a given resolution, the highest count rate in a detector will be achieved when the thickness of moderator is chosen to make F as large as possible. A direct experimental measurement of N and σ^2 and hence of F has been made at energies in the region of 100 eV and 1 keV for a range of moderator thicknesses. The results were presented at the Third Euratom Conference on Accelerator Targets Designed for the Production of Neutrons, Liege, September 1967.

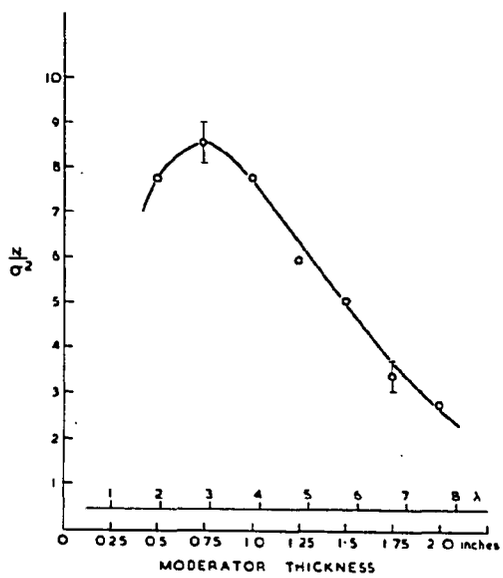

Fig. 42. Figure of merit plotted against moderator thickness for the 100 eV region.

The experiment involved measuring the shape and area of neutron resonances by observing the capture γ-rays from a sample illuminated with a neutron beam leaving various thicknesses of polyethylene moderator, under experimental conditions chosen so that the widths of the observed resonances were dominated by the moderator effects. A tantalum sample 0.004 ins thick was used to study the 100 eV region and an iron sample 0.040 in thick to study the 1 keV region. A Moxon-Rae detector on a 3.99 metre flight path was used to measure the γ-ray yield as a function of neutron energy.

Fig. 41 shows the relative figures of merit plotted against moderator thickness for the 100 eV region. It can be seen that the maximum value of F occurs at ~ 0.75 in polyethylene and this is also the case for the 1 keV region. These results are in reasonable agreement with Michaudon's calculations.

In the analysis of slow neutron resonances by the "shape" method, a knowledge of the resolution function of the time-of-flight spectrometer is required. This function is, in general, formed by a folding together of the time profile of the fast neutron burst, the timing channel width and the broadening effect of

(114) Michaudon A. Reactor Science and Technology (Parts A/B) 17, 165 (1963).

the moderator. Groenewold and Groendijk[115] have obtained an analytical expression for the shape of the slow neutron burst leaving a semi-infinite moderator, assuming that a delta function pulse of fast neutrons is injected at time t = 0. The expression is

$$P(t) = \frac{1}{2} x^2 e^{-x} \ , \ x = \frac{V\lambda}{t} \qquad (1)$$

where P(t) is the probability of a neutron leaving with energy E after time t, and the other quantities, also taken at energy E, are

the neutron velocity V and

the mean free path λ, which for polythene below 10 keV is $\sim$ 0.66 cm.

The experiment showed that the time spread introduced by the moderator increased with increasing thickness. The observed shape of the resonances in the experiment suggested that the above expression could be used to give the shape of the moderation time spread for finite moderators if the mean free path was dependent on the thickness of the moderator.

A χ^2 minimising programme has been developed to calculate the mean free path for the various moderator thicknesses. The programme folds together a Monte Carlo calculation of the neutron capture yield for the resonance, the fast neutron burst profile, the timing channel width and the moderator time spread as given by equation (1). Fig. 43 shows the best fit to the experimental data for the tantalum resonance at 105 eV using a 1 in polyethylene moderator. The value of λ which gives the best fit is 0.17 in. Calculations on other thicknesses are in progress and indicate that the above expression can be used to give the shape of the moderation jitter if a modified mean free path is used.

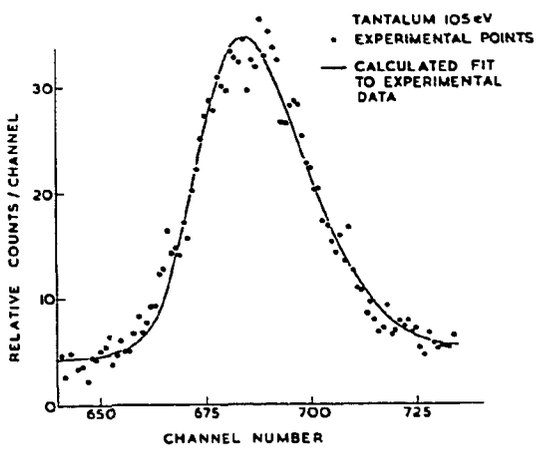

Fig. 43. Best fit to tantalum resonance at 105 eV.

(115) Groenewold H. J. and Groendijk H. Physica 13, 141 (1947).

Synchrocyclotron (P. G. Davies)

Analysis of machine running

	Hours	Hours	%
Scheduled experimental time*	3827		100.0
Time lost due to breakdowns		146	3.8
Available experimental time		3681	96.2
	3681		100.0

Experimental usage

(1)	Neutron Time-of-Flight (I) (A. Langsford, P. Clements)	845	23.0
(2)	M. Wigan	758	20.6
(3)	Neutron Time-of-Flight (II) (A. Langsford, M. S. Coates)	405	11.0
(4)	A.E.R.E./Queen Mary College (I. M. Blair, J. Edgington)	394	10.7
(5)	Neutron Time-of-Flight (III) (A. Langsford, R.H.E.L., Southampton University)	367	10.0
(6)	Neutron Time-of-Flight (IV) (A. Langsford, H. Marshak)	226	6.1
(7)	C. Whitehead	96	2.6
(8)	R.H.E.L. (G. Manning)	96	2.6
(9)	Imperial College, London	32	0.9
Machine not required		462	12.5
		3681	100.0

Cyclotron improvement program

Ion source

The ion source mechanism has been manufactured, vacuum tested and handed over for further testing.

Beam tunnels

Both tunnels have been handed over and the North tunnel has actually been used for an experiment. False floors have been installed in the East tunnel. Work is underway to provide cabling between the experimental areas and the counting room.

Modulator

Construction and D.C. testing of the modulator is complete, except for some minor modifications found necessary during the final installation.

---

*During most of this period an intermittent shift rota was worked and maintenance, setting up, etc. was carried out during scheduled rest days.

New R.F. system (P. E. Dolley, R. E. N. Horne and G. Huxtable)

The programme of measurement (at low power levels) and adjustment of the electrical characteristics of the new R.F. resonator has been completed, and the indications are that the design aims will be achieved. High power tests of the resonator, driven by its associated oscillator, will start early in November. A modulated D.C. power supply has been completed and is now being commissioned.

The R.F. programme is now running about three months later than expected, owing to production delays, to the low-power measurements and adjustments taking longer than expected, and to some modifications which have been found necessary as a result of testing. As a result the shut-down date has been postponed to December.

Development of assorted electronic equipment for control of the machine is continuing.

Modifications to the pulsed beam deflection system (P. H. Bowen)

Work on the new beam deflection system for neutron time-of-flight experiments has been delayed by late delivery of the 60 kV, 100 mA E.H.T. power supply. However the thyratron pulse shaping circuit has now been tested at full power and after a few minor modifications works satisfactorily. The next stage, to connect this circuit to the prototype deflection system for testing in vaccuo, is well advanced.

Beam acceleration studies (J. P. Scanlon)

(a) Radial oscillation generation

The effect of the choice of dee shape on the generation of radial oscillations in the internal beam of the modified synchrocyclotron was discussed in the last Progress Report (PR/NP 12). Since that time calculations made elsewhere have indicated that some additional effect exists which would damp out any radial motion caused by the dee cut-back by the time the beam had reached a large radius in the machine. To test this a new and more accurate orbit code has been written. The results with the new code agree well with the original ones; our conclusions are unchanged.

However the exercise has shown that to obtain reliable quantative results considerable care must be taken, and further work is being carried out to optimize the computing methods and to provide more general solutions for arbitrary dee shapes and dee voltage variation.

(b) Phase matching in the central region

The orbit code SPUTNIK has been used to calculate initial orbits of particles emitted from a calutron ion-source with a puller electrode electrically connected to the dee. The general conclusion is that after several orbits all particles are concentrated in the phase region 0°-45°. Measurements of the frequency sweep of the new R.F. system indicate that the initial stable phase will be in the region of 80°. This figure taken together with the results referred to in (a) above means that all particles will be expected to develop considerable radial amplitudes. A range between 1 and 3 inches seems likely. This is a far from ideal situation, and though it will be accepted initially, further calculations are being made to study the behaviour of particle orbits from a calutron source at positive D.C. potential with a negative D.C. puller. Results to date show that with such a source it should be possible to accelerate particles over a range of phases which includes the stable phase, without losing the other inherent properties of the calutron system.

(c) Ion source movement

This has been built, apart from the central feed tube, and has been vacuum tested.

(d) Ion source

A calutron source has been constructed, together with a test rig, for use in the model magnet. A 500 amp filament supply and pulsed arc power supply are now available. An improved puller insulator has been tested in the VEC. This is again a 1" long boron nitride insulator, and it has run at 35 kV, 21 Mc/s, in a field of 16.5 Kgauss for 10 hours without any sign of deterioration. Life tests must await installation in the synchrocyclotron.

Beam extraction (D. West)

The essential computations for the regenerator and for the extractor channel are now finished. The design has been carried through for particles of zero amplitude of radial oscillation. The calculations went through the following stages:

(a) the determination of field strength integrals versus radius for regenerators which would give a constant phase angle in the induced radial motion. Available radial field plots in the 110" synchrocyclotron are used in this calculation, and the regenerator is assumed to be localised at a single azimuth,

(b) evaluation of stability limits on vertical motion through these constant phase regenerators,

(c) the determination of channel configurations compatible with (a) and (b). In report SCI TP(67) 31 (July 1967) four possible combinations of extractor and regenerator were evaluated. This report also highlighted the need for horizontal focusing in the channel,

(d) the computations in (c) were revised to allow for the necessary finite angular size of the regenerator. Report SCI TP(67) 34 (November 1967) lists six possible combinations of extractor and regenerator.

The extractor engineering design, which had to start before these computations were completed, is compatible with these possible alternatives. The decision as to which is used will depend on two factors unknown at present, namely, how difficult it is to shim and to achieve the specified field configurations in the regenerator.

Preliminary measurements of field configurations in trial regenerators are to be carried out before the machine shut-down occurs. Calculations on shimming are being carried out by Dr. I. M. Blair. It is also intended to do some measurements before the shut-down. A plan of extractor installation, making allowance for these uncertainties, has been drawn up (SCI TP(67)32, July 1967).

The computer programmes used in the computations will also be required for assimilating the results of the field survey to be taken during the shut-down. To avoid the continuing use of Atlas I the programmes are being re-compiled on to the IBM 360/65 by a firm of programmers, but considerable difficulty is being encountered.

Magnetic beam extraction coil (O. N. Jarvis)

In previous Progress Reports (PR/NP 11 and 12) mention was made of the suggestion by Kim[116] that the performance of a regenerative beam extractor could be improved by the use of a small time-dependent field coil within the synchrocyclotron. The expected advantages of such a system were

(a) Improved extraction efficiency.

(b) Extraction of particles with large radial oscillation amplitudes.

---

(116) Kim H. I.E.E.E. Trans. Nuc. Sci. 13, 4, p. 58 (1966).

(c) Minimal energy spread in the extracted beam.

(d) A long beam extraction period (good duty cycle).

Computer studies have been made using orbit codes written at C.E.R.N. by Vogt-Nillsen. Results show that for a regenerative extractor designed to extract protons from a 48" radius orbit the use of a "Kim coil" would allow extraction of particles with radial oscillation amplitudes up to 1.25". For larger amplitudes there are severe vertical defocussing effects and such particles would be lost.

It was originally hoped that such a system would replace the present electronic slow extraction system (the "Cee") but it appears that both are required simultaneously. The required strength for the coil is about 200 gauss over a 42° sector.

Numerical studies have yet to be made of the transition between the state in which the particle orbit motion is mainly controlled by the (decreasing) field of the Kim coil to that in which it is controlled by the field of the regenerator.

Magnet survey (G. C. Cox)

Mechanical components for the semi-automatic survey equipment(117) have been assembled by the manufacturers. Fine adjustments to gearing and alignment will still be required prior to delivery. Calibration of the apparatus is expected to start in November and a test jig is being built for this purpose.

The electronic drive units and control apparatus are 75% complete. Exhaustive testing of these units will not be possible until the mechanical equipment has been delivered, but in preliminary tests the circuits appear to function satisfactorily.

Measurements of spectra from internal neutron producing targets (M. S. Coates, D. A. J. Endacott, D. B. Gayther, G. D. James and A. Langsford)

Measurements have been made on the 27 metre flight path of the synchrocyclotron of neutron spectra from a moderated and an unmoderated target. The data were obtained during the preliminary stage of an experiment intended to yield an accurate measurement of the relative fission cross section of ^{235}U over the energy range $\lesssim 20$ keV $\rightarrow$ 14 MeV. A gas scintillation fission fragment detector(118) placed at 17 metres from the pulsed neutron source received a collimated neutron beam from a circle 3 cm diameter and determined the fission yield. The neutron spectrum was measured by a thin ^{10}B plug(119) detector containing 20 g of ^{10}B in the form of a disc 7.5 cm in diameter. This detector was placed at 27 metres on the same flight path and collimated to view the same source position and area as the fission counter. This detector has yet to be cross calibrated against a similar detector(119) of known efficiency (which could not be used in the experiment because the flux was too high). However a sufficiently accurate estimate of the efficiency of the ^{10}B detector for investigating the general form of the spectra was obtained from the fission counter data by *assuming* the fission cross sections given in BNL 325(120) and combining them with a Monte Carlo calculation in the energy range below $\sim$ 100 keV where the ^{10}B neutron absorption cross section is known to have a $\frac{1}{V}$ dependence and the (small) effects of multiple scattering can be reliably predicted.

---

(117) Nuclear Physics Division Progress Report AERE - PR/NP 12 (1967).

(118) James G. D. Argonne National Laboratory Report ANL-7320, p. 16 (1967).

(119) Nuclear Physics Division Progress Report AERE - PR/NP 12, p. 13 (1967).

(120) Hughes D. J. and Schwartz R. B. BNL 325, 2nd Edition (1958).

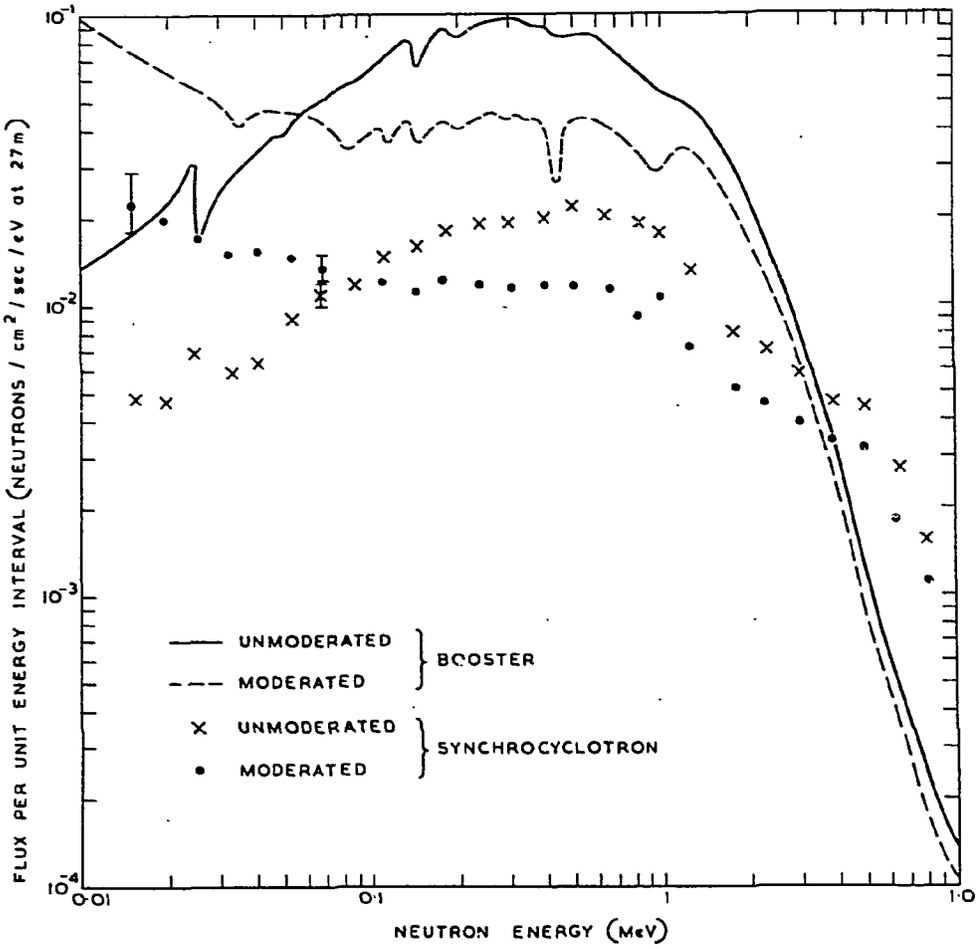

Fig. 44. Comparison of neutron spectra available from the synchrocyclotron and from the electron Linac.

The spectra are shown in Fig. 44, where the counts are grouped in $\frac{1}{4}$ lethargy intervals (~ 25% energy resolution) normalised together to an accuracy of ±10% using the monitored value of the proton beam intensity. Error bars shown at representative points give the statistical standard deviation. Variation in the intensity of the internal proton beam striking the target leads to a normalising error of ±10% in comparing "moderated" and "unmoderated" spectra. Measurements were made in the backward direction relative to the incident 140 MeV proton beam. The moderated target was a water filled copper walled tank (0.16 cm wall thickness; 15 cm wide, 4.1 cm high and 2.5 cm thick in the beam direction) set immediately in front of a heavy alloy (~ 90% W) bar (15 cm × 4.1 cm × 2.5 cm) i.e. on the side downstream for neutrons, and the unmoderated target was the heavy alloy bar. In both cases most of the neutrons are produced in the heavy alloy. The spectra differ significantly from some previously published target spectra(121) made on the synchrotron using lead and uranium with polyethylene as a moderator. In part this is due to the differences in target materials, but a reassessment of the detector efficiencies used in the evaluation of these earlier spectra indicates that the neutron population below ~ 700 keV had been underestimated and that the spectra at low energies are similar to the heavy alloy spectra.

It is also interesting to note that the shapes of the spectra below ~ 2 MeV obtained here are similar to those of the moderated and unmoderated spectra on the neutron booster target of the 45 MeV linac. These measurements have been reported previously(122) and the data have recently been

(121) Nuclear Physics Division Progress Report AERE - PR/NP 8, p. 37 (1965).

(122) Nuclear Physics Division Progress Report AERE - PR/NP 9, p. 17 (1966).

re-evaluated using an improved detector efficiency determination[119]. In addition measurements have been extended to higher energies. For comparison the booster results are also shown in Fig. 44, with the spectra normalised together to an accuracy of ± 10% using the electron beam intensity. The flux intensity scale was derived using estimated values of the absolute efficiencies of the detectors. It is difficult to assess the accuracy of this procedure, but the error is considered to be ~ 25% for each spectrum set.

Machine operating conditions (representative of normal running) for the measurements are shown in Table IV. The parameters appropriate to the expected performance of the cynchrocyclotron after conversion are also given.

TABLE IV

Machine parameters

	Synchrocyclotron		Linac
	(before modification)	(expected after modification)	
pulse length	10 nsec (protons)	10 nsec (protons)	100 nsec (electrons)
pulse repetition frequency	200 pps	1,000 pps	192 pps
current during pulse	500 mA	1,000 mA	500 mA

It should be noted that the measured fluxes correspond to neutrons travelling backward with respect to the proton beam. In the forward direction the available neutron flux from the synchrocyclotron at energies of a few MeV and above greatly exceeds that available from the electron linac.

Good and Rae have made detailed comparisons of various pulsed neutron sources allowing for the different experimental resolutions[123]. Following the treatment of these authors the outputs of the booster and synchrocyclotron are shown in Fig. 45 for a condition of constant energy resolution

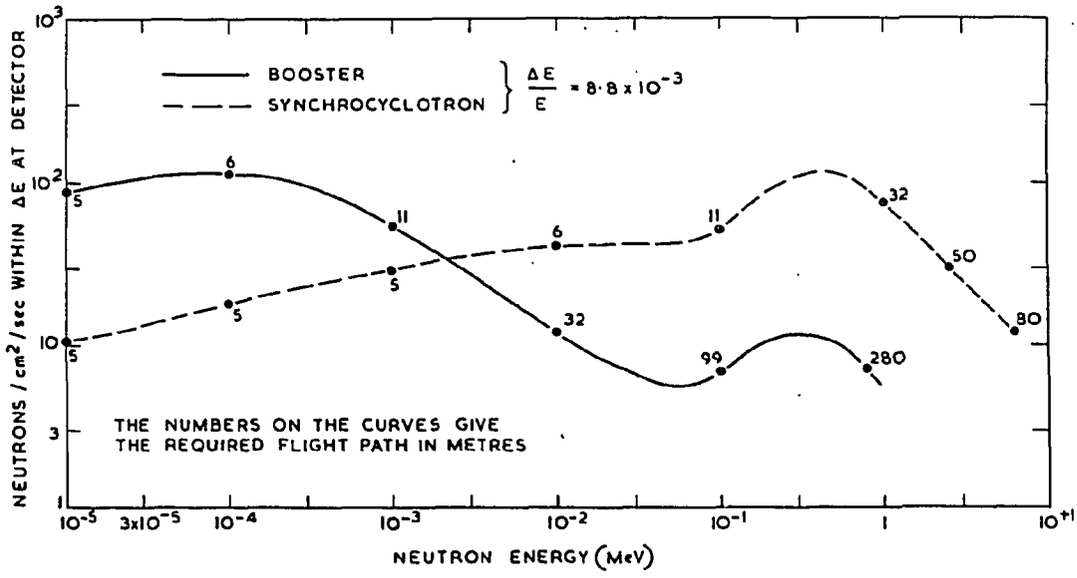

Fig. 45. Comparison of neutron counting rates available from the synchrocyclotron and from the electron linac for time of flight measurements at a fixed resolution $\Delta E/E = 8.8 \times 10^{-3}$.

(123) Good W. M. and Rae E. R. AERE Report NP/GEN 21 (1962).

$\left(\frac{\Delta E}{E} = 8.8 \times 10^{-3}\right)$. The source spectrum in each case has been taken as the unmoderated spectrum at high energies and the moderated spectrum at energies below that at which these spectra have equal intensity, as determined from Fig. 44. For convenience the spectra have been smoothed. The effects of moderation jitter are included in the calculation and neutron overlap at high machine cycle rates has been allowed for by assuming a boron filter is used which has a 1% transmission of unwanted neutrons at the end of a cycle. The machine parameters used are those given in Table IV, but taking the maximum cycle rate of 400 pps for the booster. The required flight path length in metres is shown at several energies. The maximum lengths available on the booster and synchrocyclotron at present are 300 m and 100 m respectively.

REPORTS AND PUBLICATIONS

REPORTS

AERE - R 5224 The average neutron total cross section of ^{10}B from 100 eV to 10 MeV and absorption cross section up to 500 KeV. K. M. Diment.

AERE - R 5381 A method of time calibration for time-of-flight experiments in nuclear physics. A. Langsford and P. E. Dolley.

AERE - R 5475 Comments on radio frequency and optical bremsstrahlung from extensive cosmic-ray showers. J. V. Jelley.

AERE - R 5503 The atmospheric electric field as a source of RF emissions from EAS, and some notes on bremsstrahlung. W. N. Charman and J. V. Jelley.

AERE - R 5507 The Harwell-Grove radio installation for detecting extensive air showers at low elevation, over a 9 km baseline. W. N. Charman, J. H. Fruin and J. V. Jelley.

AERE - R 5508 Antennas, receivers and problems of the radio detection of large air showers. J. V. Jelley.

AERE - R 5509 Servo systems for Cherenkov light receivers. J. H. Fruin and J. V. Jelley.

AERE - R 5556 Measurement of the correlation parameter C_{NN} in proton-proton scattering. O. N. Jarvis, T. W. P. Brogden, B. Rose, J. P. Scanlon, J. Orchard-Webb and M. R. Wigan.

AERE - R 5573 Electronic conduction through thin unsaturated oxide layers. G. Dearnaley.

AERE - R 5585 Measurements of the differential cross section and polarization in proton-proton scattering at about 143 MeV. G. F. Cox, G. H. Eaton, C. P. Van Zyl, O. N. Jarvis and B. Rose.

AERE - R 5588 A theory of the oxide-coated cathode. G. Dearnaley.

AERE - R 5592 Excitation of isobaric analogue states in ^{20}Ne, ^{24}Mg and ^{28}Si. B. Lawergren, G. C. Morrison and A. T. G. Ferguson.

AERE - R 5618 Neutron scattering at 6 MeV from light nuclei. W. M. Currie, J. Martin and D. T. Stewart.

MEMORANDA

AERE - M 1967 Report on the conference on semi-conductor nuclear particle detectors and circuits, Gatlinburg, May 1967. G. Dearnaley and K. Kandiah.

PUBLICATIONS

ASGHAR M. Spin Assignments of Low Energy Resonances in ^{239}Pu. Nuc. Phys. A98, 33 (1967).

AULD E. G., CRABB D. G., McEWEN J. G., BIRD L., WHITEHEAD C. and WOOD E. 63 MeV Deuteron Scattering on C, Al and H. Nuc. Phys. A101, 65 (1967).

BANERJEE S. K., O'REILLY W. and JOHNSON C. E. Mössbauer effect measurements on Fe Ti Spinels with Local Disorder. J. App. Phys. 38, 1289 (1967).

CHARMAN W. N., FRUIN J. H., JELLEY J. V., PORTER R. A. and SMITH F. G. Evidence for Radio Pulses from Extensive Air Showers at Large Zenith Angles. Zh. Eksperim. i Teor. Fiz. 53 (1), 88 (1967).

CHARMAN W. N. Atmospheric Electric Field as a possible cause of Radio Pulses from Extensive Air Showers. Nature 215, 497 (1967).

CRABB D. G., McEWEN J. G., ALD E. G. and LANGSFORD A. Detection Efficiency of Plastic Scintillation Counters for Neutrons in the Energy Range 20-130 MeV. Nuclear Instruments and Methods 48, 87 (1967).

CURRIE W. M. and EVANS J. E. Levels in ^{33}P. Phys. Lett. 24B, 399 (1967).

DEARNALEY G. and WILKINS M. A. Crystal Wafer Orientation by Proton Channelling. Journal Sci. Instrum. 44, 880 (1967).

DEARNALEY G. Semi-conductor Detectors in Nuclear Physics Research. "Nuclear Structure" Ed. : Hossain, Rashid and Islam (North-Holand 1967).

EDWARDS P. R., JOHNSON C. E. and WILLIAMS R. J. P. Mössbauer Spectra of some Tetrahedral Iron (II) Compounds. J. Chem. Phys. 47, 2074 (1967).

GAYTHER D. B. and GOODE P. D. Neutron Energy Spectra and Angular Distributions from Targets Bombarded by 45 MeV Electrons. J. Nuc. Energy 21, 733 (1967).

JAIN A. P. and CRANSHAW T. E. Anomalous Temperature Dependence of the Hyperfine Field at Sn in Cobalt. Phys. Lett. 25A, 421 (1967).

JAIN A. P. and CRANSHAW T. E. Mössbauer effect at ^{119}Sn in AuMn, AgMn, CuMn and AuFe alloys. Phys. Lett. 25A, 425 (1967).

JARVIS O. N., HARVEY B. G., HENDRIE D. L. and MAHONEY J. The Inelastic Scattering of 17.8 MeV Protons from ^{58}Ni, ^{60}Ni and ^{120}Sn and the Determination of Spin and Parity Assignments for ^{58}Ni from α-particle Scattering. UCRL-17352 and Nuc. Phys. A102, 625 (1967).

JELLEY J. V. Cerenkov Radiation from Extensive Air Showers. Progress in Elementary Particles and Cosmic Ray Physics. Edited by J. G. Wilson and S. A. Wouthuysen, Vol. 9, Chapter II, p. 41 (1967).

JELLEY J. V. Comments on Radio Frequency and Optical Bremsstrahlung from Extensive Cosmic Ray Showers. Phys. Lett. 25A, 346 (1967).

JOHNSON C. E., KNOWLES P. F. and BRAY R. C. Mössbauer Evidence for the form of Iron in Xanthene Oxidase. Biochem. J. 103, 10C (1967).

JOHNSON C. E. and RIDOUT M. S. A Mössbauer Effect Study of Antiferromagnetic $FeCl_2$ $4H_2O$. J. App. Phys. 38, 1272 (1967).

JOHNSON C. E. Hyperfine Interactions in Ferrous Fluosilicate. Proc. Phys. Soc. 92, 748 (1967).

JOLLY R. K., MAXSON D. R., NEILSON D. C. and JONES G. A. Ground State Spin of ^{129}Te by Polarization Measurements of Protons Scattered via Analogue Resonances. Phys. Lett. 25B, 265 (1967).

LANGSFORD A., BOWEN P. H., COX G. C., DOLLEY P. E., RIDDLE R. A. J. and SALTMARSH M. J. M. Fast Forward Neutron Production in the d(p,n)2p Reaction for 95.7 and 143.9 MeV Protons. Nuc. Phys. A99, 246 (1967).

RAE E. R., MOYER W. R., FULLWOOD R. R. and ANDREWS J. L. Gamma-Ray Spectra from Radiative Capture of Thermal and Resonance Neutrons in Mercury and Tungsten. Phys. Rev. 155, 1301 (1967).

RAE E. R. Fundamental Methods in Neutron Spectroscopy. Chapter 14, Fundamentals in Nuclear Theory, IAEA Vienna (1967).

IN COURSE OF PUBLICATION

ARMITAGE B. H. and HOOTON B. W. Energy Loss of Oxygen and Sulphur Ions in Matter. Nuclear Instruments and Methods.

CHARMAN W. N. Radio Pulses from Extensive Air Showers as a result of Movement of Slow Electrons in the Atmospheric Electric Field. J. Atmos. Terrestial Physics.

DEARNALEY G. Solid State Radiation Detectors. Contemporary Physics.

DEARNALEY G. Electronic Conduction through thin Unsaturated Oxide Layers. Phys. Lett.

DEARNALEY G., FREEMAN J. H., GARD G. A. and WILKINS M. A. Implantation Profiles of ^{32}P channelled into Silicon Crystals. Can. Journ. Phys.

JAMES G. D. Multilevel Analysis of ^{239}Pu Fission Cross Section near 83 eV. J. Nuc. Energy.

MAXSON D. R., JOLLY R. K. and KNOX K. C. A Polarimeter for Isobaric Analogue State Spin Measurements. Nuc. Instrum. and Methods.

JOLLY R. K., GOLDBERG M. D. and SENGUPTA A. K. Collective Excitations via Inelastic Deuteron Scattering from even Nickel and Zinc Isotopes. Nuc. Phys.

LAWERGREN B., MORRISON G. C. and FERGUSON A. T. G. Excitation of Isobaric Analogue States in the ^{27}Al(d,n) ^{28}Si Reaction. Nuc. Phys.

MARTIN J., STEWART D. T. and CURRIE W. M. Neutron Scattering at 6 MeV from Light Nuclei. Nuc. Phys.

MOXON M. C. The Neutron Resonance Parameter and Average Capture Cross Section of ^{165}Ho. Nuc. Phys.

CONFERENCE PAPERS

Invited Papers:

SOWERBY M. G. Some Notes on the $^{6}Li(n,\alpha)$ Cross Section from Thermal Energies up to the $(n, \alpha + d)$ threshold (1.718 MeV); and,
Methods of Neutron Flux Determination Based on Standard Cross Sections for White Spectrum Measurements (e.g. Linacs). IAEA Panel Meeting on Nuclear Standards Needed for Neutron Cross Section Measurements, Brussels, 8-12th May (1967).

DEARNALEY G. Basic Limitations of Semi-Conductor Detector Performance. Symposium on Semi-Conductor Nuclear Particle Detectors and Circuits, Gatlinburg, 15-18th May (1967).

MURRAY G., FREEMAN J. M., JENKIN J. G. and BURCHAM W. E. Q-values of (p,n) Reactions. International Conference on Atomic Masses, Winnipeg, Canada, 28th August-1st September (1967).

FREEMAN J. M. Superallowed Fermi beta decays and the Weak Interaction Vector Coupling Constant. American Physical Society, Division of Nuclear Physics, Madison, Wisconsin, 23-25th October (1967).

Contributed Papers:

Proceedings of the Second International Conference on Magnetic Resonance in Biological Systems, Stockholm, June 1966. (Pergamon Press 1967)

JOHNSON C. E., BRAY R. C. and KNOWLES P. F. Mössbauer Effect Studies of the Iron in Milk Xanthine Oxidase, p. 417.

JOHNSON C. E. Note on Hyperfine Splitting in Mössbauer Spectra in Large Magnetic Fields, p. 405.

The Tenth International Conference on Cosmic-Rays, Calgary, July 1967

CHARMAN W. N. and JELLEY J. V. The Atmospheric Electric Field as a Source of RF Emissions from EAS, and some Notes on Bremsstrahlung.

CHARMAN W. M., FRUIN J. H. and JELLEY J. V. The Harwell-Grove Radio Installation for detecting extensive Air Showers at low elevation, over a 9 km baseline.

JELLEY J. V. Antennas, Receivers and Problems of the Radio Detection of Large Air Showers.

FRUIN J. H. and JELLEY J. V. Servo systems for Cerenkov light receivers.

PORTER R. A., SMITH F. G., TORBITT W. S. and JELLEY J. V. Experimental tests of the mechanism of the Radio Emission from Showers.

Conference on Astronomical Optics, London, 7-9th July 1967 (IPPS)

HEWITT A. V. and CHARMAN W. N. Spectrometry with a Cascade Image Intensifier.

13th General Assembly of I.A.U., Prague, 11-18th August 1967

HEWITT A. V. and CHARMAN W. N. A Cascade Intensifier System for Coudé-Focus Spectrometry.

HEWITT A. V. and CHARMAN W. N.; MILSOM A., PALMER D. A. and STANDEN P. (Royal Greenwich Observatory, Herstmonceaux). Stellar Spectroscopy with a Cascade Image Intensifier.

Third Euratom Conference on Accelerator Targets Designed for the Production of Neutrons, Liege, 18-19th September 1967

PATRICK B. H., BOWEY E. M., MOXON M. C. and RAE E. R. Optimisation of Moderators for Pulsed Neutron Targets.

Conference on Atomic Collision and Penetration Studies with Energetic Ion Beams, Chalk River, 18-21st September 1967

DEARNALEY G., FREEMAN J. H., GARD G. A. and WILKINS M. A. Implantation Profiles of ^{32}P channelled into Silicon Crystals.

International Conference on Solid State Physics Research with Accelerators, Brookhaven, 25-28th September 1967

DEARNALEY G., FARMERY B. W., MITCHELL I. V., NELSON R. S. and THOMPSON M. W. Channelling of Protons through Thin Crystals.

International Conference on The Physics Problems of Reactor Shielding, Harwell, 26-28th September 1967

AVERY A. F., EGERTON MISS J., COATES M. S. and GAYTHER D. B. Comparison of Spectra Calculated by Discrete Ordinate Methods with Time-of-Flight Measurements in Polythene, Graphite and Sodium.

Conference on Low Energy Nuclear Physics, Manchester, September 1967 (IPPS)

EARWAKER L. G. and MONTAGUE J. H. Properties of the 6.35 and 6.49 MeV Levels in ^{11}C.

FERGUSON A. T. G., NILSSON N. and STARFELT N. Isobaric analogue states in ^{32}S populated by the $^{31}P(d,n)^{32}S$ reaction.

JOLLY R. K., MAXSON D. R., NEILSON G. C. and JONES G. A. Some Spin assignments by polarization measurements of protons scattered via analogue resonances.

MARSHAK M. and LANGSFORD A. The Interaction of Intermediate Energy Neutrons with Aligned Holmium Nuclei.

WHITEHEAD C. and SHERWOOD A. C. Investigations of Ge(Li) Counters with 150 MeV Protons.

IAEA Symposium on Fast Reactor Physics and Related Safety Problems, Karlsruhe, 30th October - 2nd November 1967

SCHOMBERG M. G., SOWERBY M. G. and EVANS F. W. A new method of Measuring alpha (E) for ^{239}Pu.

International Conference on Elementary Particles, Heidelberg, September 1967

BIRD L. and WHITEHEAD C. (A.E.R.E.); AULD E. G. (R.H.E.L.), CRAB D. G., ORR R. and McEWEN J. G. (Southampton University); AITKEN D. K., BENNETT G., HAQUE J. F., JENNINGS R. E. and PARSONS A. S. L. (University College, London). Inelastic π-p reactions in the region of 3.2 GeV/c.

Divisional Staff

Division Head: Dr. B. Rose

Group Leaders: Dr. P. E. Cavanagh
Dr. T. E. Cranshaw
Dr. G. Dearnaley
Dr. A. T. G. Ferguson
Dr. J. M. Freeman
Dr. J. V. Jelley
Dr. E. R. Rae
Dr. A. E. Taylor

J. M. Adams
B. H. Armitage
Dr. I. M. Blair
P. H. Bowen
Dr. W. N. Charman
B. P. Clear
Dr. C. F. Coleman
Dr. W. M. Currie
K. M. Diment
Dr. L. G. Earwaker
P. D. Goode
Dr. B. W. Hooton
Dr. O. N. Jarvis
R. I. MacDonald
N. J. Pattenden
D. R. Porter
M. S. Ridout
Dr. J. P. Scanlon
A. C. Sherwood
W. Spencer
B. W. Thomas
J. F. Turner
S. Waring
Dr. C. Whitehead
E. Wood

G. V. Ansell
D. A. Boyce
Miss E. M. Bowey
Dr. M. S. Coates
D. W. Colvin
G. C. Cox
G. B. Dean
P. E. Dolley
J. H. Fruin
Dr. D. B. Gayther
A. G. Hardacre
G. Huxtable
Dr. G. D. James
Dr. A. Langsford
M. C. Moxon
Dr. B. H. Patrick
F. D. Pilling
Dr. B. W. Ridley
B. D. Rogers
M. G. Schomberg
Dr. M. G. Sowerby
D. J. Tripp
Dr. C. A. Uttley
D. West
M. A. Wilkins

Fellows, Temporary Research Associates and Attached Staff in Nuclear Physics Division

Dr. A. Asami	T.R.A.	
R. A. Bell	Attached	Oxford University
Dr. H. C. Benöhr	Attached	Institut für Theoretische Physik der Universität Tübingen
Dr. R. Chapman	Fellow	
P. J. Clements	Attached	Oxford University
Dr. T. W. Conlon	Fellow	
K. Gul	Attached	Oxford University
Dr. R. K. Jolly	Fellow	
M. Khalequzzaman	Attached	Bedford College, London University
Dr. L. G. Lang	T.R.A.	
Dr. C. D. McKenzie	T.R.A.	
Dr. J. Martin	S.F.T.A.	
Dr. H. A. Medicus	T.R.A.	
C. M. Newstead	Attached	Oxford University
Dr. W. T. Oosterhuis	Attached	Carnegie Institute of Technology, Pittsburgh, U.S.A.
Dr. J. Poate	Fellow	
W. D. N. Pritchard	Attached	Exeter University
Mrs. S. Ramavataram	Attached	Oxford University
Dr. D. C. Robinson	Fellow	
Dr. W. E. Stein	Attached	Los Alamos Scientific Laboratory
Dr. T. T. Thwaites	Attached	Pennsylvania State University, U.S.A.
Dr. C. L. Wick	Fellow	